X-ray fluorescence analysis

Tokyo University of Science
Department of Applied Chemistry

Izumi NAKAI

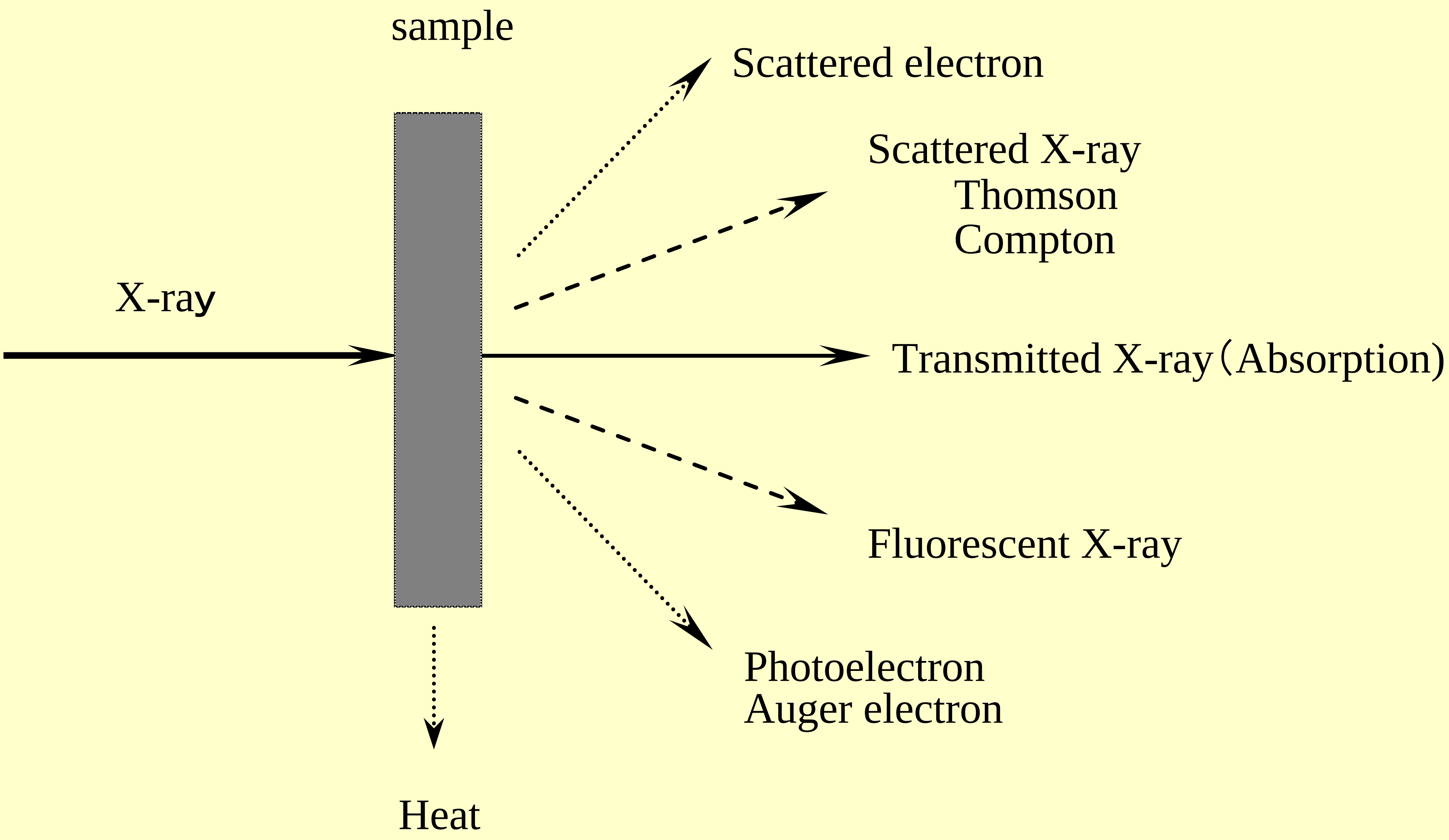

sample

Scattered electron

Scattered X-ray
Thomson
Compton

X-ray

Transmitted X-ray（Absorption)

Fluorescent X-ray

Photoelectron
Auger electron

Heat

Interaction of X-ray with matter

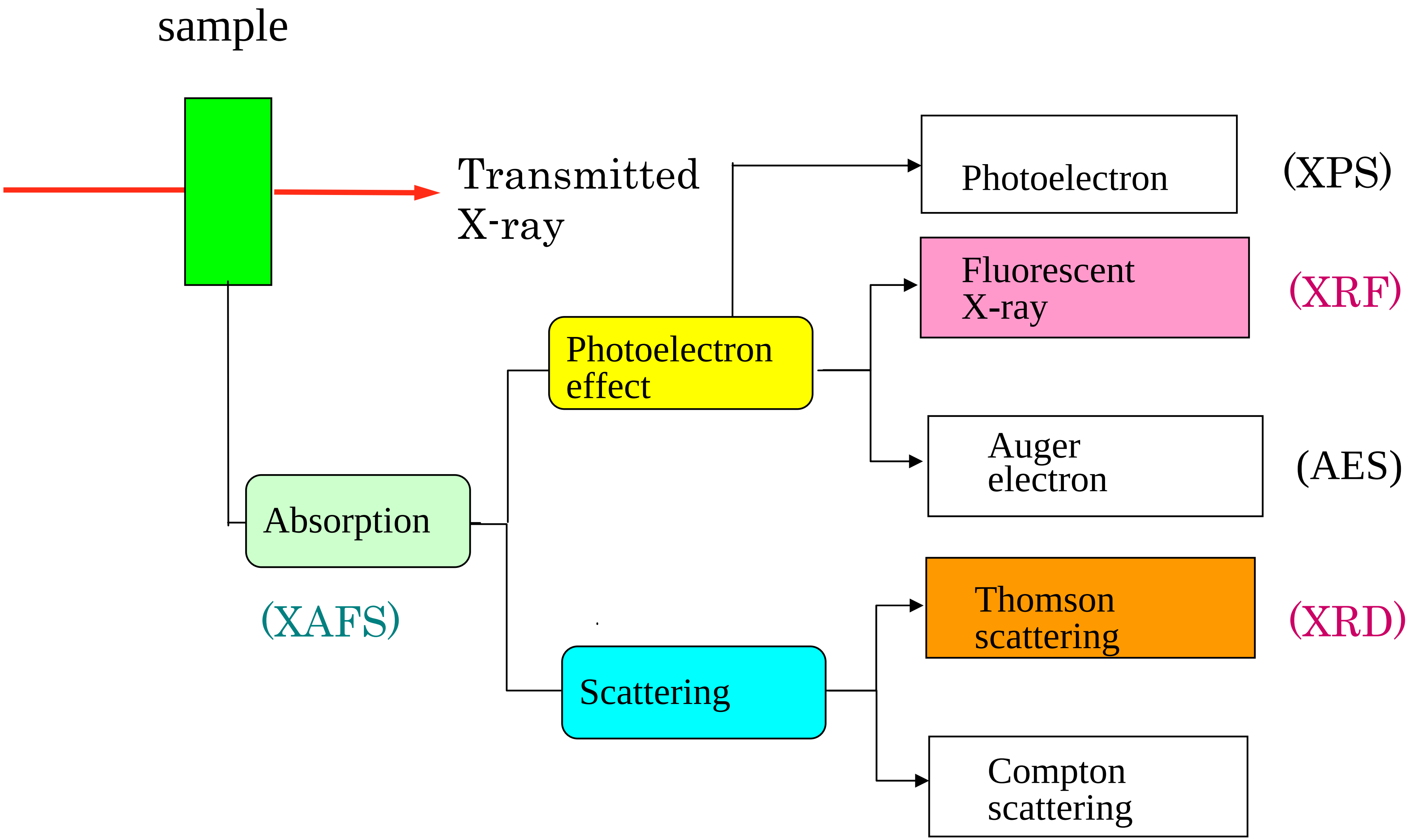

Interaction of X-ray with matter and X-ray analysis

Relationship between λ and E

Particle : energy E [keV]

Wave : wavelength λ [Å]

$E = hc/\lambda = 12.398/\lambda$ [keV],

Wavelength λ

ex. 1 Å = 12.398keV

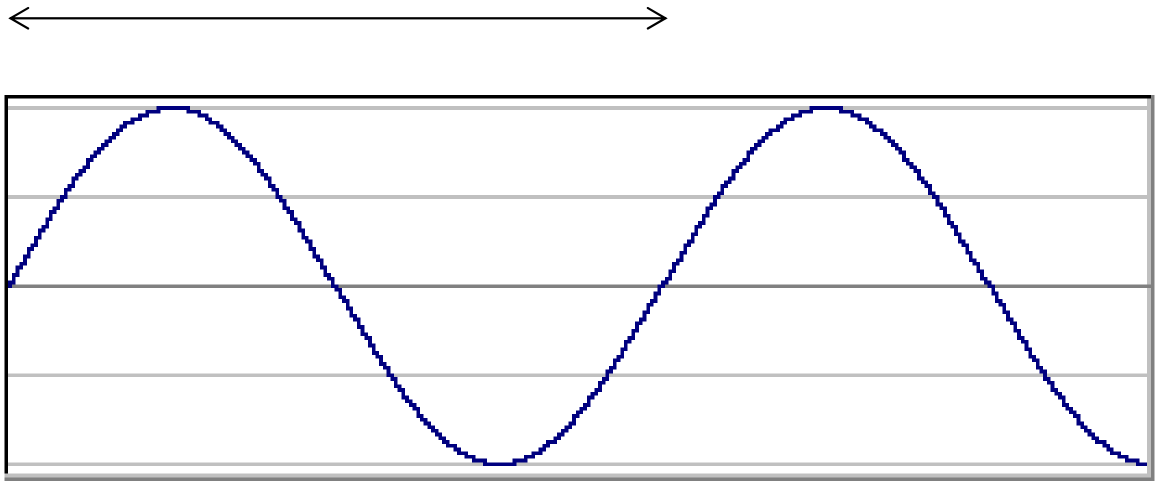

λ = long

Energy = low

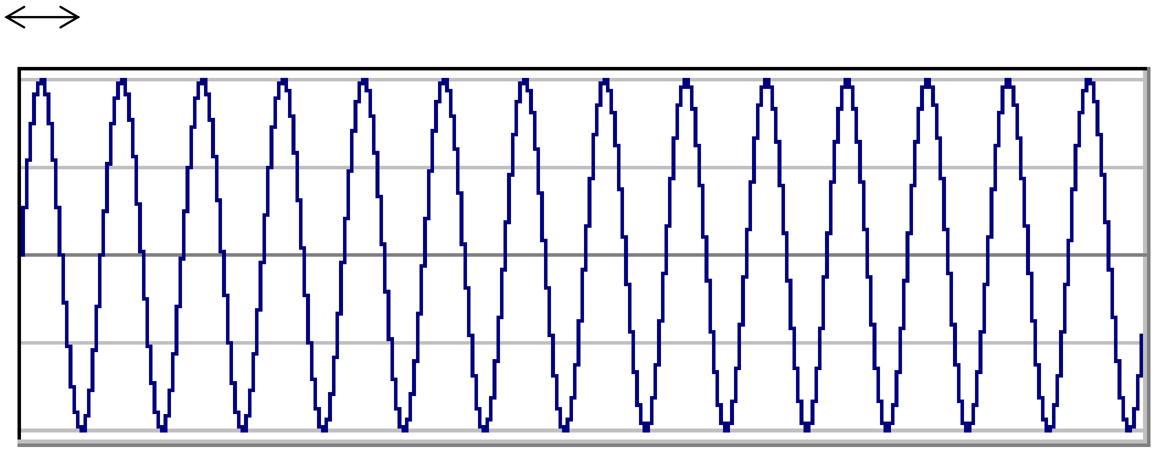

λ = short

Energy = high

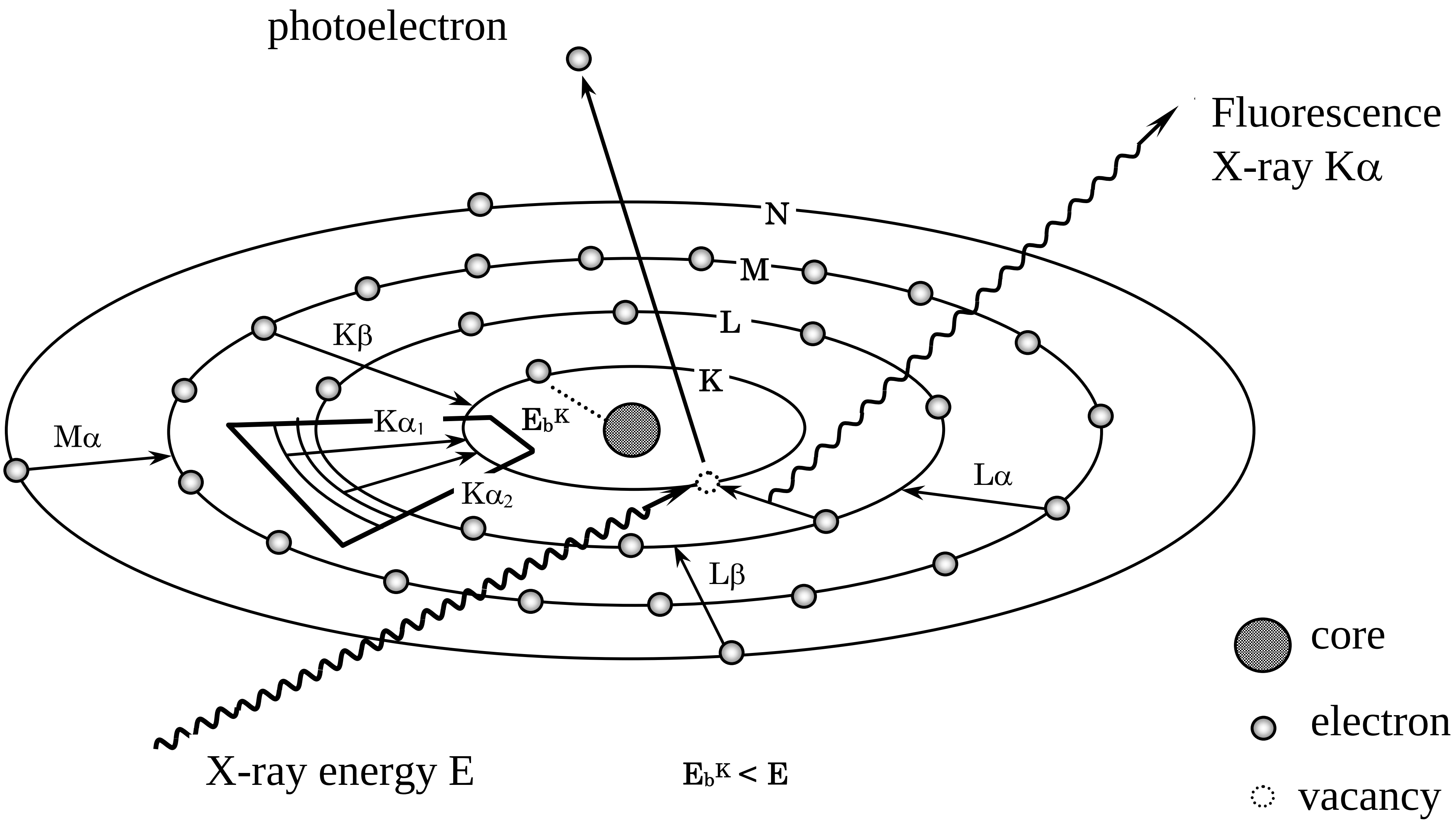

X-ray energy E > Binding energy Eb

Bohr model and emission of X-ray fluorescence

Principle of X-ray fluorescence (XRF) analysis

Energy ΔE characteristic to each element

Qualitative analysis

Intensity number of X-ray photons → concentration

Quantitative analysis

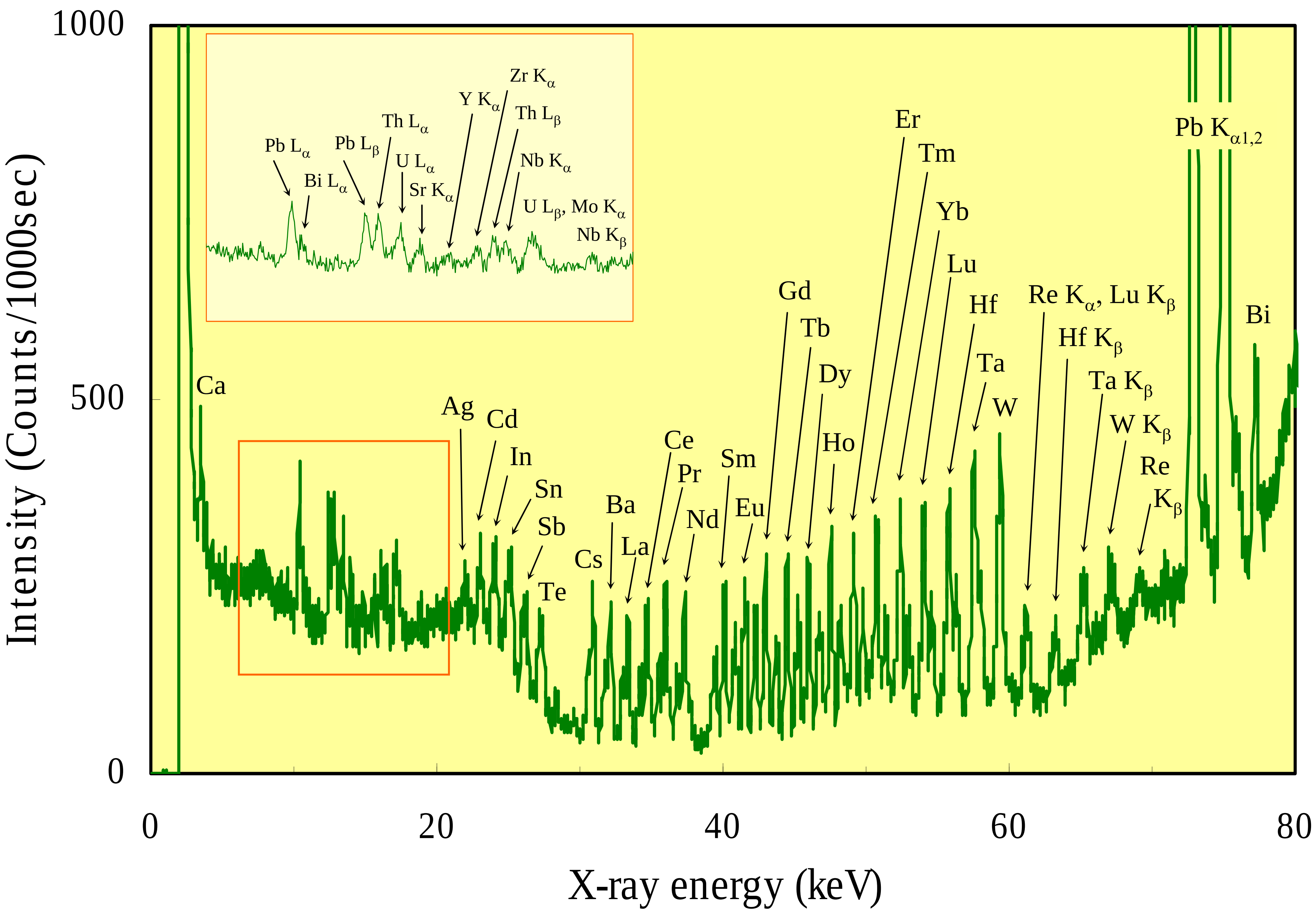

XRF spectrum of NIST SRM612 glass

d-spacing

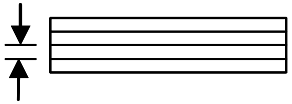

Analyzing crystal

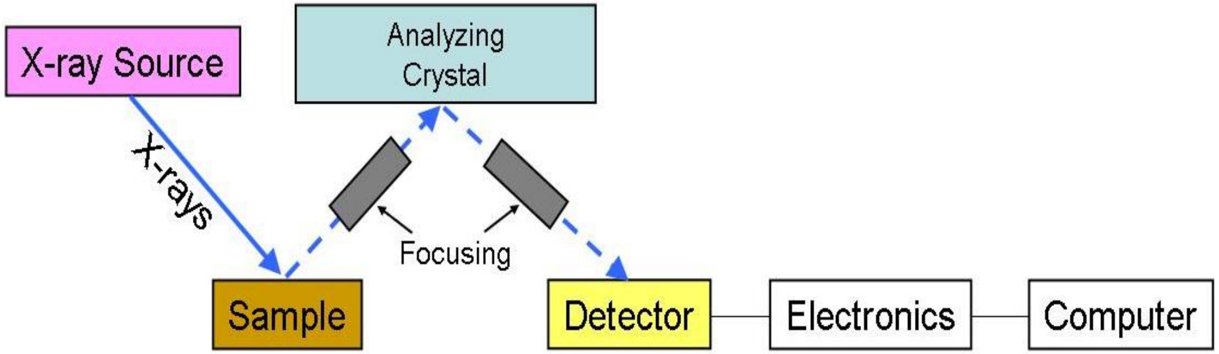

(a) WDS

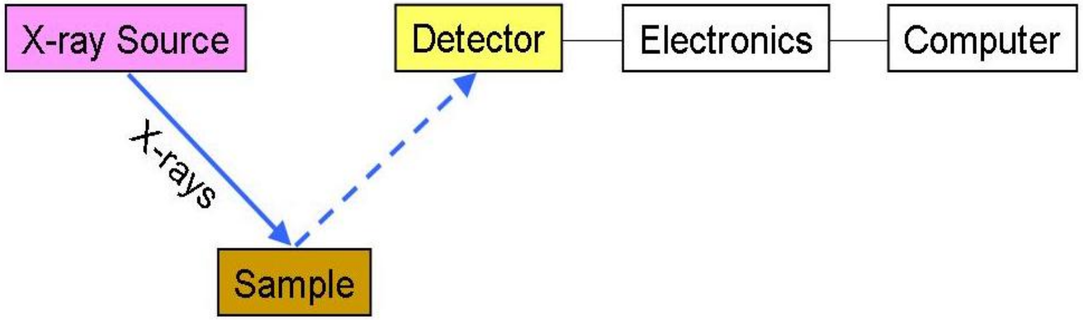

(b) EDS

XRF analysis

(a) Wavelength dispersive spectroscopy

(b) EDS Energy dispersive spectroscopy

©http://www.postech.ac.kr/dept/mse/axal/index.html

Principle of analyzing crystal

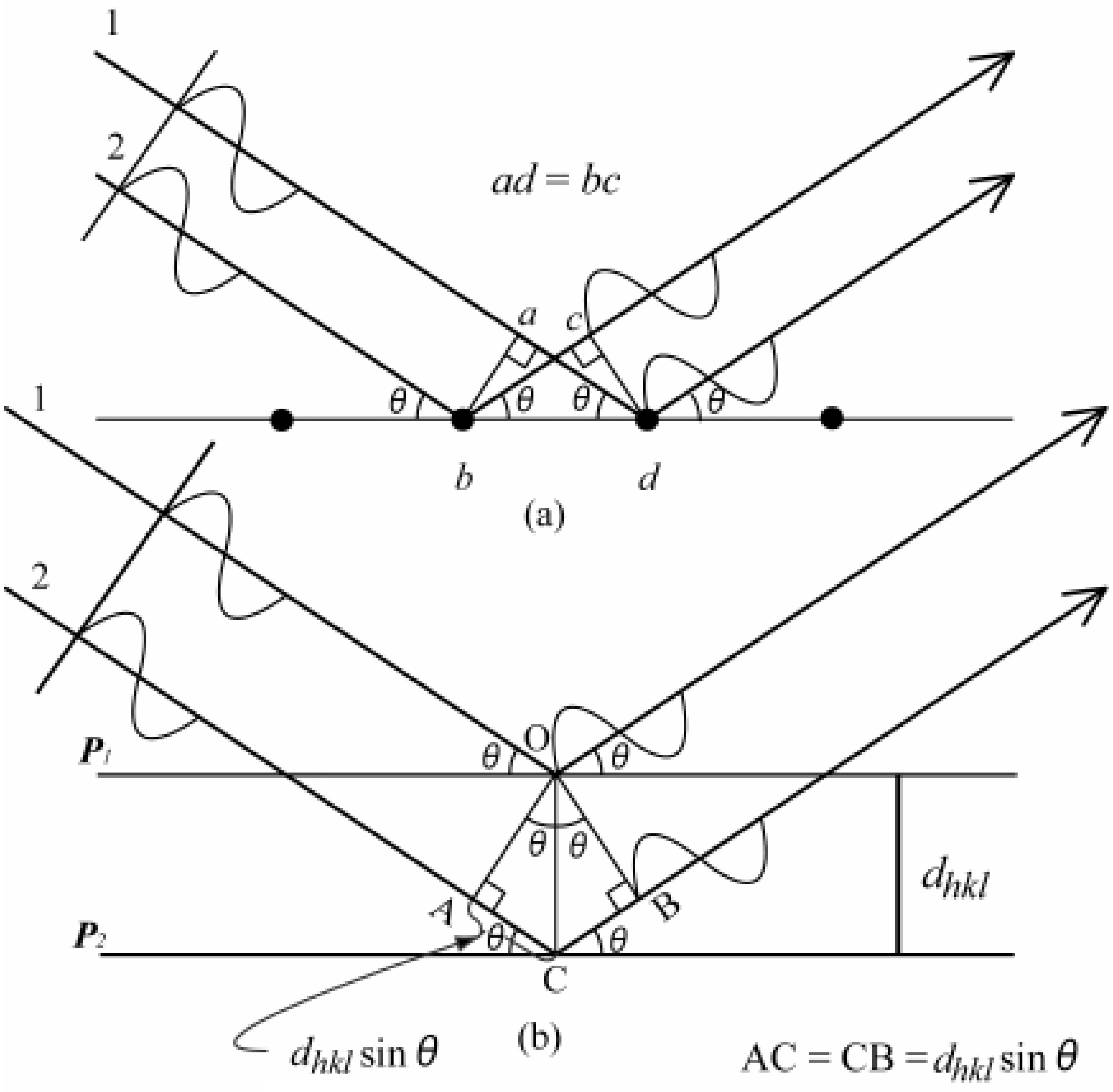

Bragg condition $n\lambda = 2d\sin\theta$

5.1 X-ray Fluorescence Analysis

Commonly used analyzer crystal: LiF, ADP (ammonium dihydrogen phosphate), Ge, graphite, InSb, PE (*tetrakis*-(hydroxymethyl)-methane: penta-erythritol), KAP (potassium hydrogen phthalate), RbAP (rubidium hydrogen phthalate) and TIAP (thallium(I) hydrogen phthalate). In addition, synthetic multilayer is used to detect the light elements in the range Li to Mg.

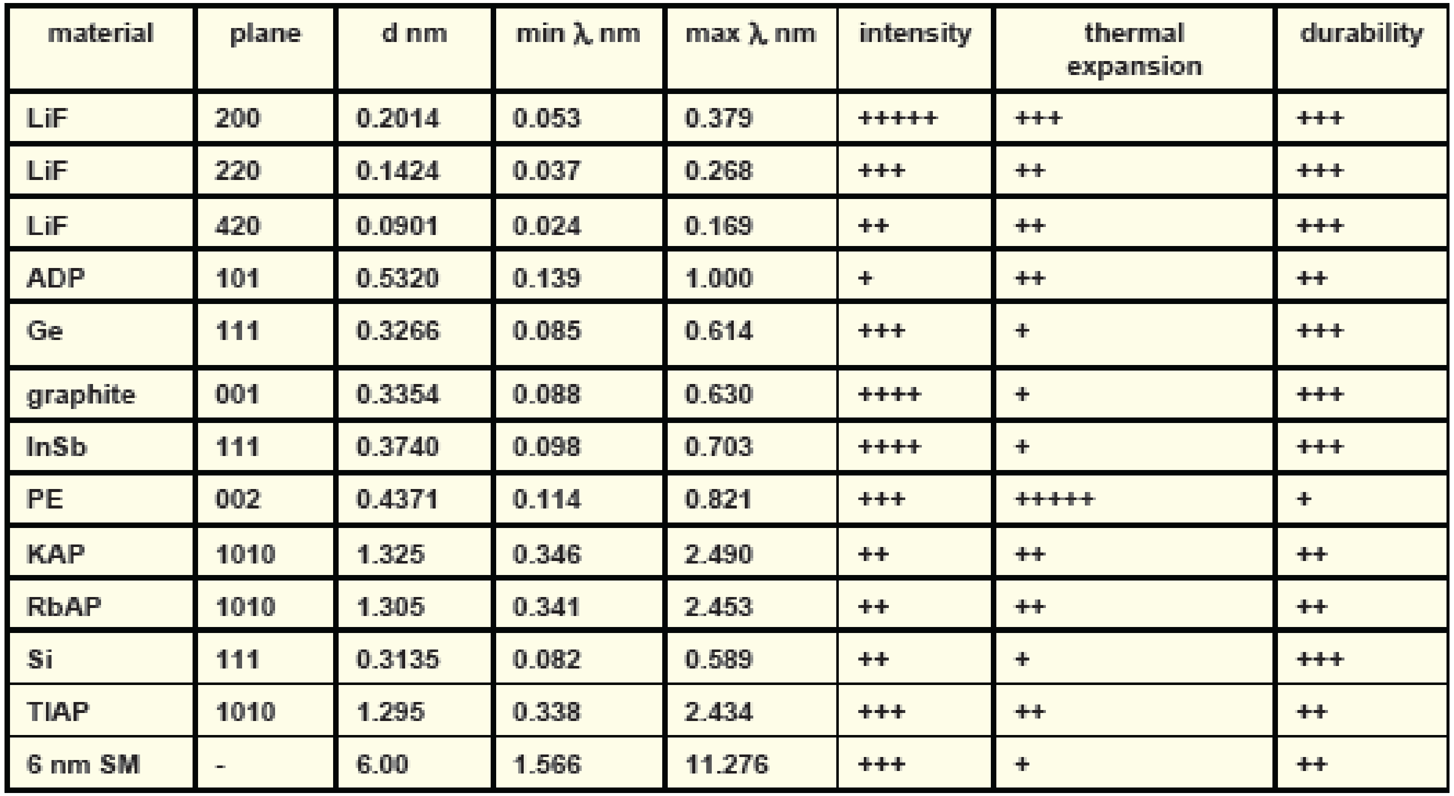

material	plane	d nm	min λ nm	max λ nm	intensity	thermal expansion	durability
LiF	200	0.2014	0.053	0.379	+++++	+++	+++
LiF	220	0.1424	0.037	0.268	+++	++	+++
LiF	420	0.0901	0.024	0.169	++	++	+++
ADP	101	0.5320	0.139	1.000	+	++	++
Ge	111	0.3266	0.085	0.614	+++	+	+++
graphite	001	0.3354	0.088	0.630	++++	+	+++
InSb	111	0.3740	0.098	0.703	++++	+	+++
PE	002	0.4371	0.114	0.821	+++	+++++	+
KAP	1010	1.325	0.346	2.490	++	++	++
RbAP	1010	1.305	0.341	2.453	++	++	++
Si	111	0.3135	0.082	0.589	++	+	+++
TIAP	1010	1.295	0.338	2.434	+++	++	++
6 nm SM	-	6.00	1.566	11.276	+++	+	++

Principle of Si(Li) detector → a reverse-biased silicon diode.

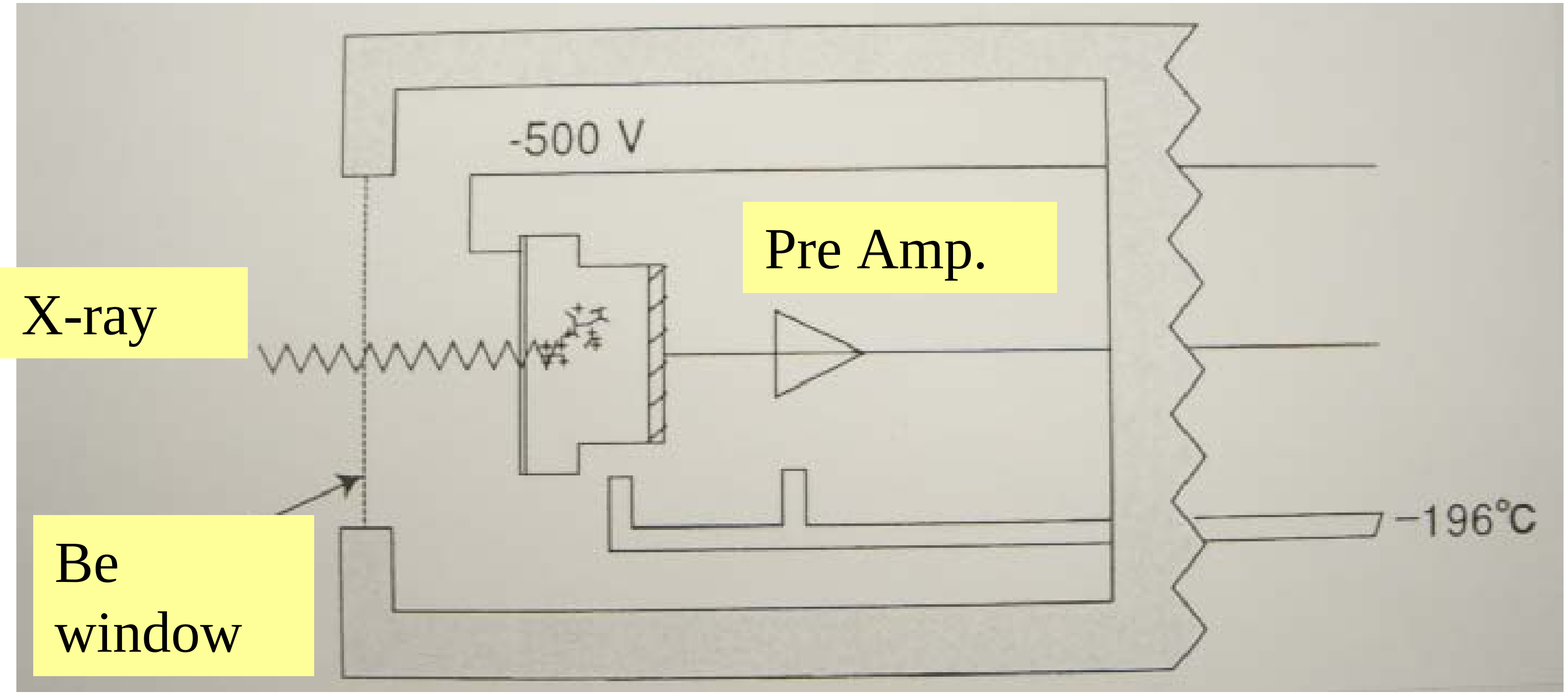

Si(Li) detector electron-hole pair 3.85eV

ex. Fe Kα 6.400keV 6400/3.85=1662 pairs

Bias voltage(-500V) cause current flow. The charge collected at the anode is converted to a voltage by an amplifier. This results in a voltage pulse that is proportional to the number of pairs created and thus to the incident X-ray energy. The resolution is determined by the energy required to create an electron-hole pair (3.8 eV).

Slides made by Prof. A. Iida (PF)

Energy Dispersive Mode vs. Wavelength Dispersive Mode

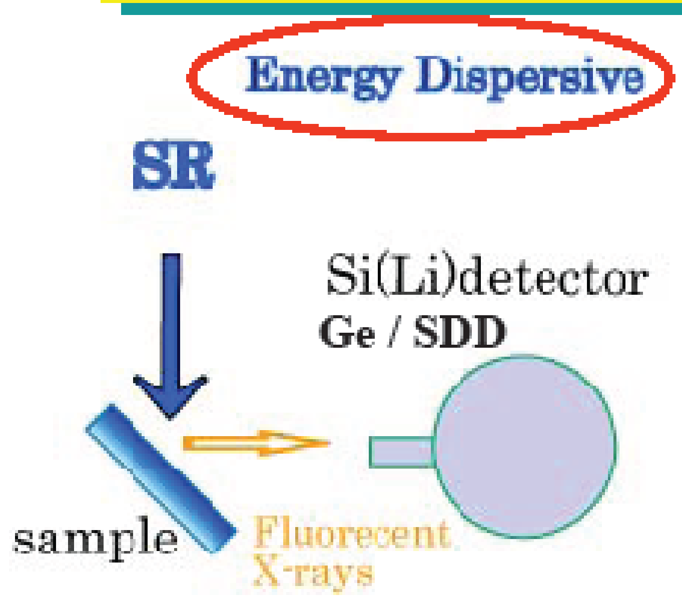

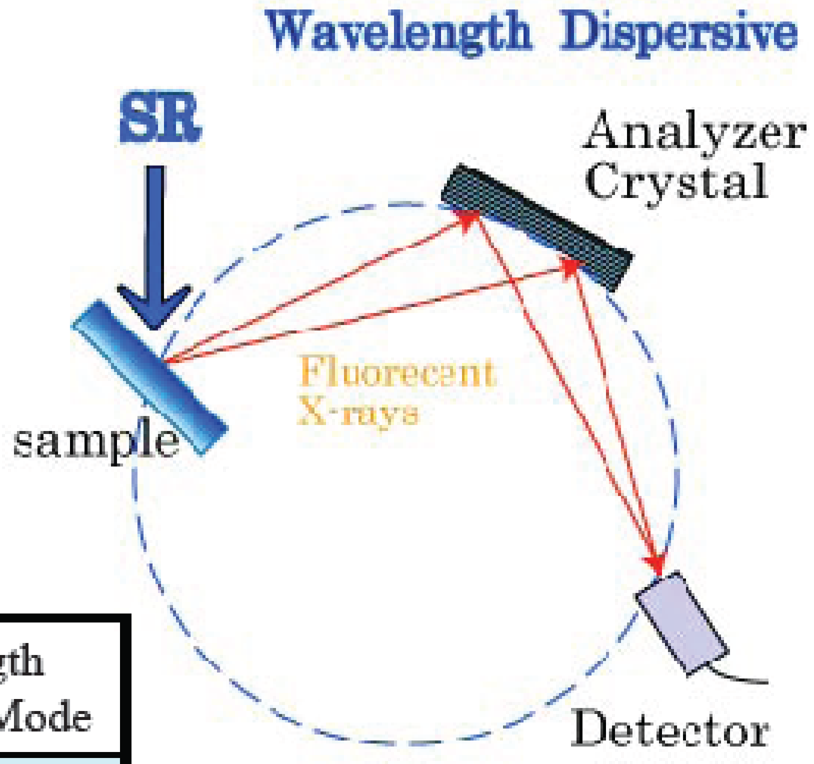

	Energy Dispersive Mode	Wavelength Dispersive Mode
Advantage	•High Efficiency •Multi-elemental detection	•High resolution •High S/B
Disadvantage	•Low resolution •Scattering background	•Low efficiency

Characteristics of SR-XRF
(X-ray fluorescence analysis)

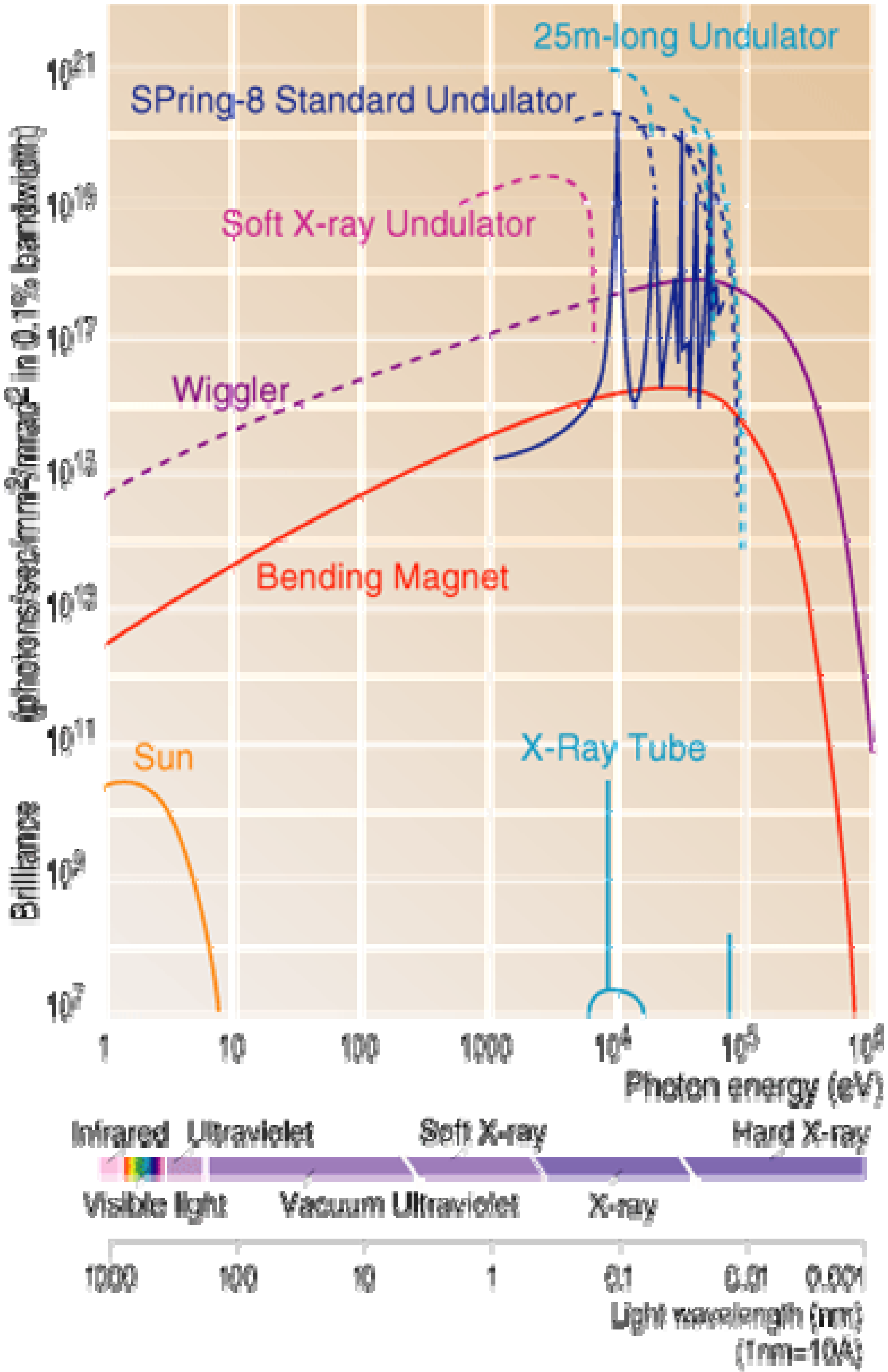
25m-long Undulator
SPring-8 Standard Undulator
Soft X-ray Undulator
Wiggler
Bending Magnet
Sun
X-Ray Tube
Brilliance (photons/sec/mm^2/mrad^2 in 0.1% bandwidth)
10^{21}
10^{19}
10^{17}
10^{15}
10^{13}
10^{11}
10^{9}
10^{7}
1
10
100
1000
10^4
10^5
10^6
Photon energy (eV)
Infrared
Ultraviolet
Soft X-ray
Hard X-ray
Visible light
Vacuum Ultraviolet
X-ray
1000
100
10
1
0.1
0.01
0.001
Light wavelength (nm)
(1nm=10Å)

Synchrotron radiation excited XRF
-SRXRF-

Advantages of conventional XRF

- Nondestructive
- Multi-elemental analysis
- Wide dynamic range
  major ~ trace
- High accuracy
- User-friendly instruments
- Easy to analyze

Advantages of SRXRF

- **High sensitivity**
  ng=>fg, ppm=>ppb
- **Chemical state analysis**
- **Micro-beam analysis**
  mm => µm
- **Total reflection analysis**
  10^{15}atoms/cm^2
  => 10^8atoms/cm^2

SR Properties and SRXRF

1) High Brilliance Source
(small size and high collimation X-ray source)

strong intensity (high density) =>**signal enhancement**
high collimation =>**micro beam analysis (focusing optics)**
=>**total reflection XRF**

2) Linear polarization
(p polarization + 90° arrangement) => **background reduction**

3) White (bending magnet), quasi-monochoromatic (Undulator) X-rays
monochoromatic X-rays => **background reduction**
(monochromator) => **selective excitation**
(S/B optimization / Resolving overlapping peak)
continuous energy scanning =>**XAFS**
(Chemical state analysis)

4)High and low energy X-ray excitaiton
=>**heavy & light trace elements analysis**

Selective Excitation :

Resolving overalpping peaks: PbLα vs. As Kα Case

As Kedge < PbL3 edge <E_0

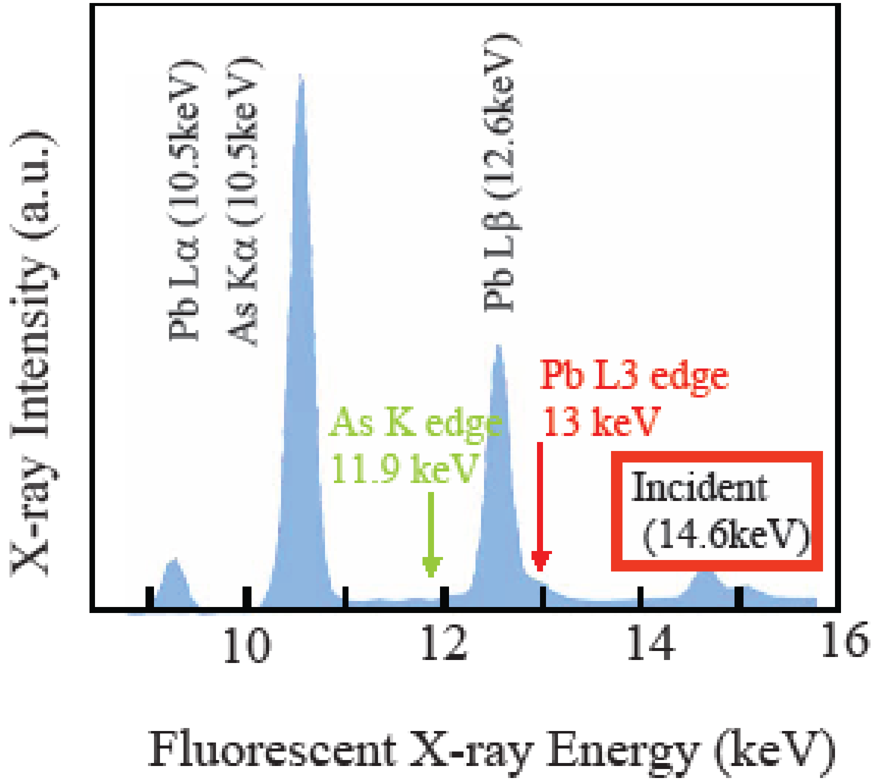

As Kedge <E_0< PbL3 edge

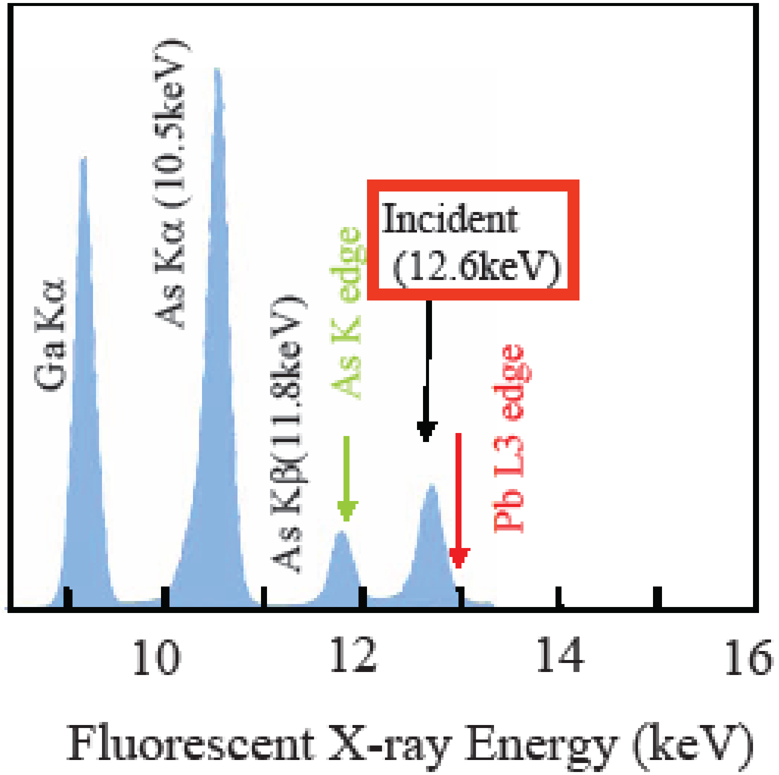

Both As K and Pb L are excited.

As K series alone is excited.
=>As quantification becomes possible.

（1）High Brilliance Source

Wavelength Dispersive Technique

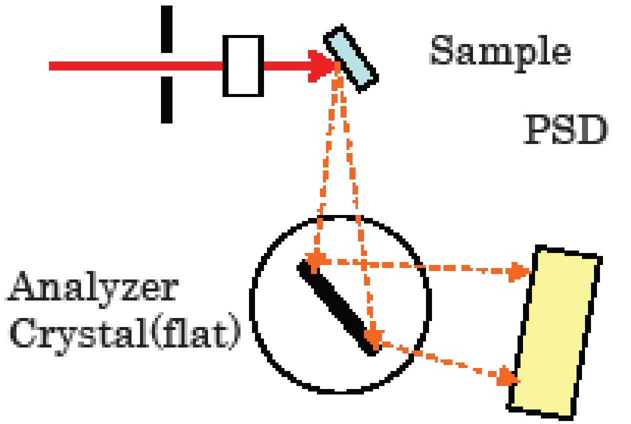

Multi-elemental geometry

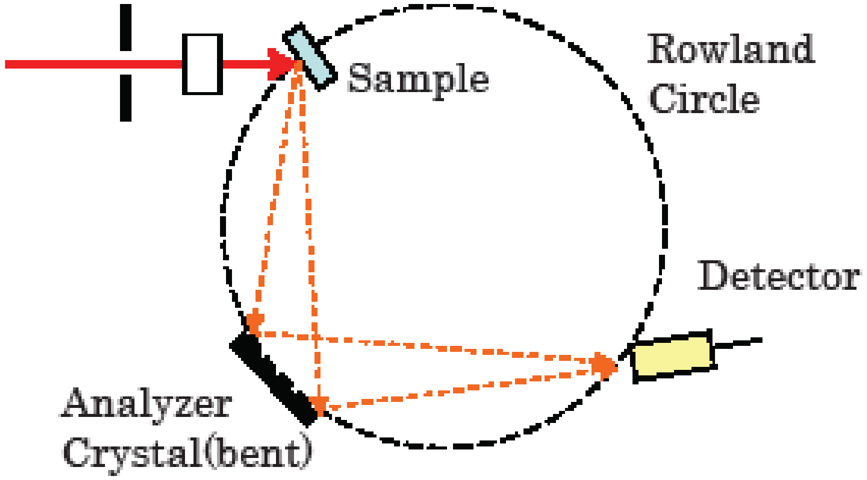

Focusing geometry

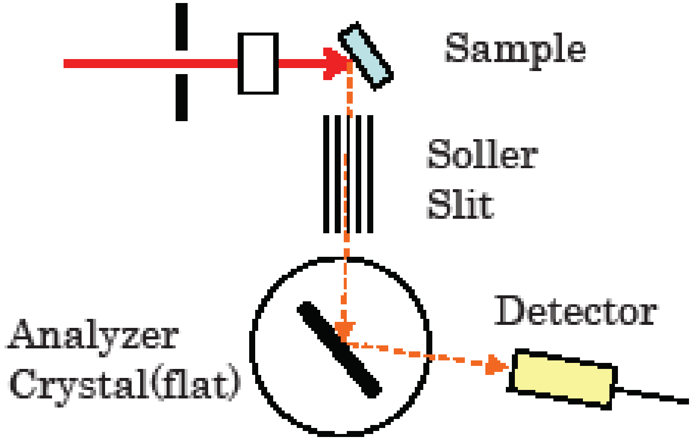

θ-2θ geometry

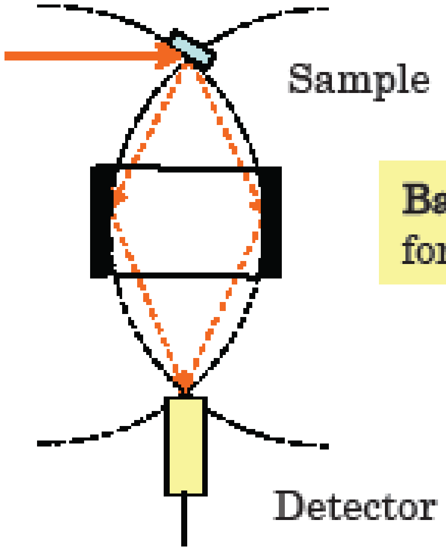

Barrel type Crystal
for 2D focusing

TXRF for Ultra Trace Element Analysis

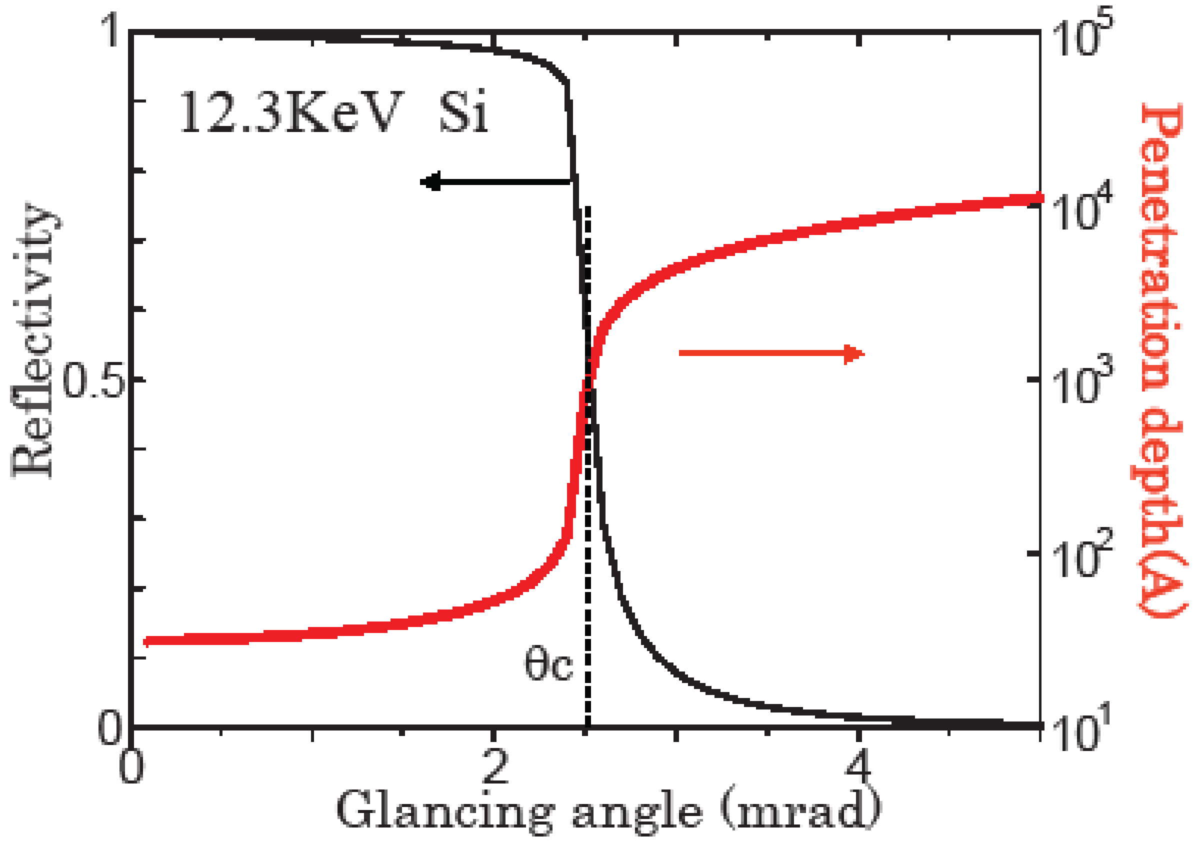

Extremely Shallow Penetration Depth

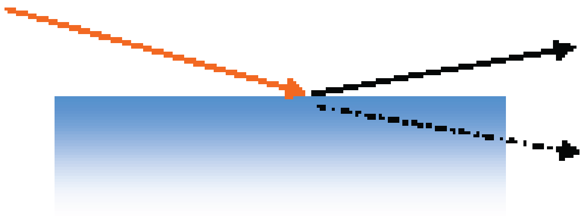

Total Reflection of X-rays
at a flat and smooth surface
(Si wafer, optical flat .....)

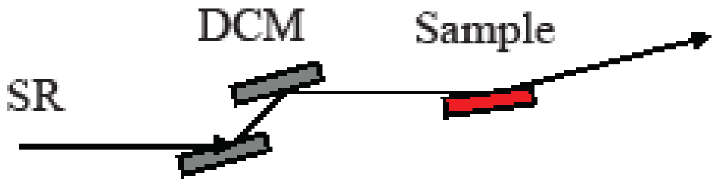

Total-Reflection X-ray fluorescence analysis
Ultra trace element analysis (TXRF)

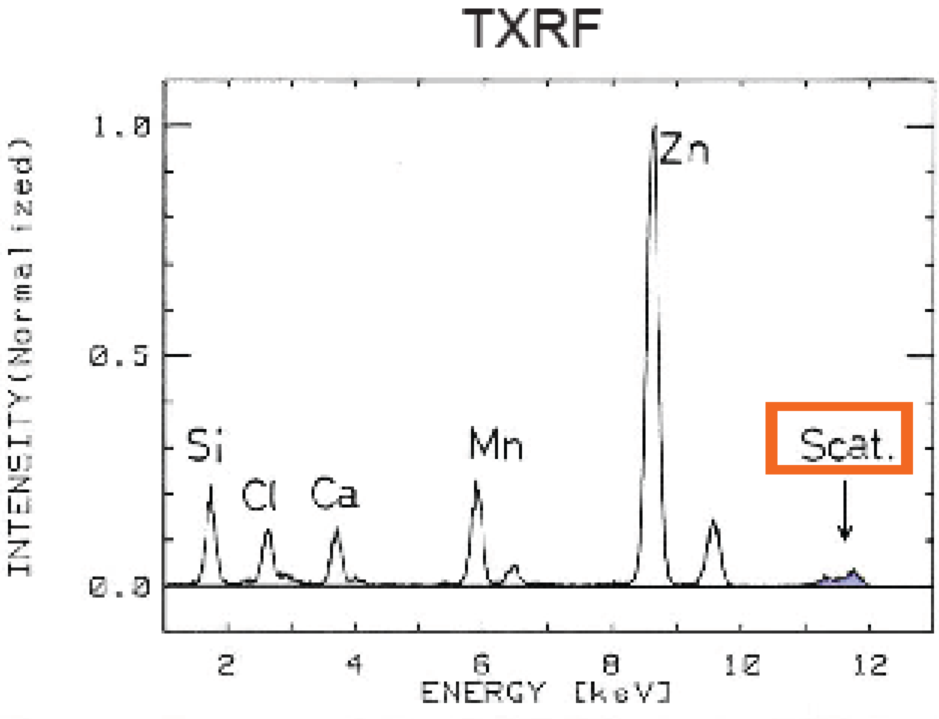

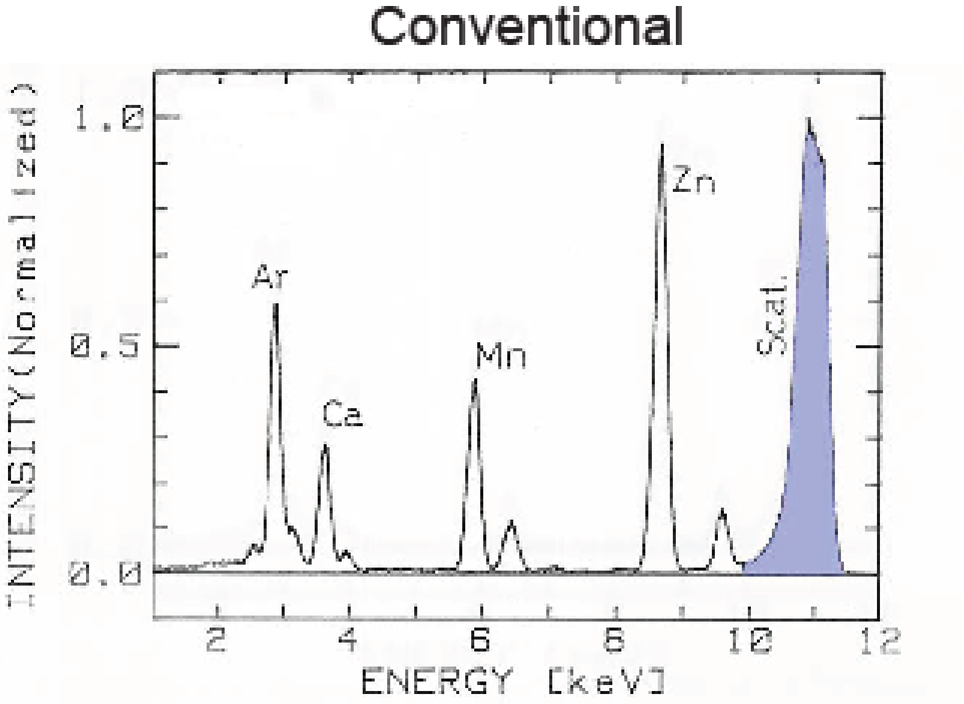

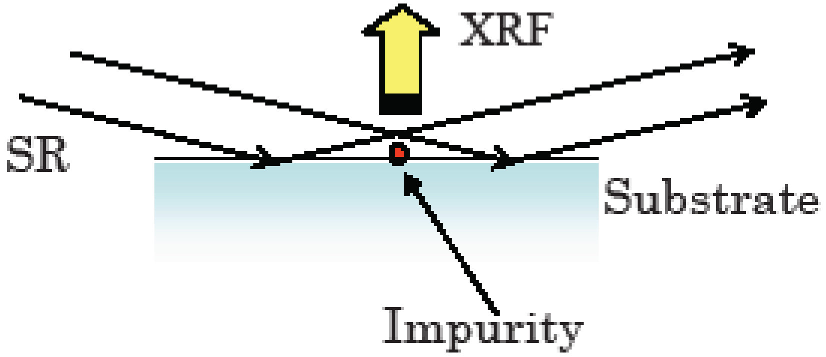

Si wafer

10^{15}atoms/cm^2=>10^8atoms/cm^2

TXRF Experiments at Beamline 40XU, SPring-8

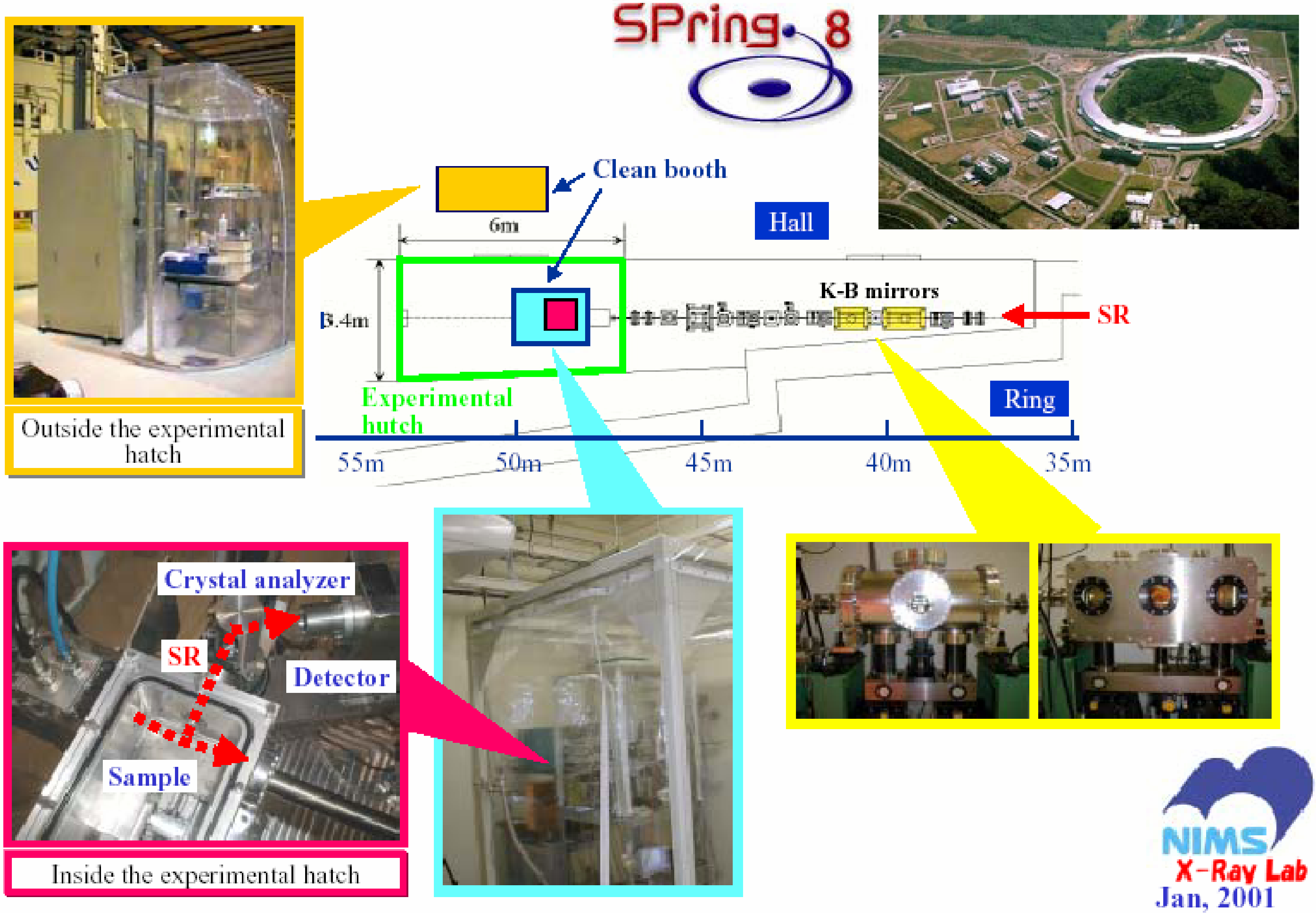

Outside the experimental hatch

Inside the experimental hatch

NIMS X-Ray Lab
Jan, 2001

©K. Sakurai(NIMS)

WD-TXRF Spectra for Trace Elements in Micro Drop

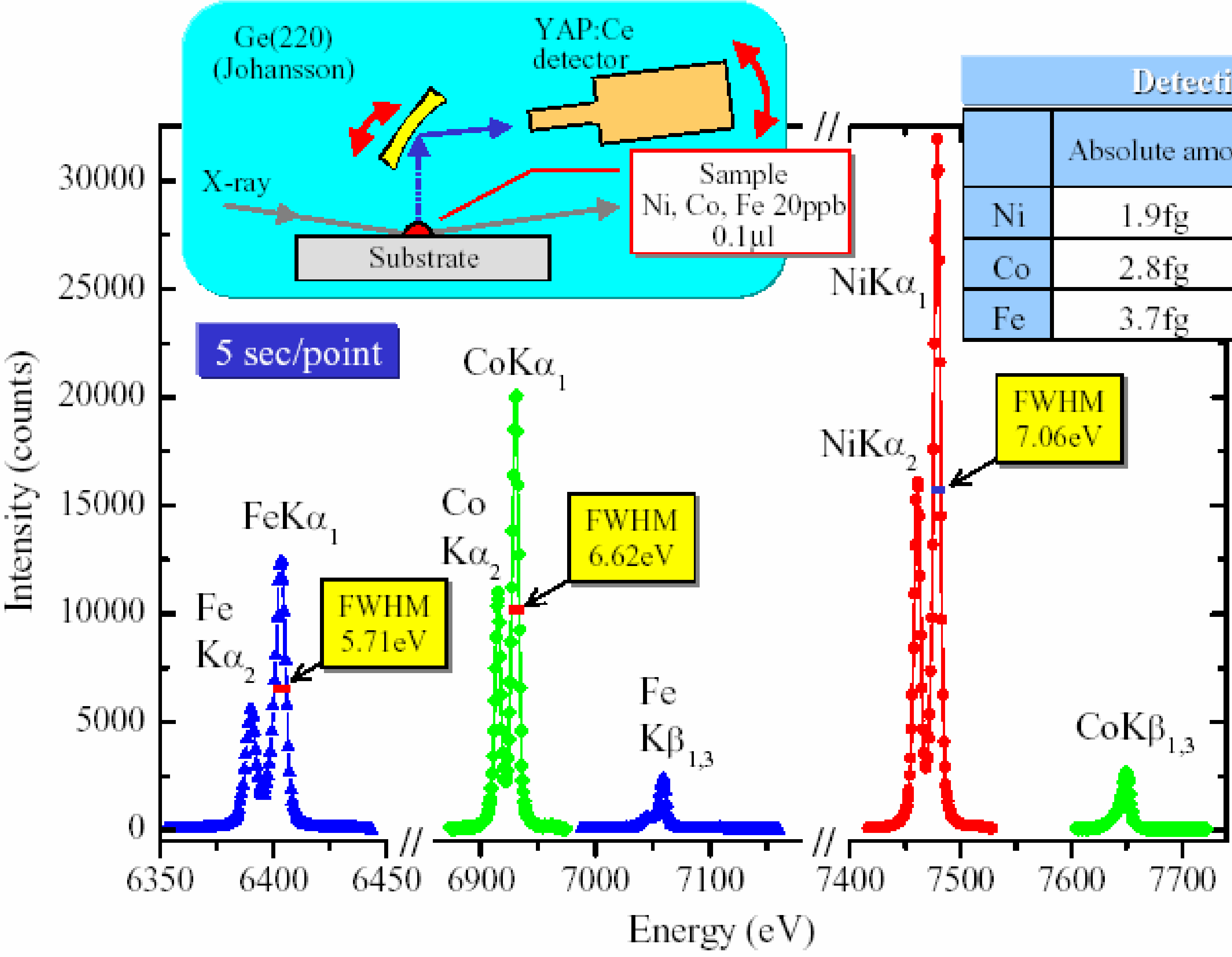

Detection limit		
	Absolute amount	Concentration of solution of 0.1μl
Ni	1.9fg	19ppt
Co	2.8fg	28ppt
Fe	3.7fg	37ppt

NIMS
X-Ray Lab
Jan, 2001

MDL（Minimum detection limit)

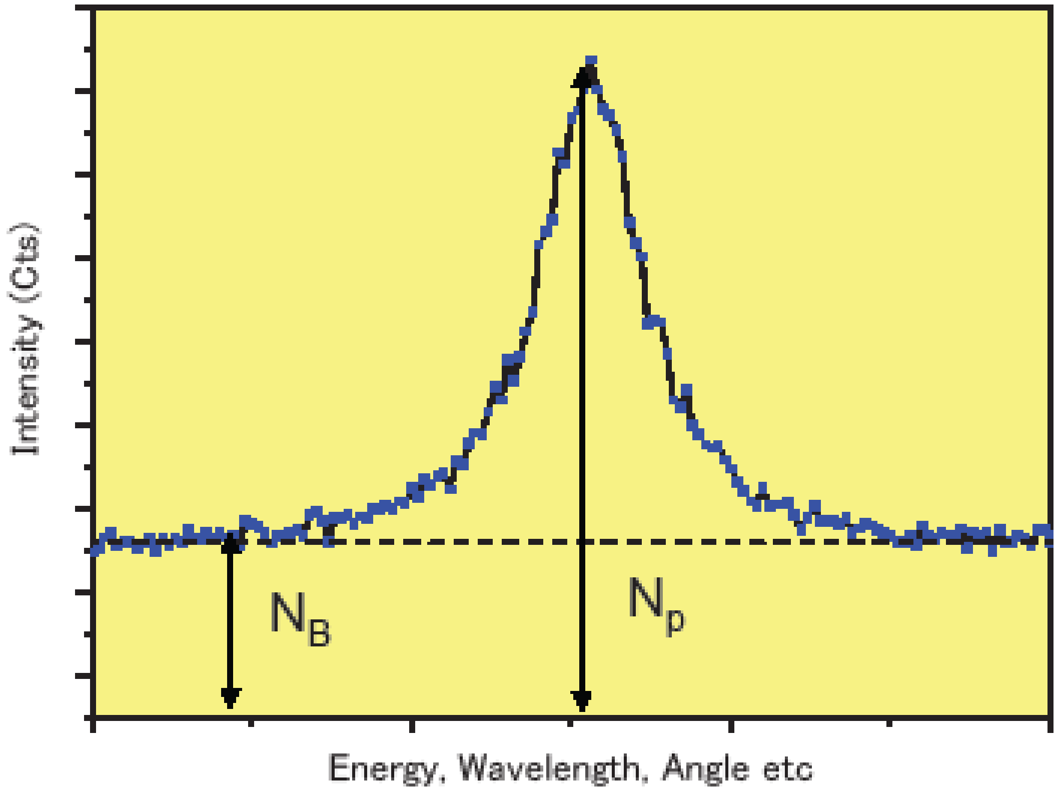

Minimum detection limit (MDL)

$$k = \frac{3C\sqrt{N_B}}{N_p - N_B}$$

Minimum quantification limit (MQL) (2k ~3.3k)

World record of MDL by total reflection SR-XRF

3.1×10^{-16}g= 0.31fg

3.1ppt(pg/g) 3×10^{6}atom

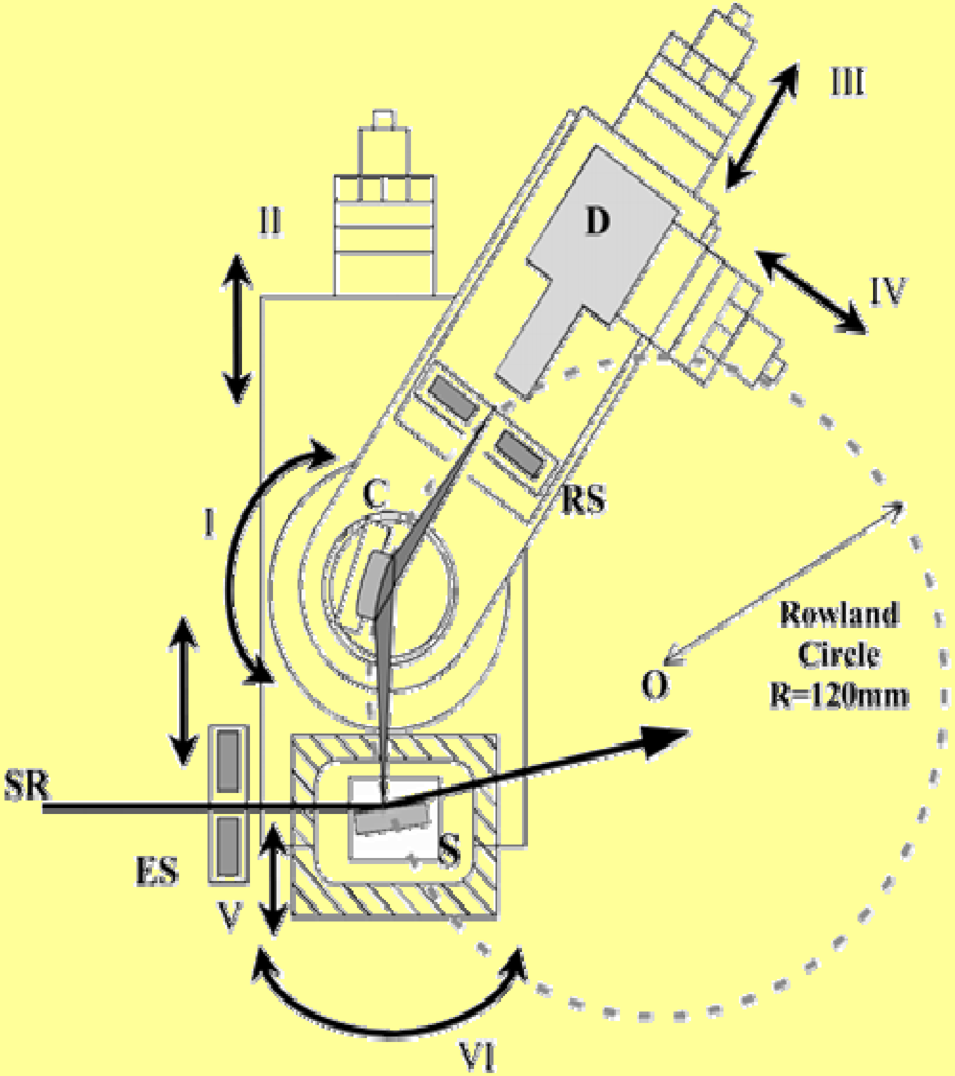

(a) Crytal monochormator

C: Ge(220)Johansson type

D:YAP:Ce scintillation counter

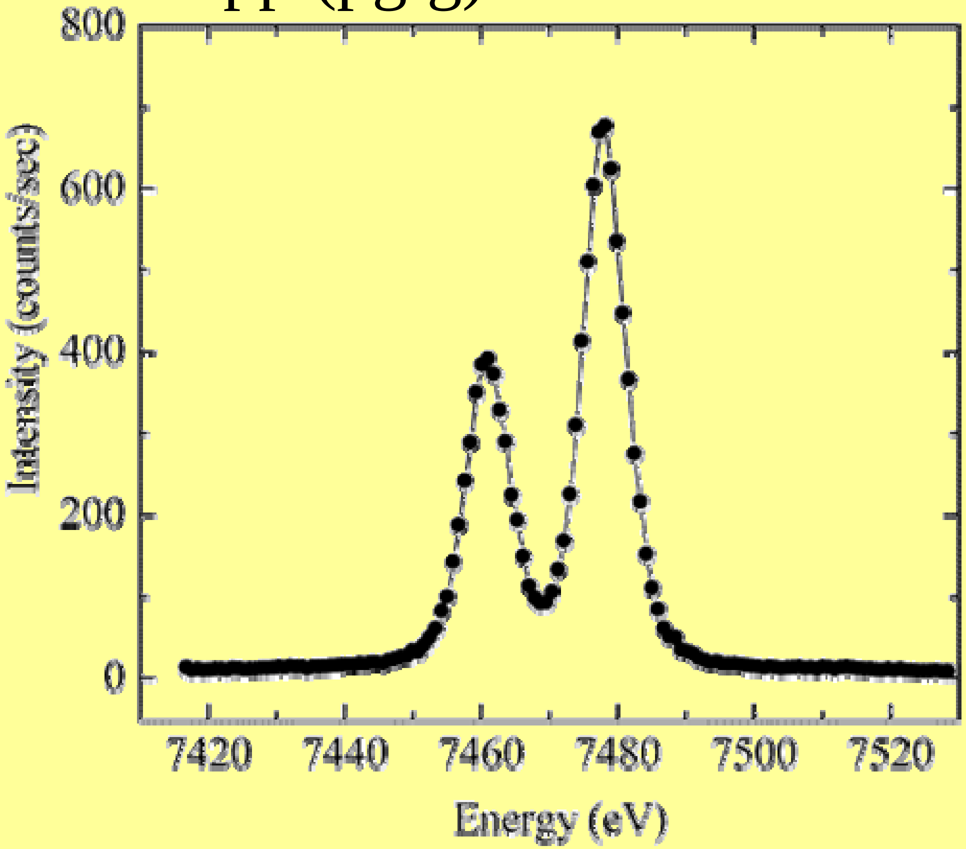

(b)XRF spectrum of 0.1ml Ni (1ng/g)solution (20s/point)

©K.Sakurai(NIMS)

Typical XRF Spectra Obtained by R=100 Spectrometer
Trace Metals in Apple and Tomato Leaves (NIST1573a and 1515)

	Mn	Fe	Co	Ni	Nd	Gd	Sm	Tb
apple	54	83	0.09	0.91	17	3	3	0.4 µg/g
tomato	246	83	0.09	0.91	-	0.17	3	0.4 mg/kg

1sec/point

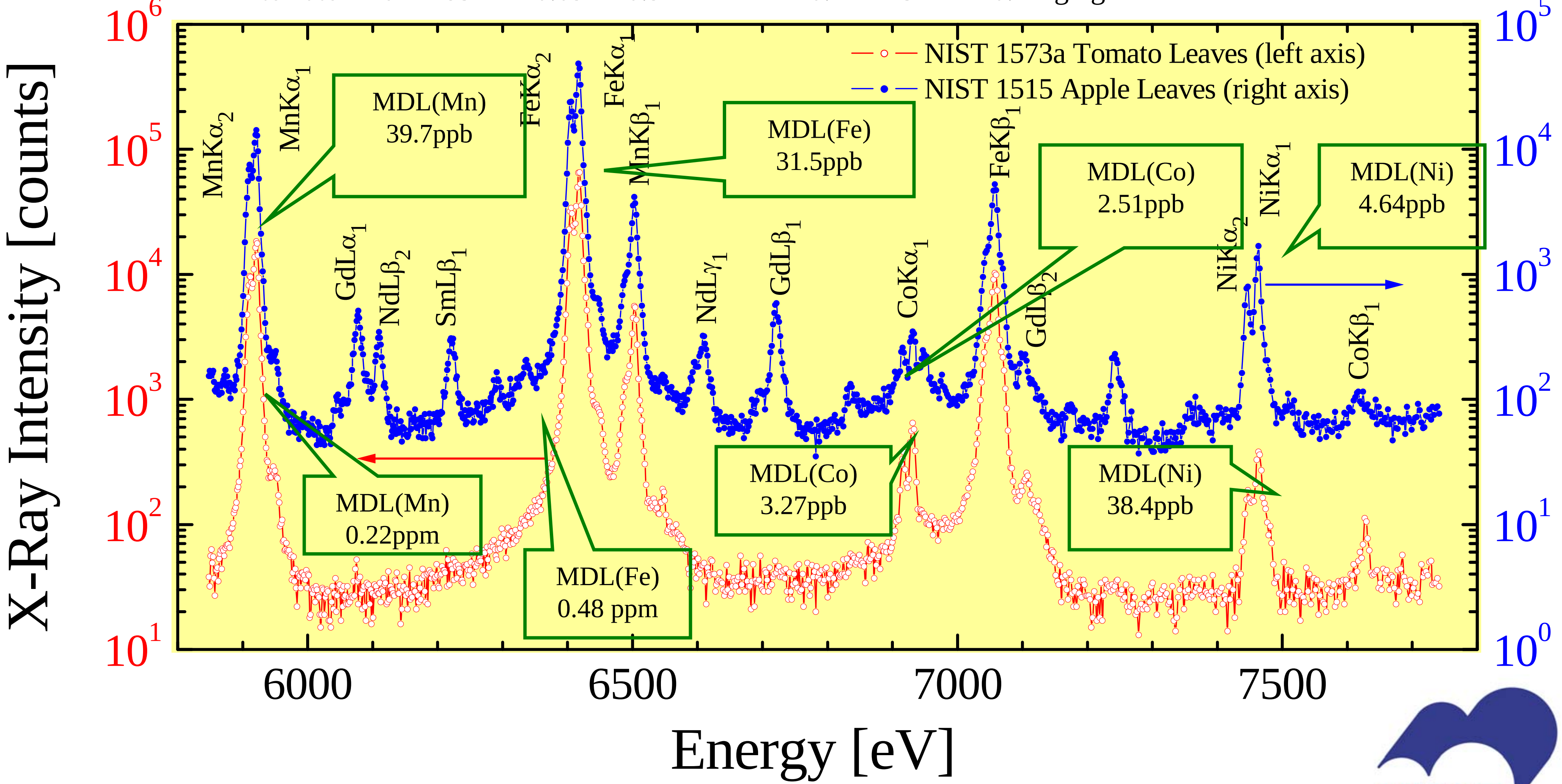

NIMS X-Ray Lab

©K. Sakurai(NIMS)

（2）parallel beam with small divergence

X-ray source and X-ray microbeam

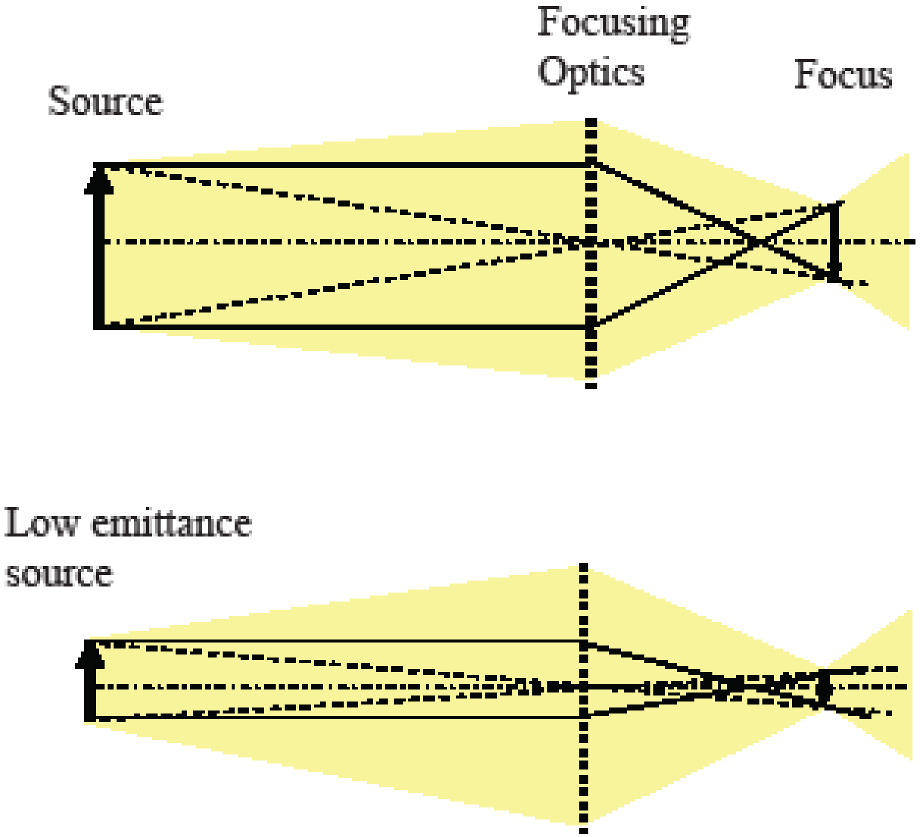

$1/a + 1/b = 1/f$ $M = b/a$

Helmhortz invariant

$y \times u = y' \times u'$

y, y' source and focus size

u, u' divergence and convergence angle

Low emittance source => small $y \times u$

Small source size and low divergence

(3rd generation ring)

⇒Smaller focus with higher intensity

⇒micro-beam to nano-beam

X-ray Focusing Elements

$n = 1 - \delta - i\beta \qquad \delta \sim 10^{-5}$

X-rays: electromagnetic wave with short wavelength

Reflection	Grazing incidence mirror
No chromatic aberration	spherical / aspherical toroidal (bent cylinder) elliptical, ellipsoidal parabolic, paraboloidal
	Capillary (single, poly)
Diffraction	Fresnel Zone plate
Energy dependence	Bragg-Fresnel lens Crystal (asymmetric reflection / bent crystal)
Refraction	Compound refractive lens

X-ray microbeam Optics

Kirkpatrick-Baez optics

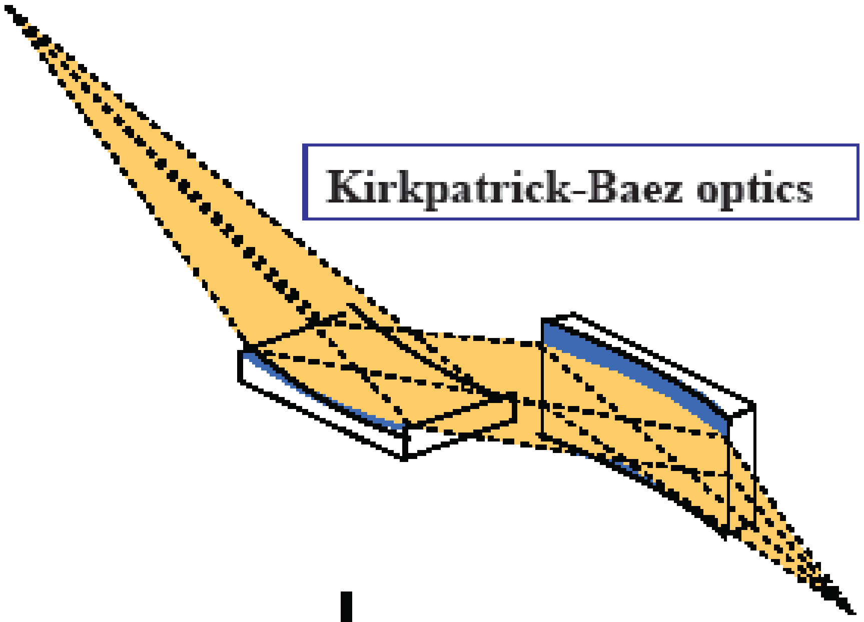

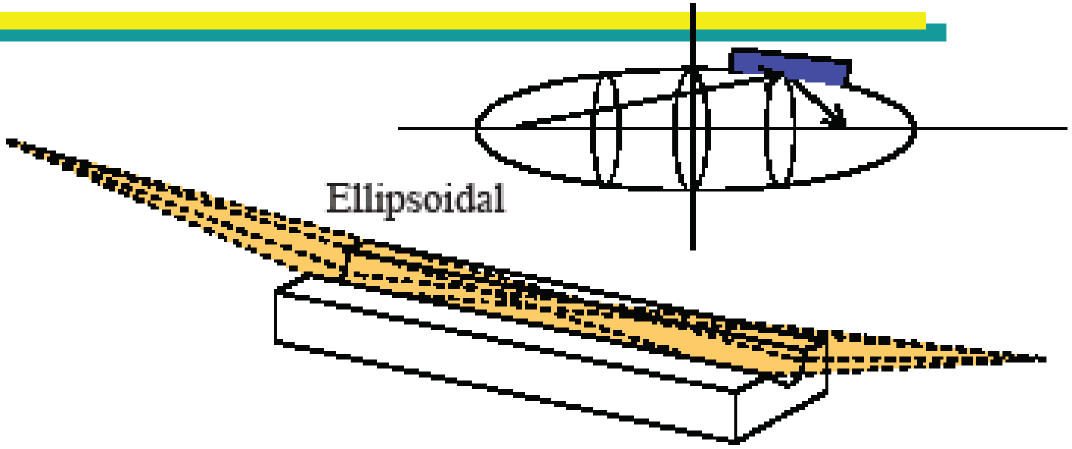

Ellipsoidal

Single tapered capillary

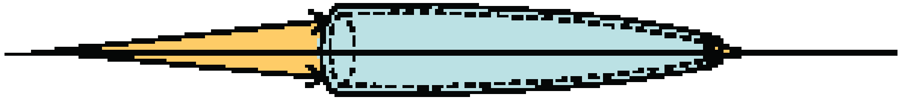

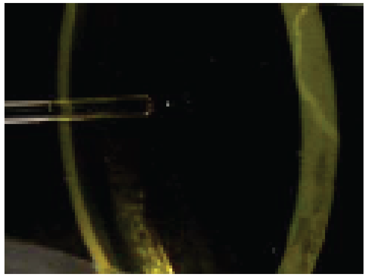

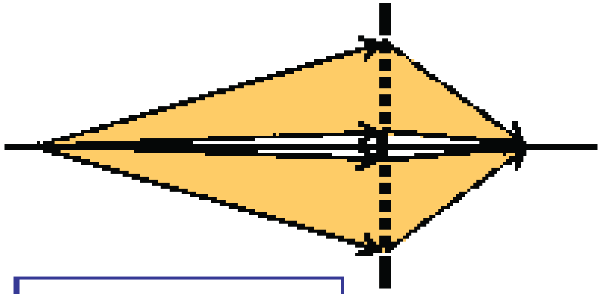

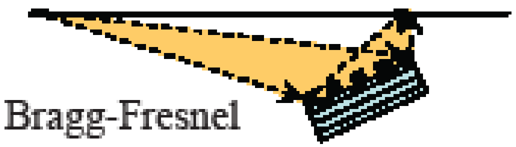

Bragg-Fresnel

Fresnel zone optics

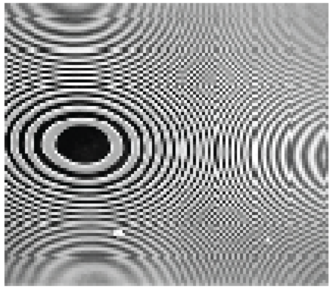

Compound refractive optics

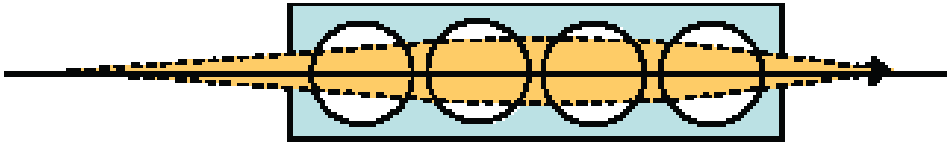

Spring-8

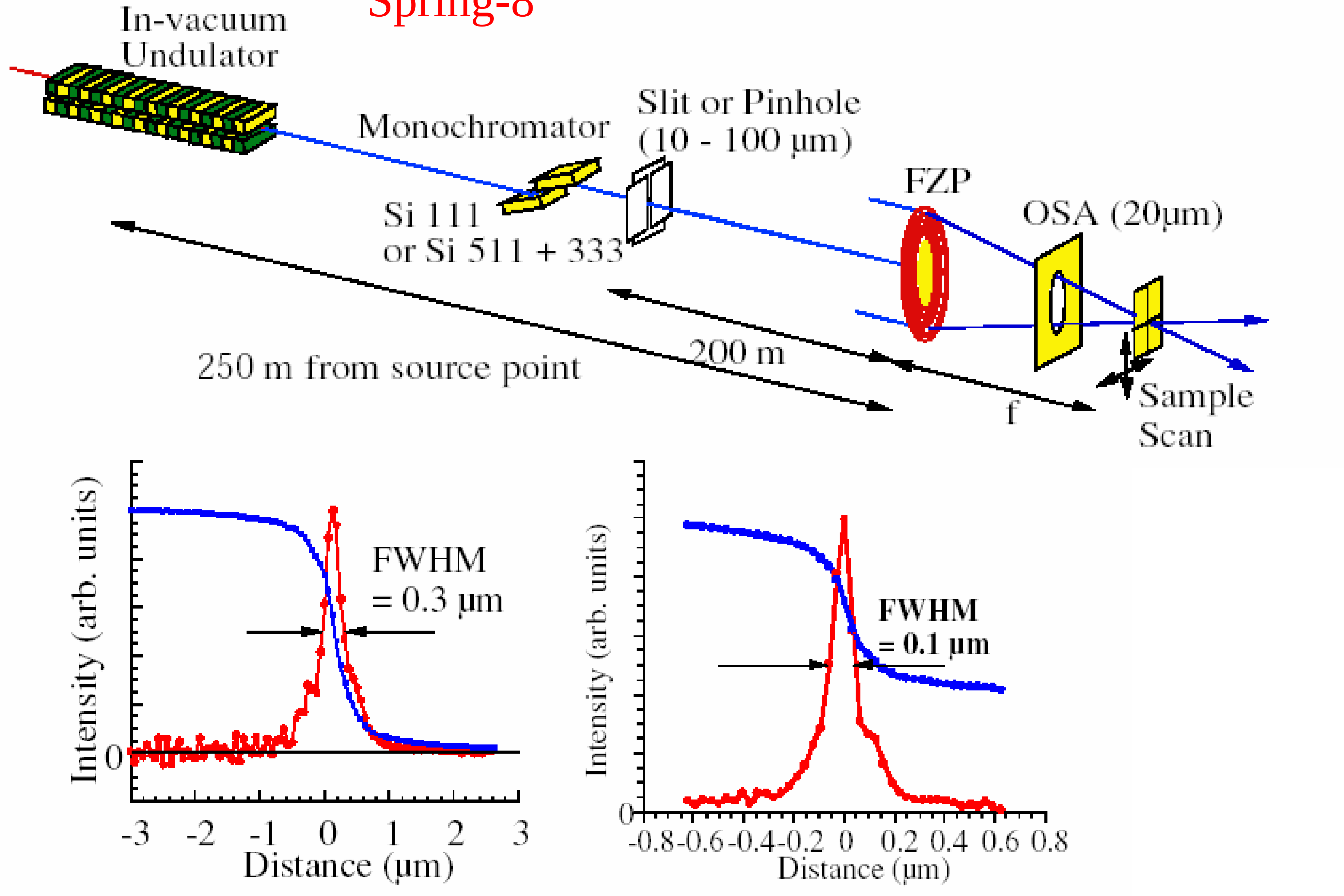

Beam profile at focal points made by FZP at 8keV

©Y.Suzuki(2002）

Application of SR-XRF to in vivo analysis of biological sample

Study of hyperaccumulator plants of As and Cd

Phytoremediation

plant

remediate

Phytoremediation is a technology that uses plants to remove, destroy, or sequester hazardous substances from the environment.

Green technology by plant

Merit : no damage, low cost
preservation of surface
etc...

Some specific kinds of plants are known to be heavy metal hyperaccumulator

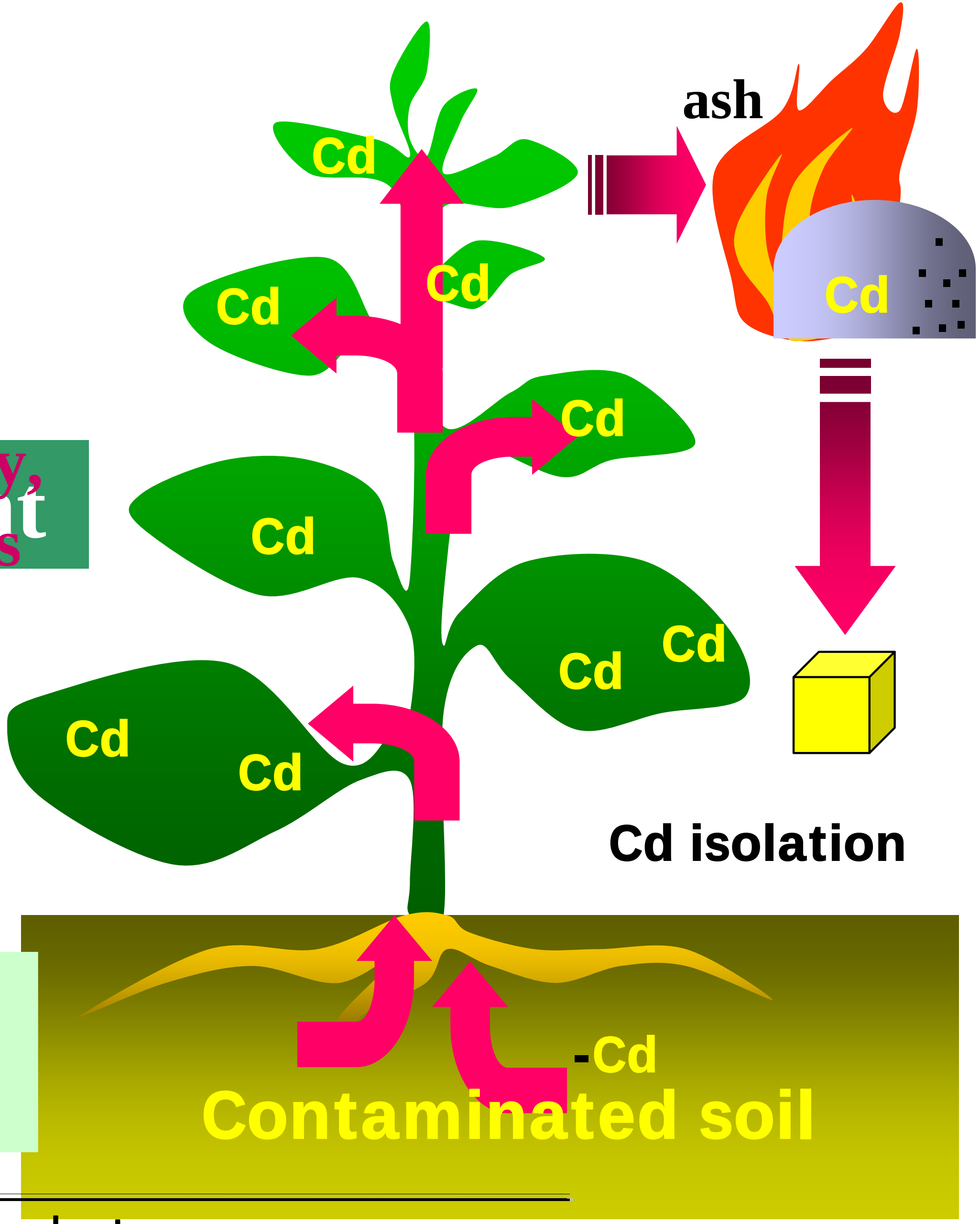

Element	conc./ ppm	plant
As[*1]	22,630	*Pteris vittata L.*(モエジマシダ)
Cd	11,000	*Athyrium yokoscense*（ ヘビノネゴザ）
Pb	34,500	*Brassica juncea* (カラシナ)

[*1] L. Q. Ma, et al., *Nature*, (2001) , **409**, 579.

Phytoremediation

Environmentally friendly low cost technique

Key:Use of hyperaccumulator plant

As

Arsenic Hyperaccumulator
Pteris vitteta L.
(モエジマシダ）

Cd

Cd Hyperaccumulator
Arabidopsis halleri ssp.*gemmifera*
（ハクサンハタザオ）

Hyperaccumulation

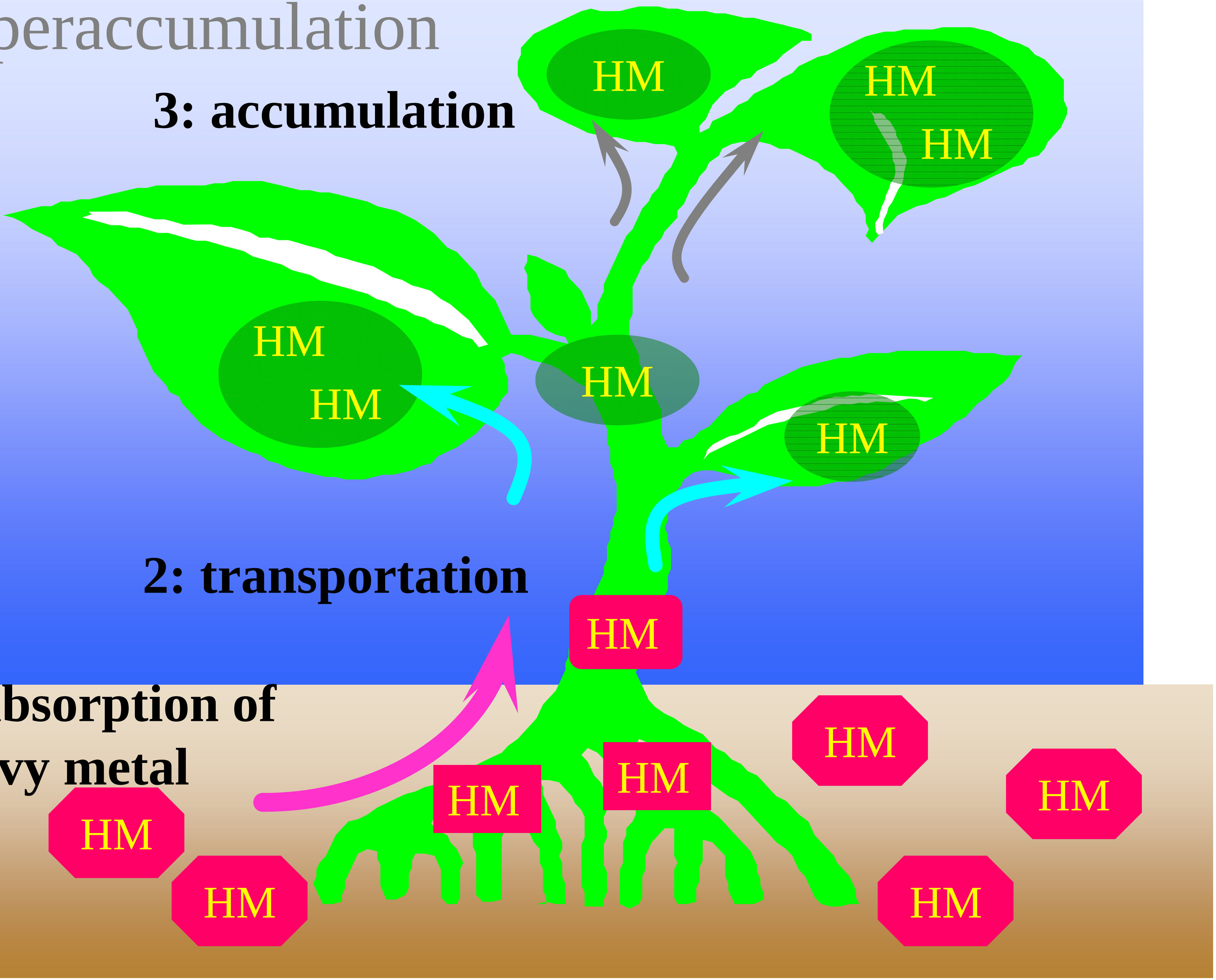

3: accumulation

2: transportation

1: absorption of heavy metal

Application of SR X-ray analyses

- Two dimensional multi-element nondestructive analysis in cell level
  → μ-XRF imaging

- in vivo chemical state analysis of metals in the plant
  → X-ray absorption fine structure (XAFS) analysis

- chemical state analysis in cell level
  → μ-XANES

As hyperaccumulator

Chinese brake fern (*Pteris vittata* L.)

(As: *ca.* 22,000 μ g /g dry weight)

Arsenic distribution and speciation in an arsenic hyperaccumulator fern by X-ray spectrometry utilizing a synchrotron radiation source
A. Hokura, R. Onuma, Y. Terada, N. Kitajima, T. Abe, H. Saito, S. Yoshida and I. Nakai
Journal of Analytical Atomic Spectrometry, 21, 321-328 (2006)

Life of fern

Pteris vittata L.

frond

sporophyte

fertilized

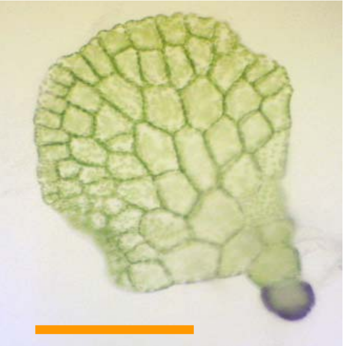

prothallium

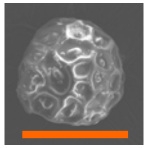

spore

Fertile pinna

Cultivation of fern

arsenic-contaminated soil

As level in soil：481 μg g^{-1}dry

Term： ～3 weeks

Average As level ：～720 μg /gdry

culture medium containing As (1 ppm 4days)

As level*

pinna：2800 - 4500 μg g^{-1}dry

midrib of a frond：84 - 250 μg /g dry

* Anal. By AAS

Sample preparation for microbeam analysis

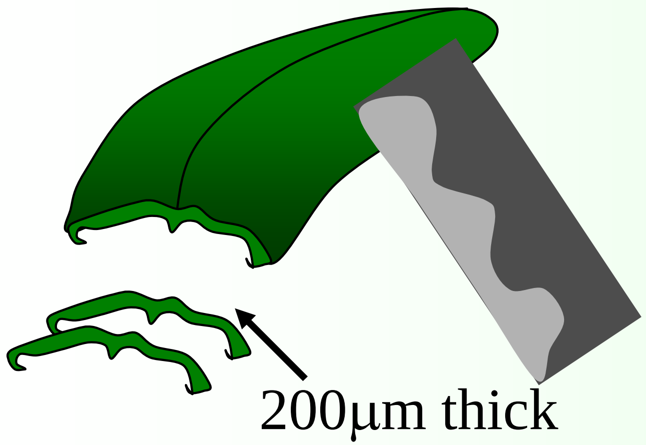

vertical slicer (Model HS-1, JASCO Co.)

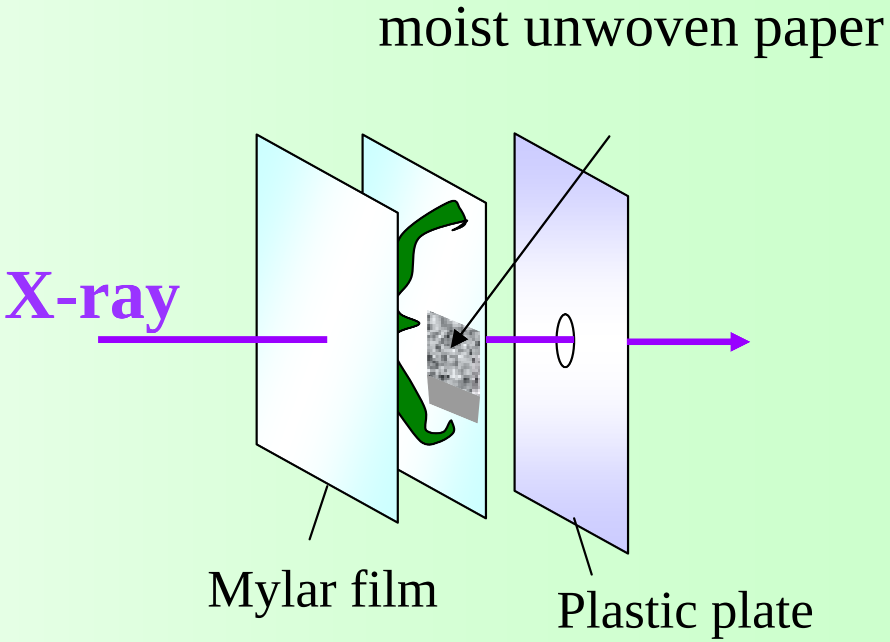

freeze dry of frozen

μ-XRF, μ-XANES

X-ray energy

As: 12.8keV

Cd: 37.0keV

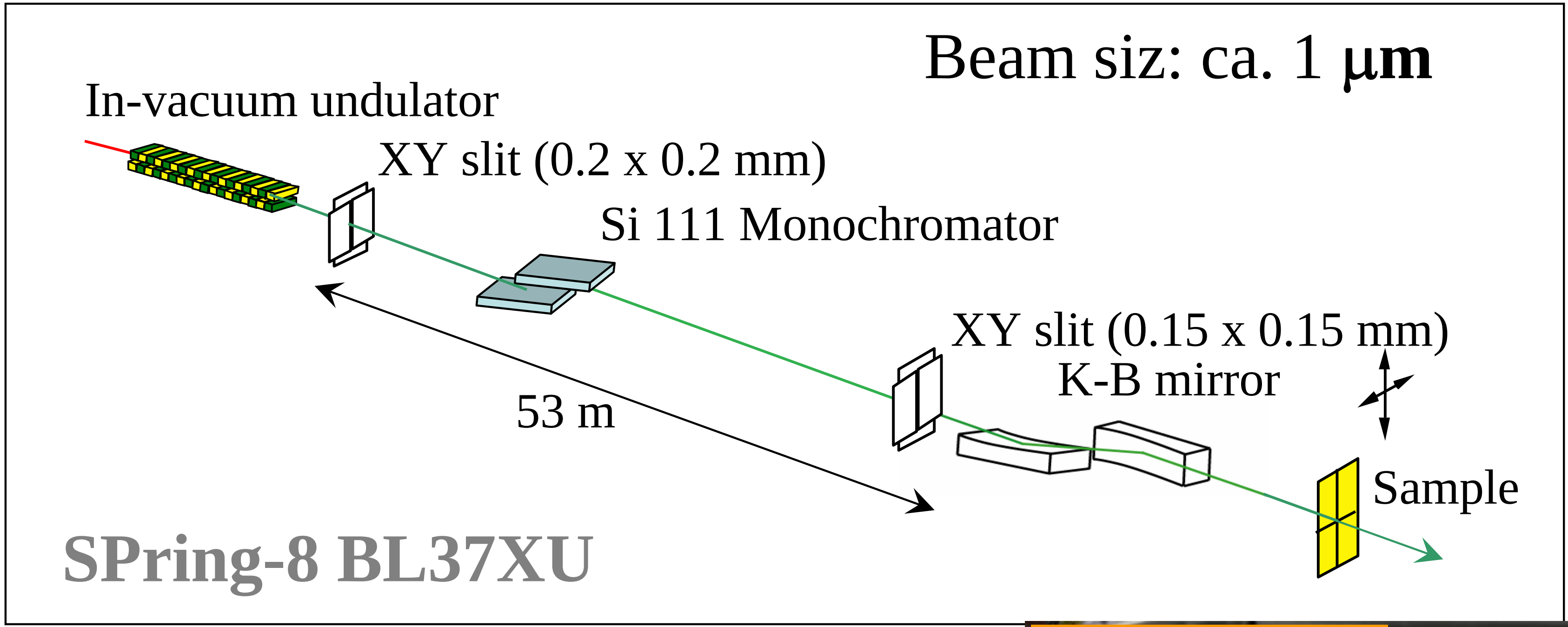

- BEAMLINE DESCRIPTION -

The light source : In-vacuum type undulator
(Period length : 32 mm, the number of period : 140)
Monochromator : Double-crystal monochromator
located 43 m from the source

Table Details of focusing optics by K-B mirror

	37 keV[1]	12.8 keV
Material	fused quartz	fused quartz
Surface	platinum coated	platinum coated
Focal length (1st mirror)	250 mm	100 mm
(2nd mirror)	100 mm	50 mm
Average glancing angle	0.8 mrad	2.8 mrad

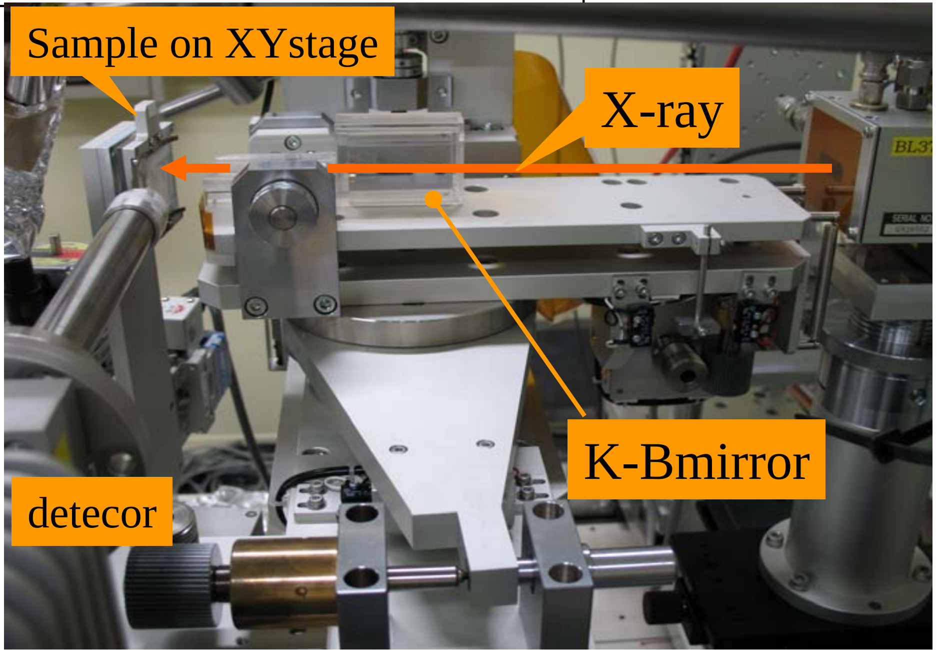

Instrument ~Spring-8 BL37XU~

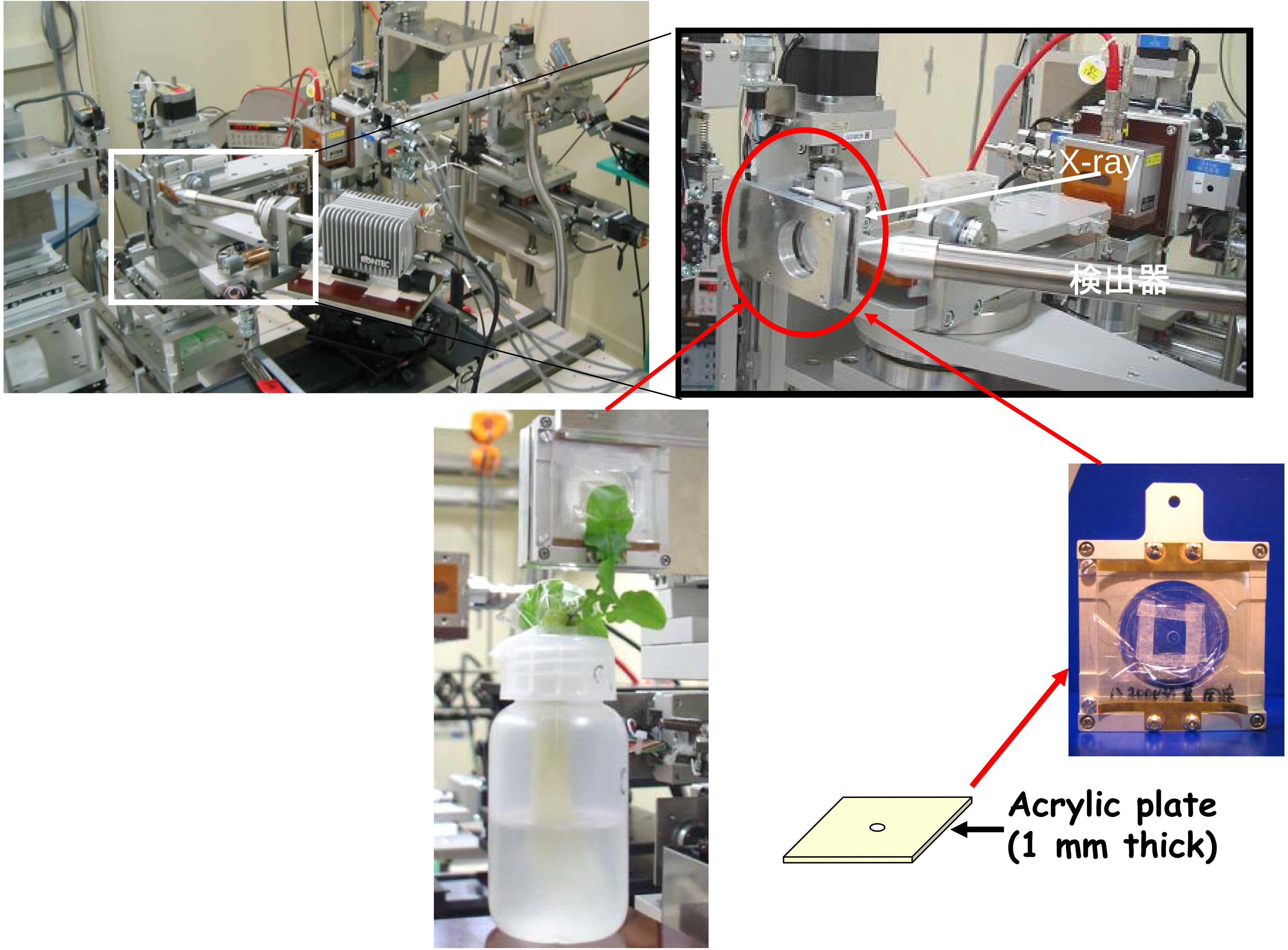

Acrylic plate
(1 mm thick)

XAFS analysis

KEK PF BL12C
As K-edge (11.863 keV)
Si(111) double crystal
Fluorescence mode
19elements-SSD

in vivo XAFS

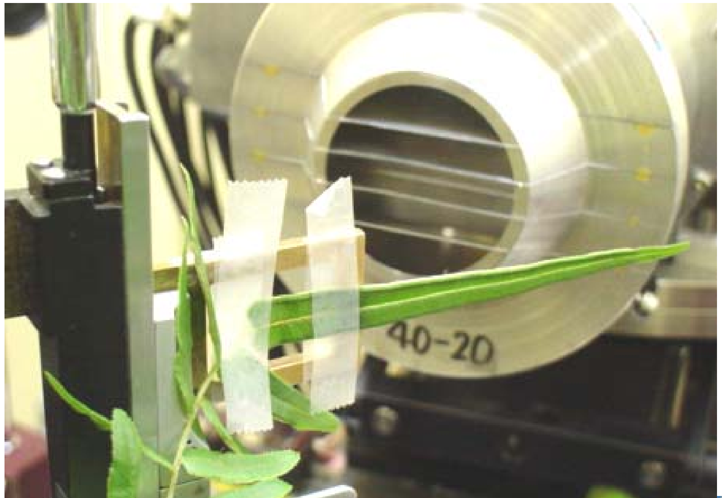

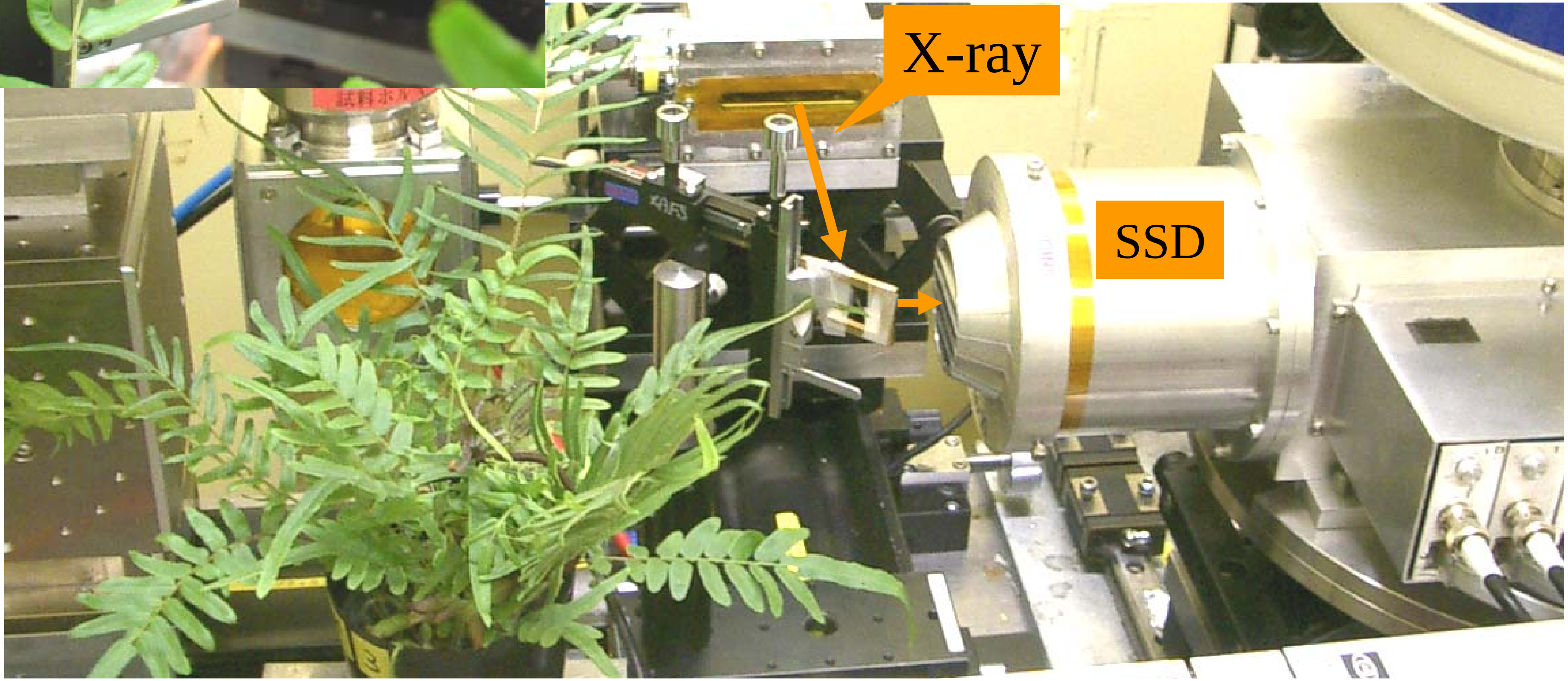

A section of pinna

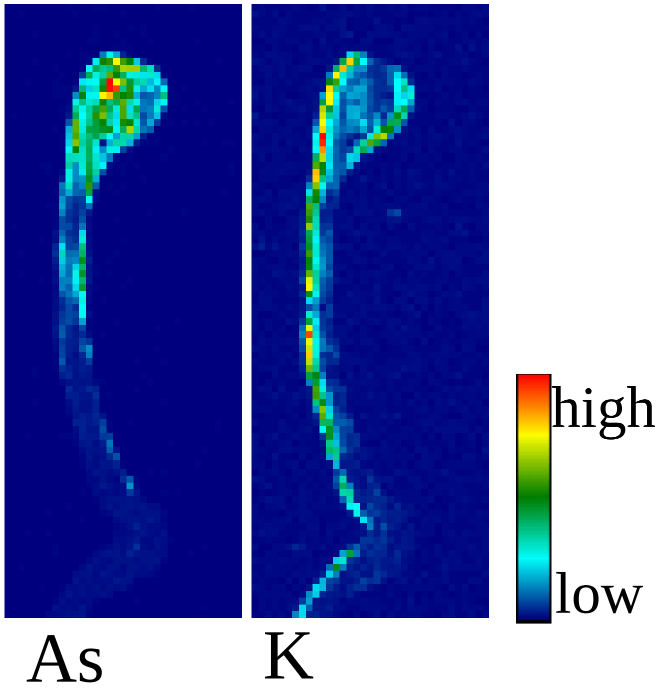

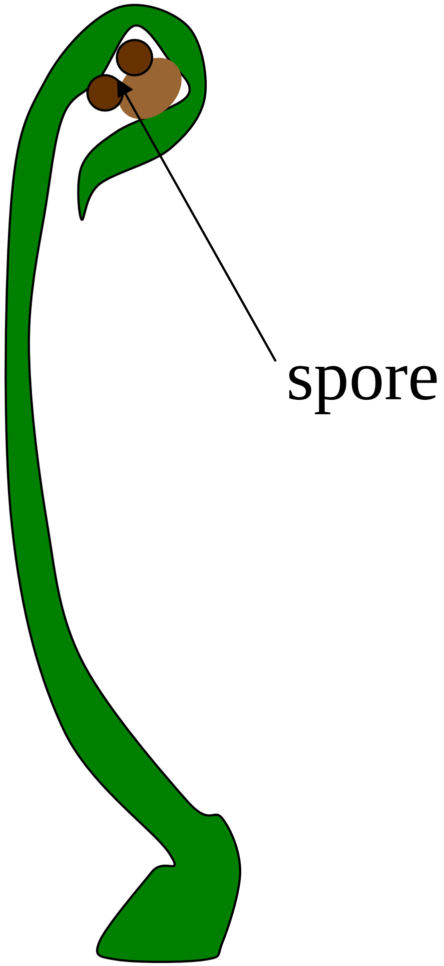

frond

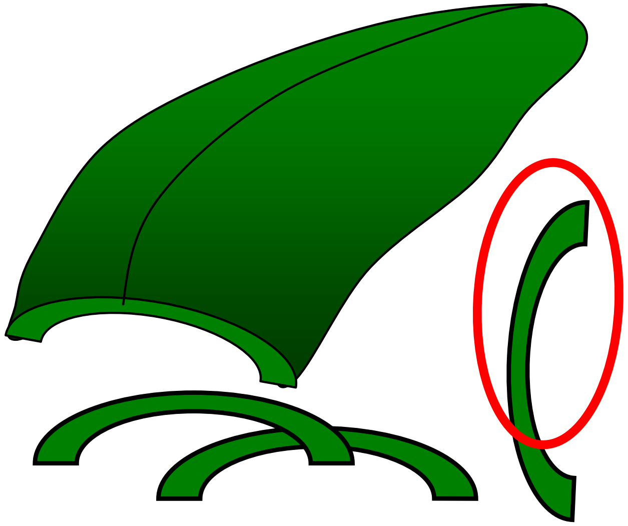

X-ray Energy : **14.999 keV**
Beam size : **50 µm × 50 µm**
Step number : **35 point × 90 point**
measurement time : **1 sec/point**

X-ray Energy : 12.8 keV
Beam size : 1.5 µm × 1.5 µm
Exposure time : 0.2 sec. / point
Point : 150 point × 150 point

M−XRF imaging at Spring-8

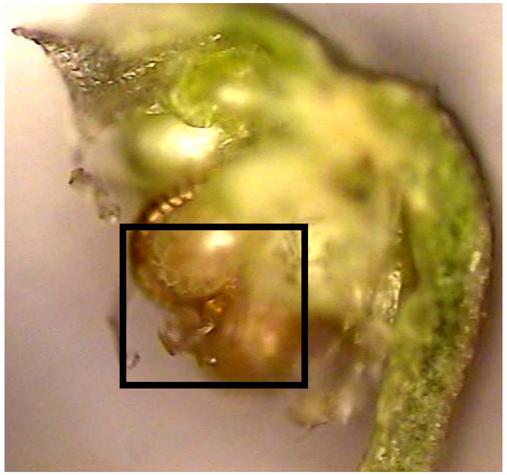

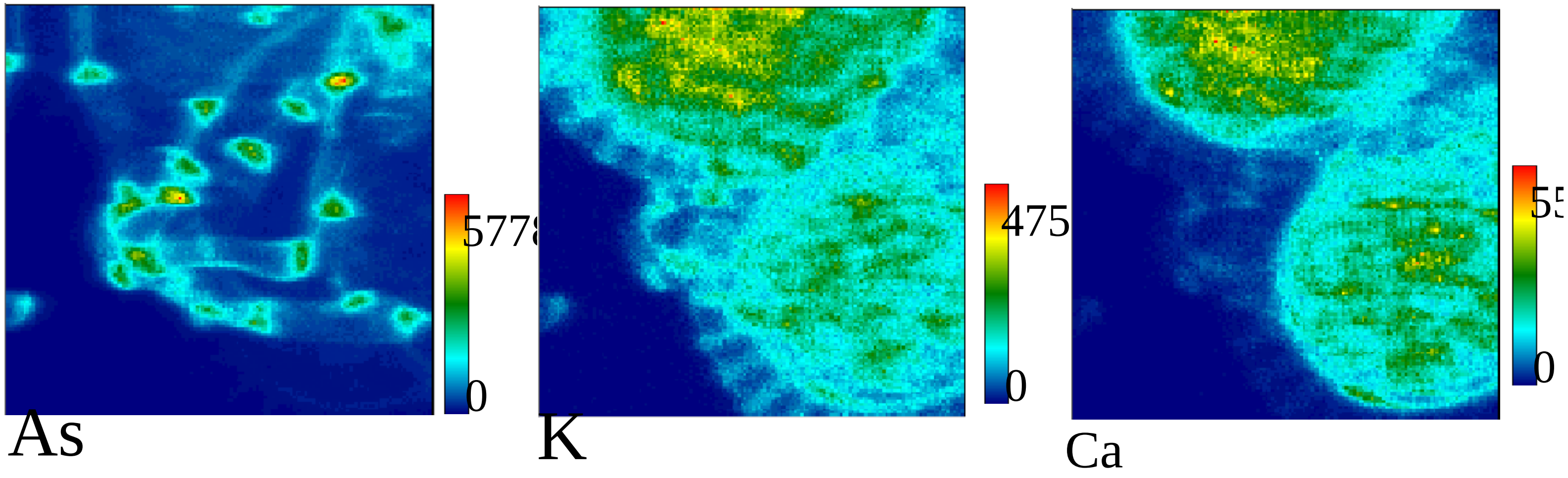

X-ray Energy : 12.8 keV
Beam size : 1.5 µm × 1.5 µm
Exposure time : 0.2 sec. / point
Point : 150 point × 150 point

As level is low at spore

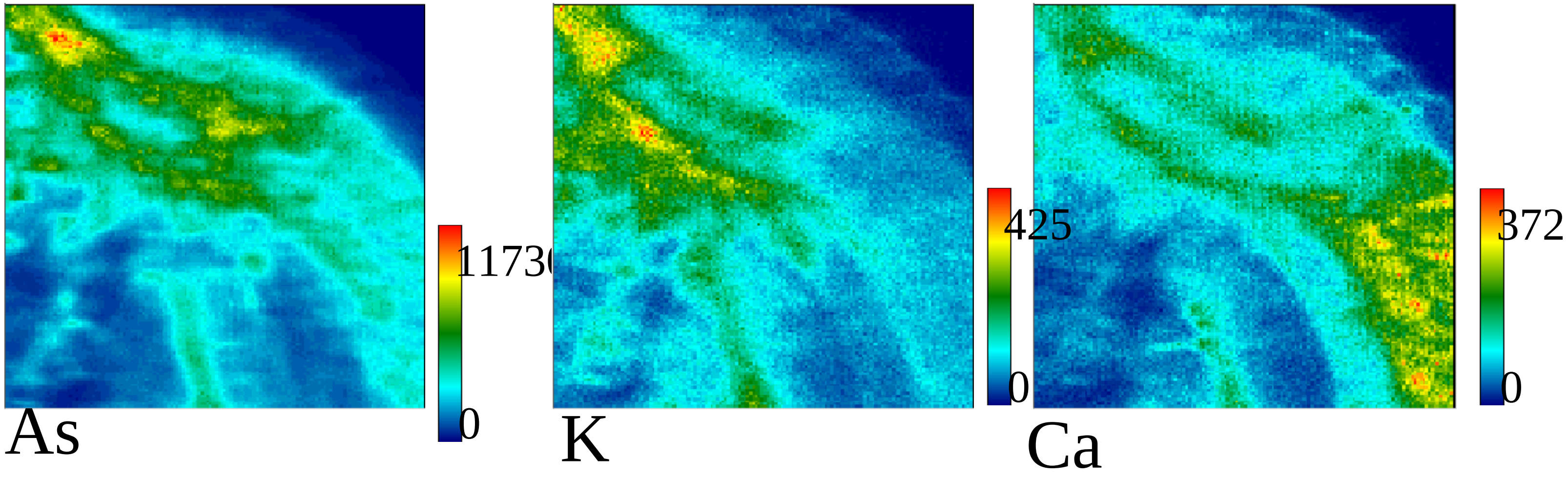

（3）Energy tunability

Chemical state analysis
by Fluorescence -XAFS

Chemical State Analysis

- **XAFS** (X-ray Absorption Fine Structure)
  - **XANES**
    - Chemical shift of absorption edge
    - The intensity of the white line
  - EXAFS
    - Local structure
    - Coordination number
- **X-ray Emission**
  - Chemical state analysis
    - Chemical shift of the K or L emission lines
    - Intensity ratio of Kα and Kβ
  - Emission Spectroscopy
    - Resonant inelastic emission spectroscopy
    - …..

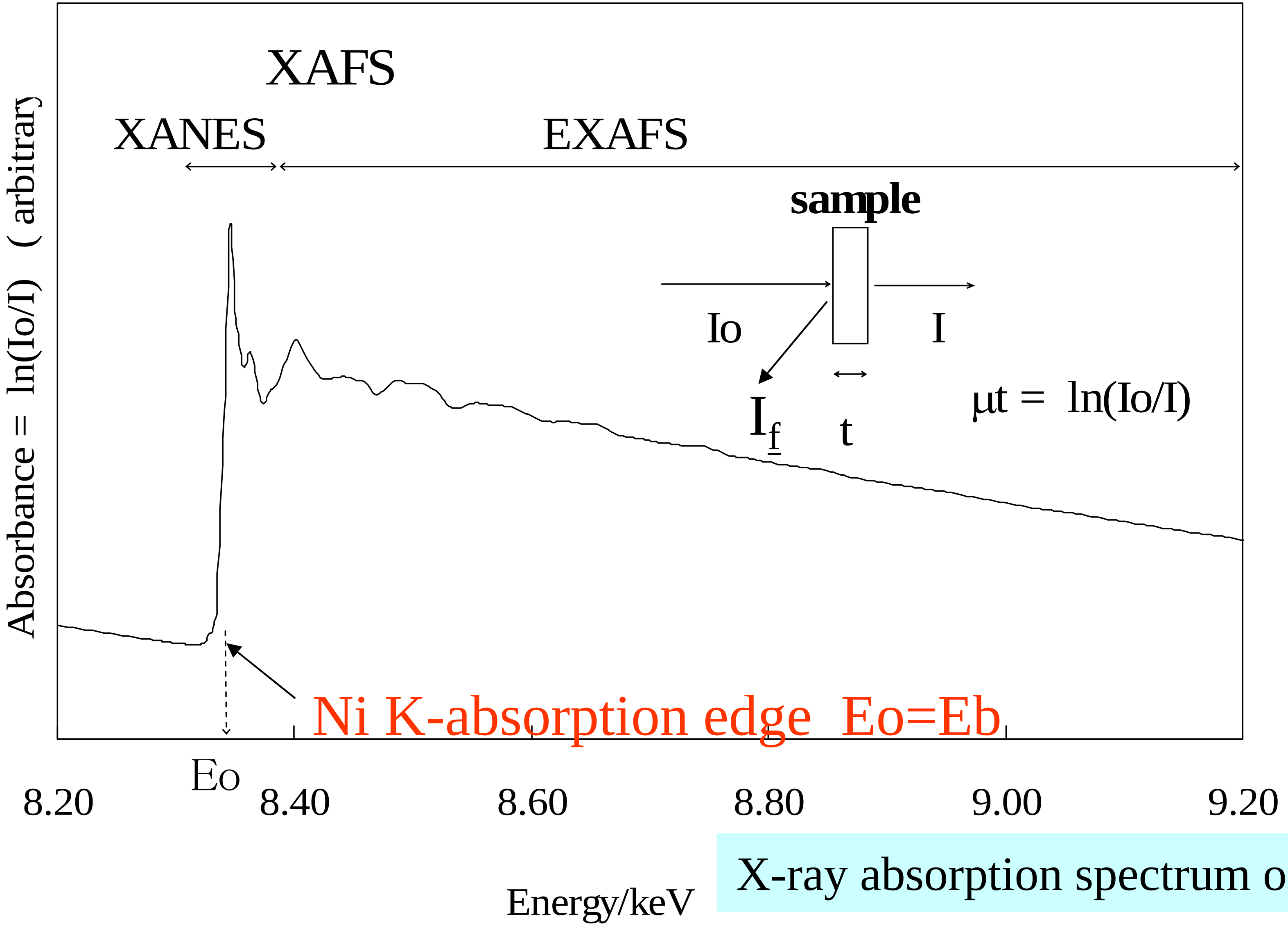

X-ray absorption spectrum of $LiNiO_2$

XANES: X-ray absorption near edge structure

electronic state, oxidation number

EXAFS: Extended X-ray absorption fine structure

local structure (atomic distance and coordination No.)

X-ray absorption by sample

$$I/I_o = \exp(-\mu t) = \exp(-\mu_M \rho t) \qquad [1]$$

μ : linear absorption coef.(cm^{-1})
μ_M : mass absorption coef.(cm^2/g)
ρ : density of sample（g/cm^3）

$$\mu_M = \Sigma \mu_{Mi} w_i \qquad [2]$$

μ_{Mi}: μ_M of component i

w_i : weight% of component i

Chemical State analysis by XANES

-Chemical Shift of X-ray Absorption edge-

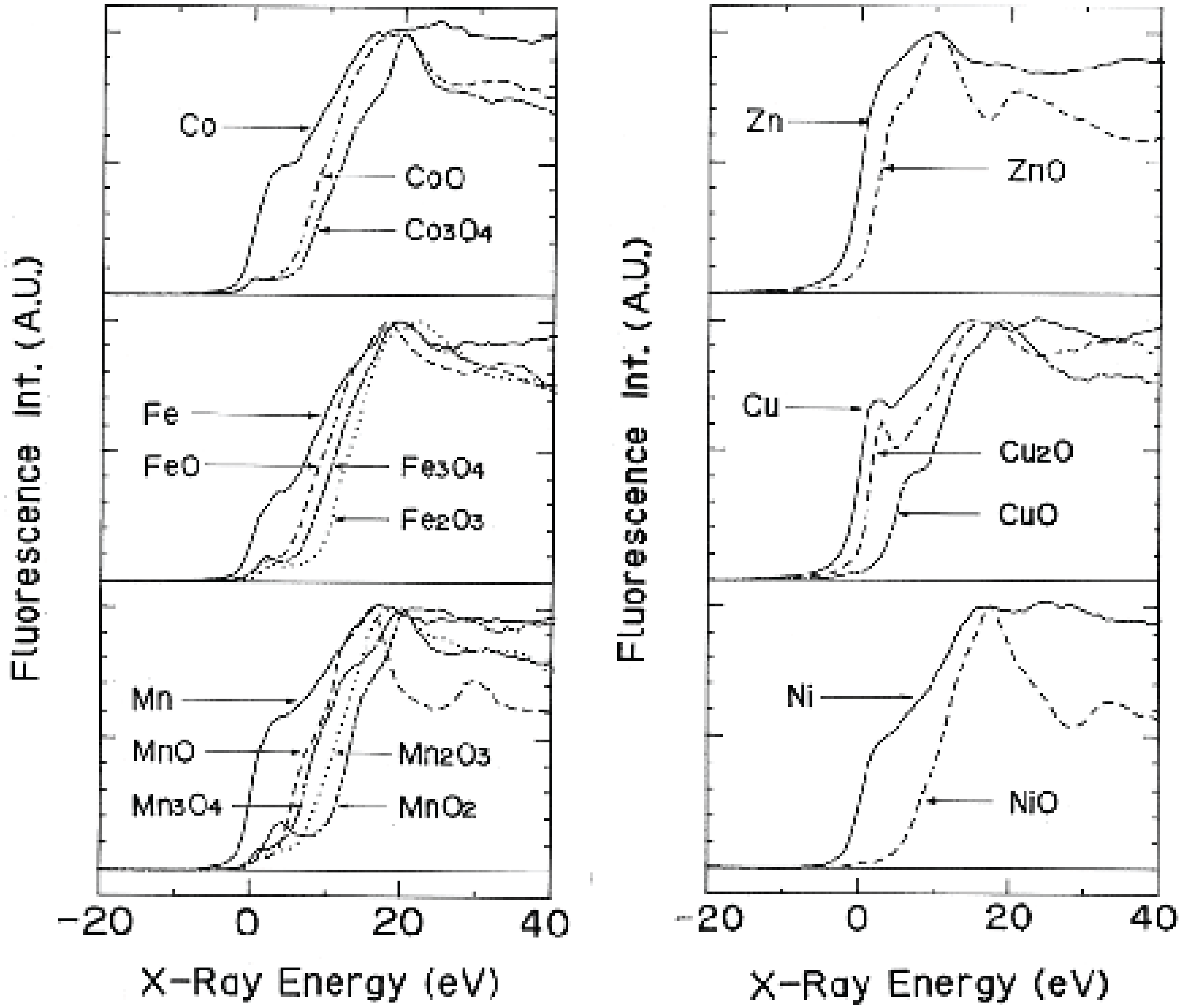

Fingerprint Method

K.Sakurai (NIMS)

As K-edge XANES analysis

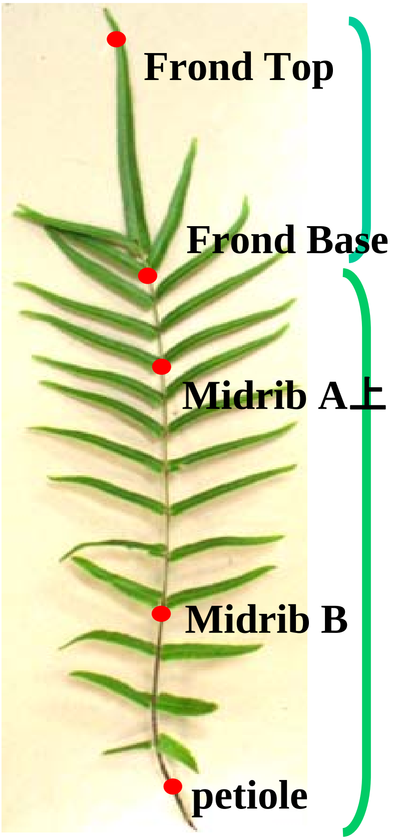

Frond

PF BL-12C

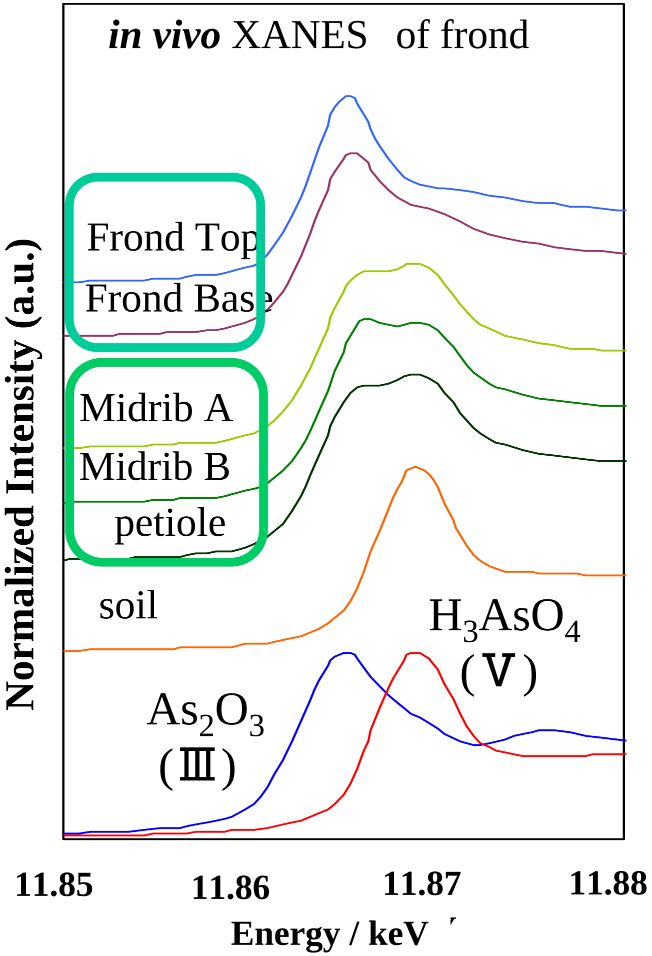

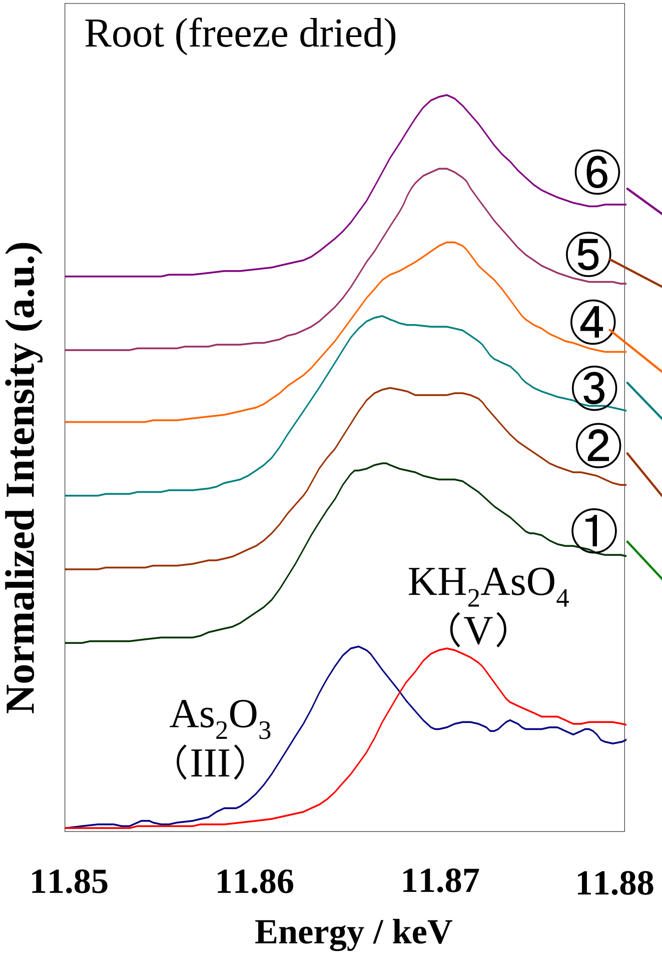

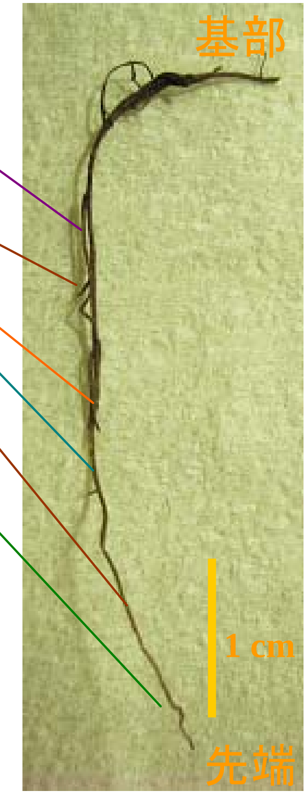

Root

Summary

- We have established μ-XRF imaging technique utilizing SR to monitor time dependent process of arsenic transfer in a leaf tissue of hyperaccumulator fern.

- This study visually revealed for the first time that arsenic transferred from root to marginal part of leaf within 30min after feeding.

- Arsenic accumulated in the region of vascular bundle and transferred to paraphysis prior to sporangium.

Arabidopsis halleri

Cd and Zn hyper-accumulator

and

Cd in Rice

Micro X-ray fluorescence imaging and micro X-ray absorption spectroscopy of cadmium hyper-accumulating plant, *Arabidopsis halleri* ssp. *gemmifera*, using high-energy synchrotron radiation

***Journal of Analytical Atomic Spectrometry*, 23, 1068-1075 (2008)**

N. Fukuda, A. Hokura, N. Kitajima, Y. Terada, H. Saito, T. Abe and I. Nakai.

Arabidpsis halleri ssp. *Genmifera* (ハクサンハタザオ)

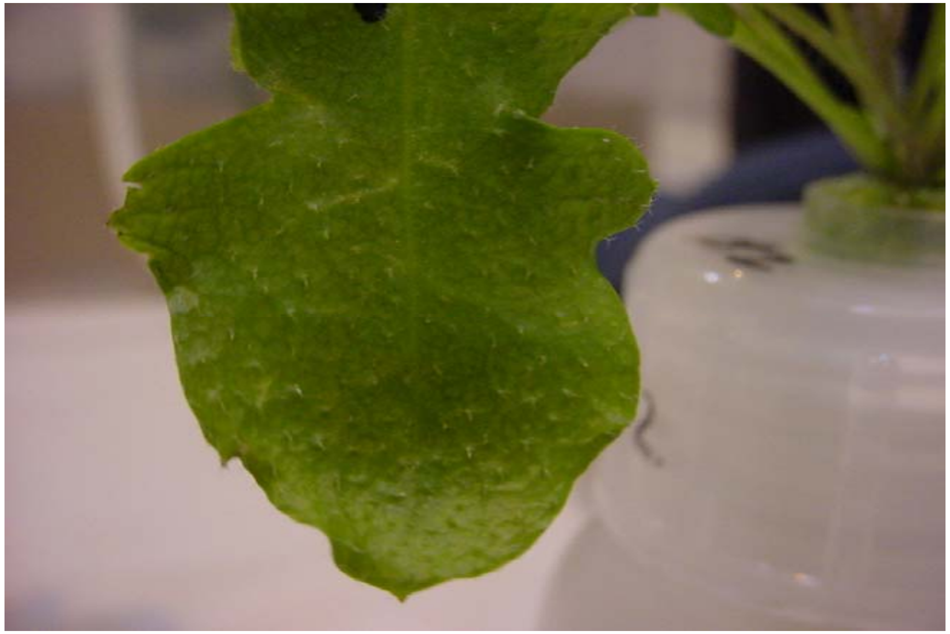

Arabidopsis halleri is known as a Cd and Zn hyper-accumulator, which contained more than 9000 mg/ kg Cd and Zn.

XRF imaging of a leaf of *A. halleri* ssp. *Gemmifera*.

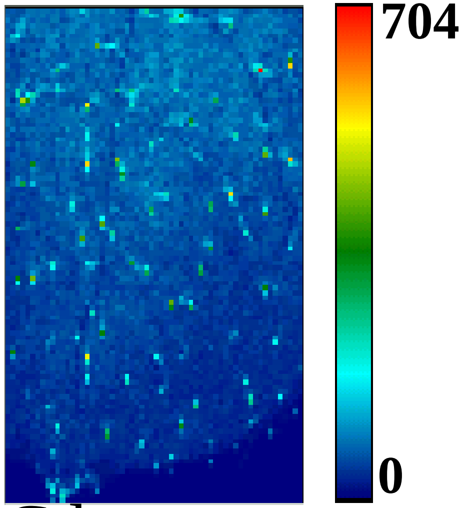

Cd

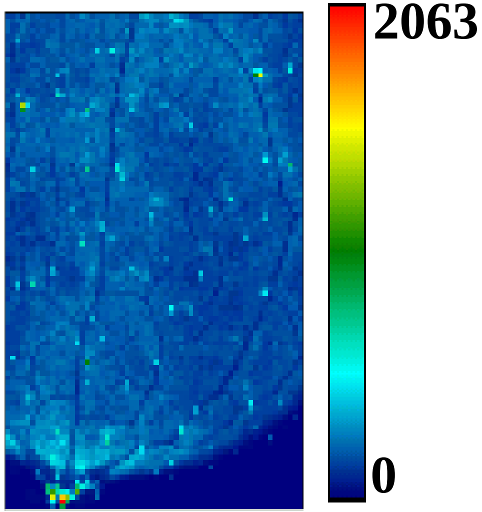

Zn

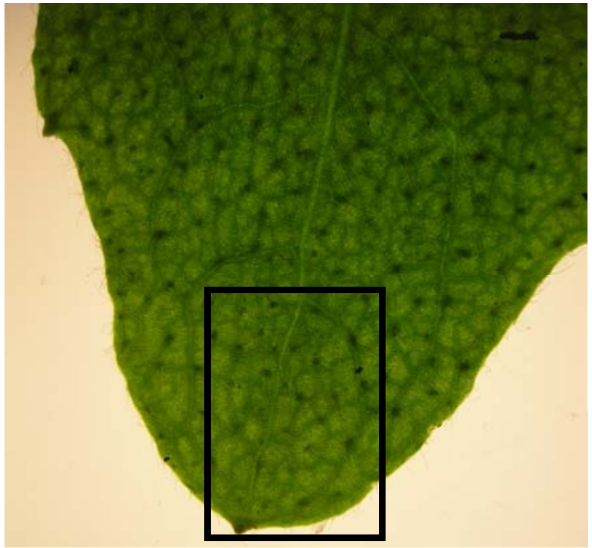

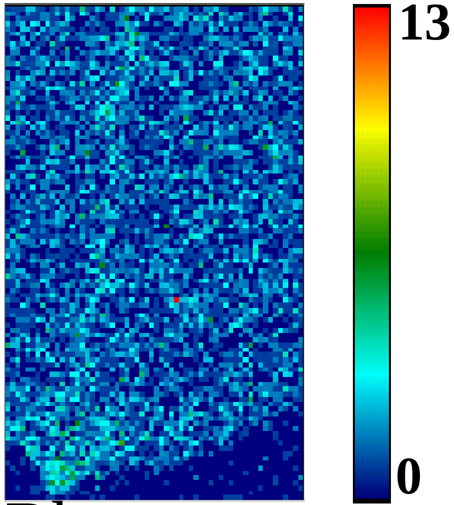

Rb

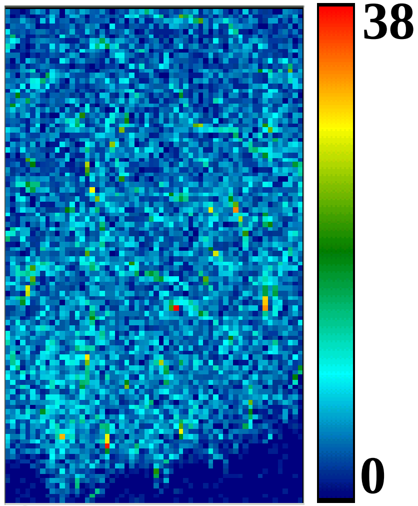

Sr

X-ray Energy : **37 keV**

Beam size : **50 μm × 50 μm**

Measurement points : **60 point × 100 point**

measurement time : **1 sec/point**

µ-XRF imaging of a trichome taken from a leaf.

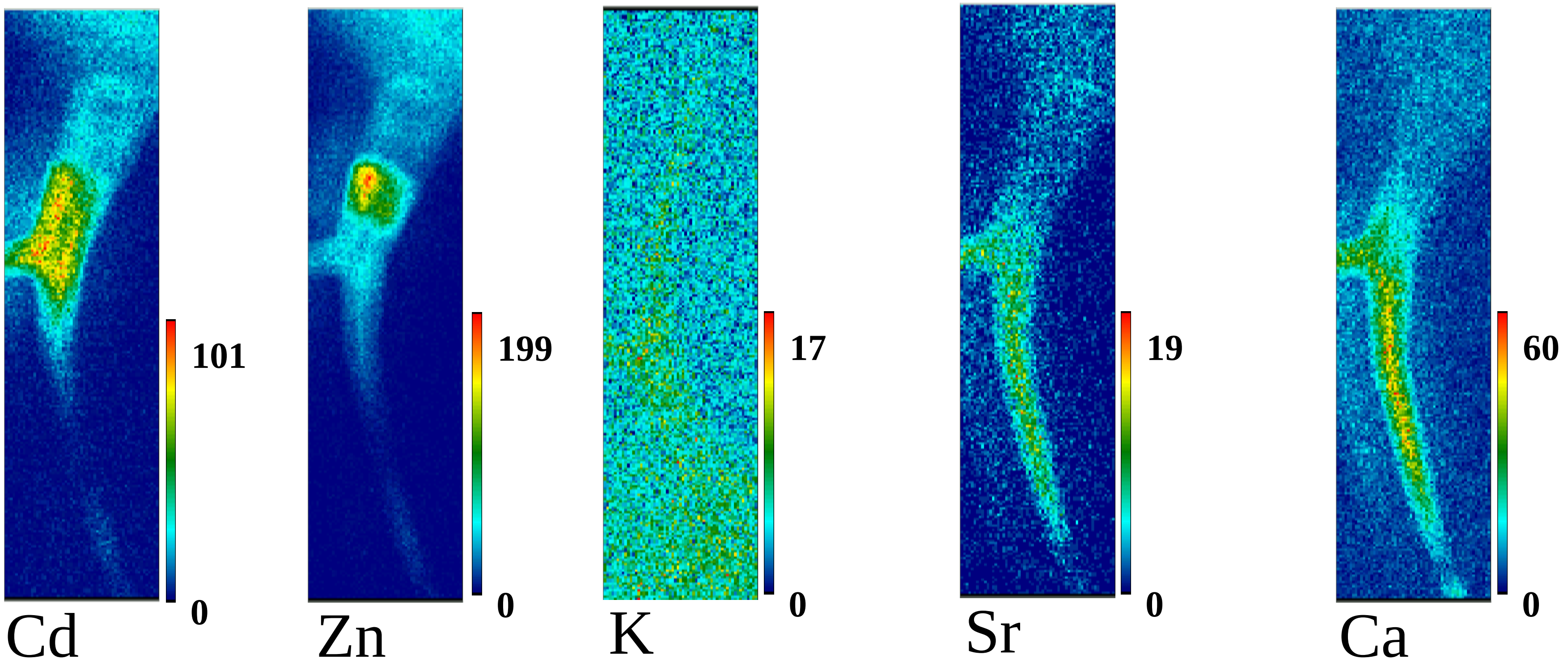

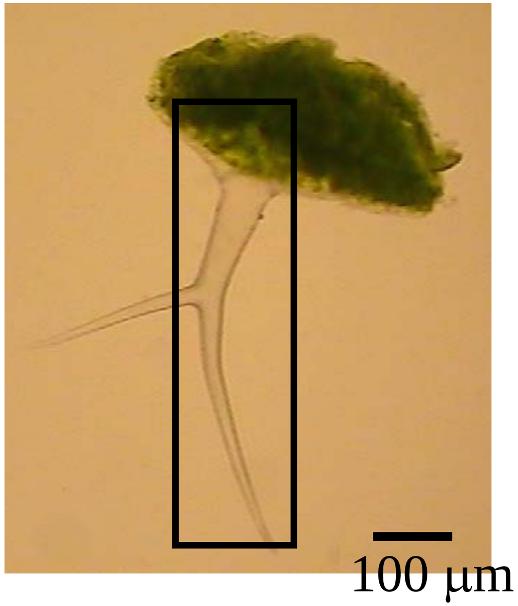

X-ray Energy : **37 keV**

Beam size : **3 µm × 3 µm**

Measurement points : **59 point × 226 point**

measurement time : **0.5 s/ point**

Trichomes are epidermal hairs present at the surface of leaves of *A. halleri*, and their functions are thought to be an exudation of various molecules.

Prospect of microbeam analysis

Microbeam → Nanobeam

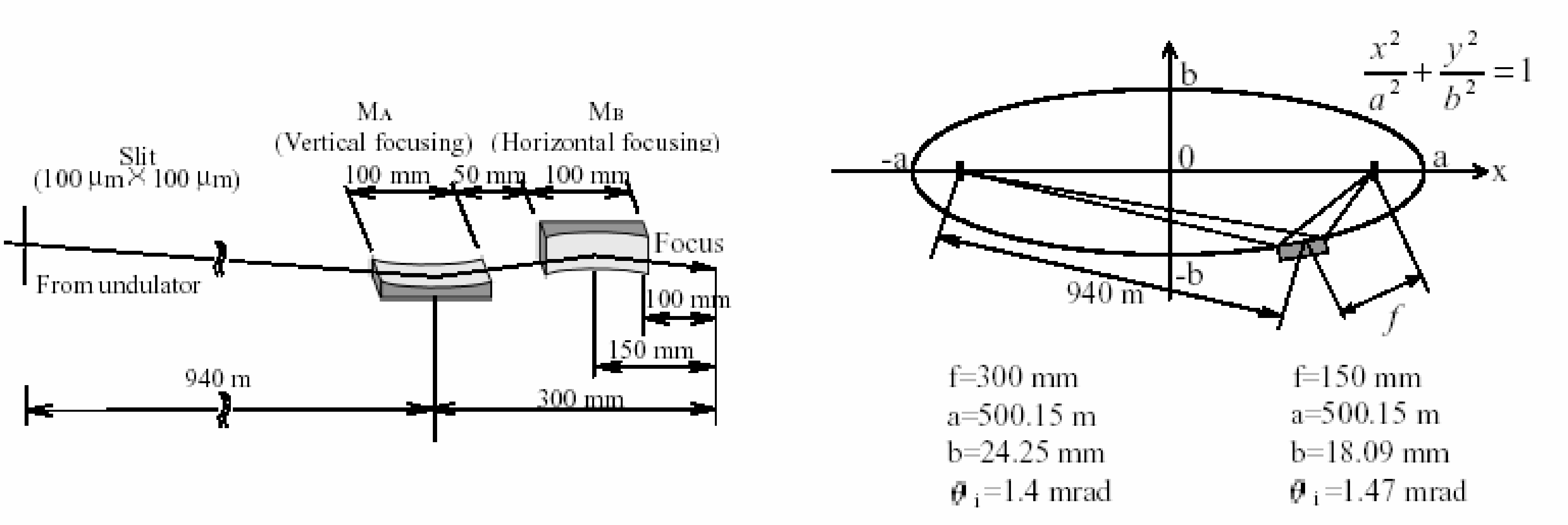

$$\frac{x^2}{a^2}+\frac{y^2}{b^2}=1$$

f=300 mm
a=500.15 m
b=24.25 mm
θ_i=1.4 mrad

f=150 mm
a=500.15 m
b=18.09 mm
θ_i=1.47 mrad

Nano-beam focusing system at SPring-8

(left)Hig precision K-B mirror

(right) Optical parameters of elliptical mirror

Yamauchi et al.（Osaka Univ.)

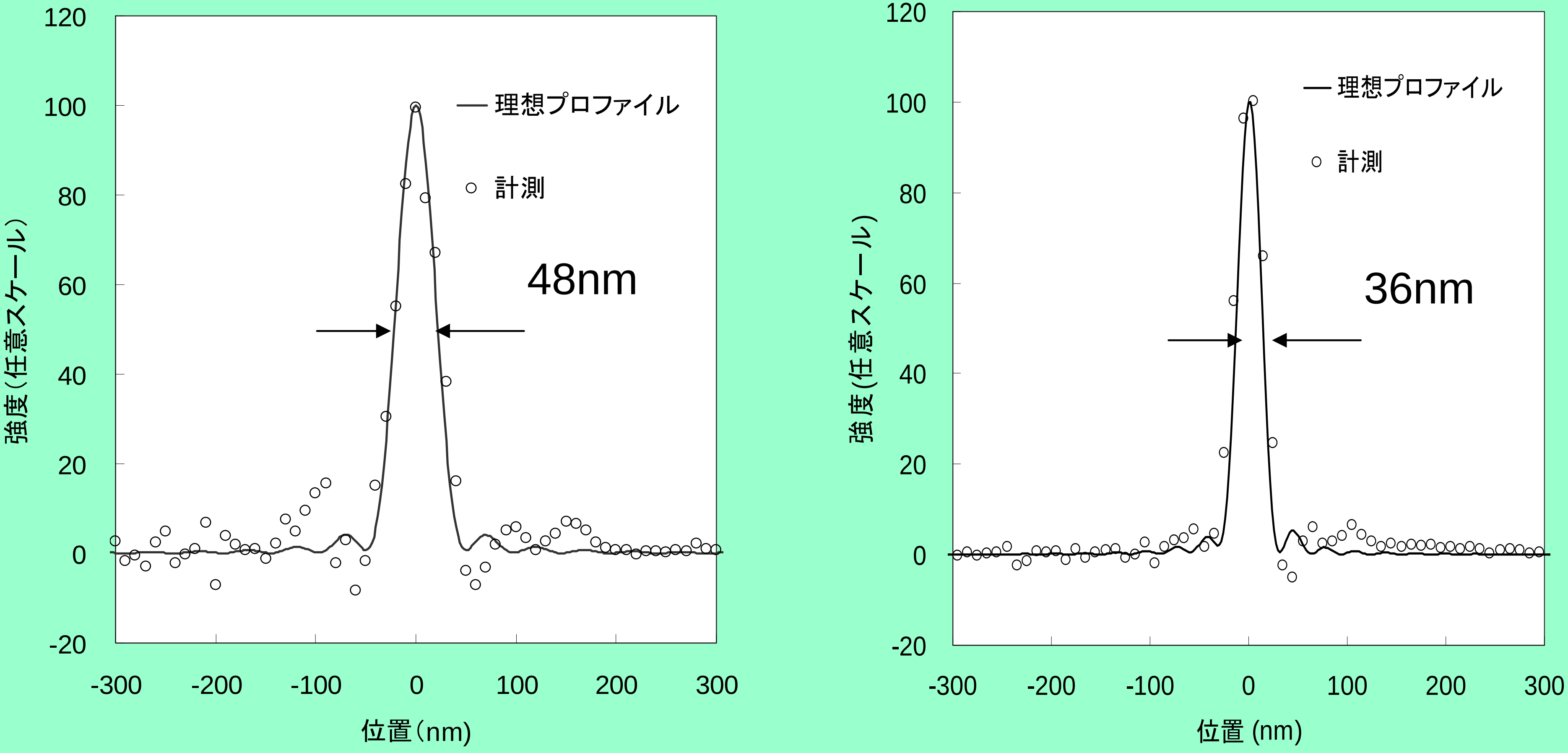

(a)vertical

(b)horizontal

Beam profile

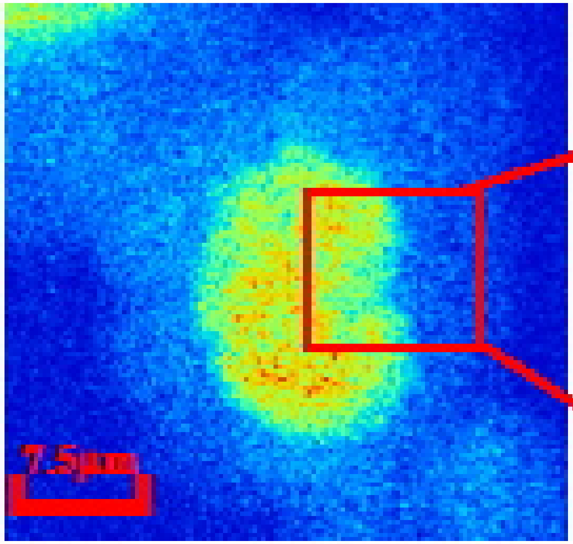

Full image of cell as iron mapping

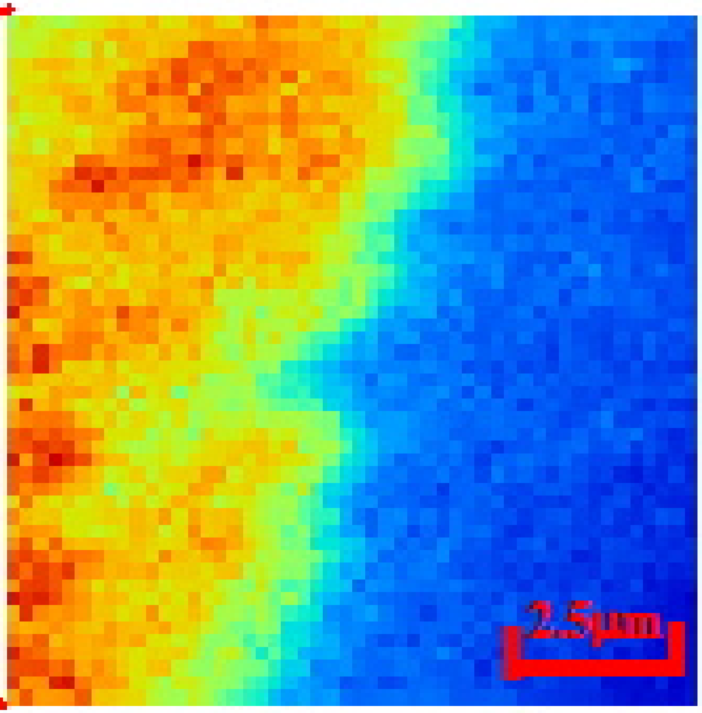

Iron mapping in a part of a nucleus

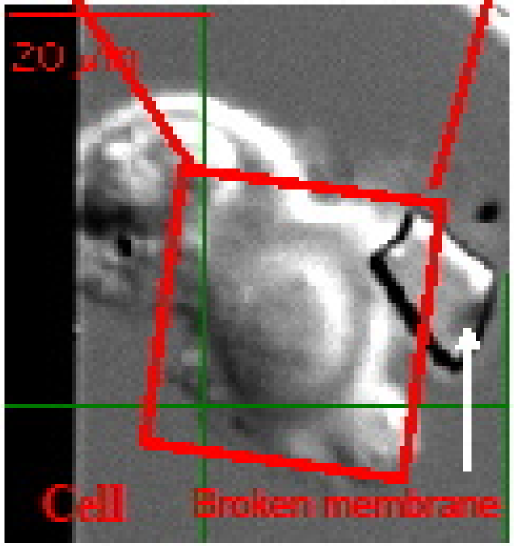

Opt. microscope

Experimental condition of the iron mapping

Sample	Human cell
X-ray Energy	15keV
Beam size	200nm x 200nm
Scanning pitch	200nm/pixel
Scan area	10µm x 10µm

TXRF-XAFS

Photon Factory BL-12C

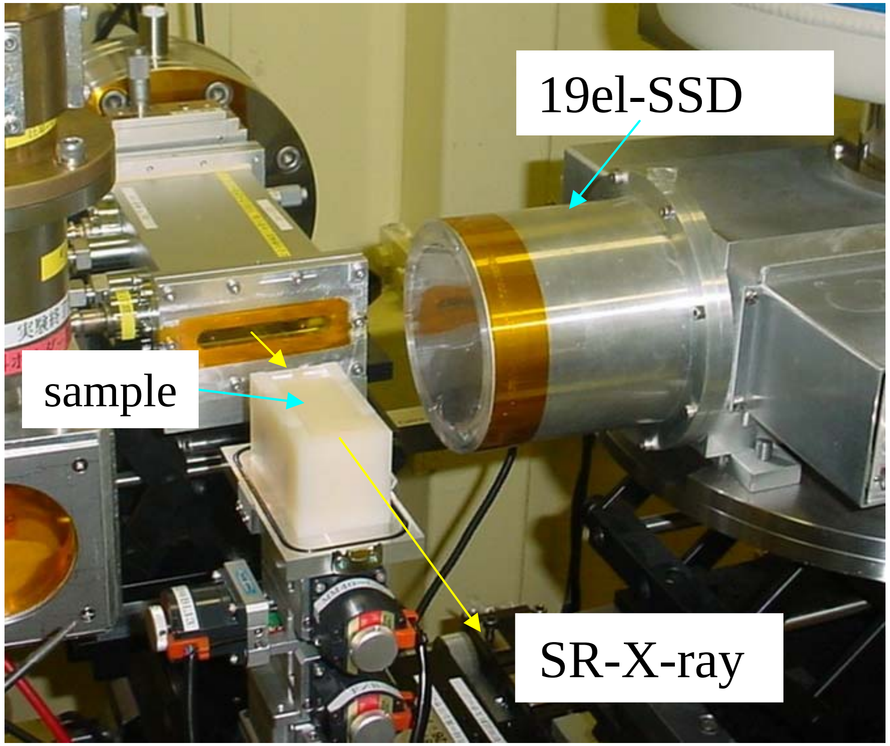

Total reflection

⇒ High S/N

Nanosheet Monolayer

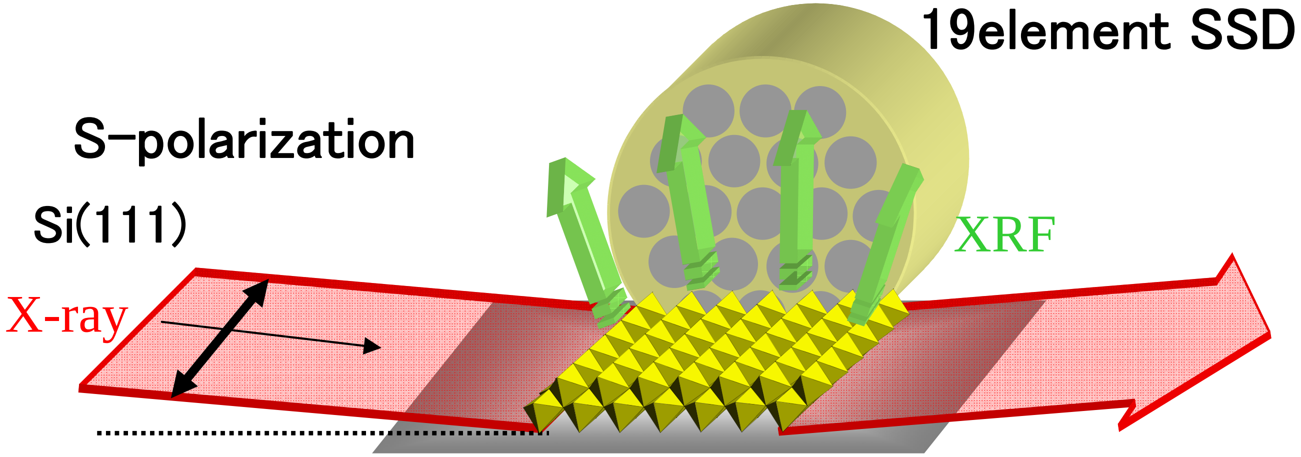

$\theta_c < 0.3°$

Material Science

Heating behavior of titania nanosheet by TXRF-XAFS

$Cs_{0.7}Ti_{1.825}\square_{0.175}O_4$

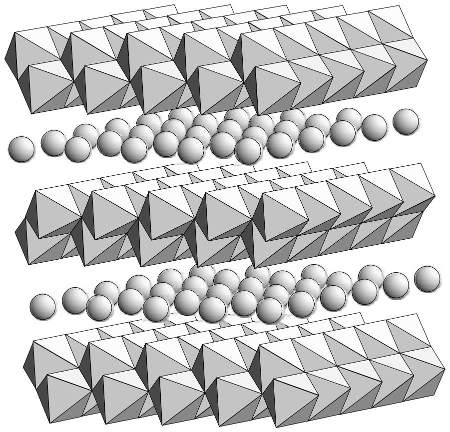

Layer structure

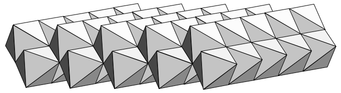

$Ti_{1-\delta}O_2^{4\delta-}$

Titania nanosheet

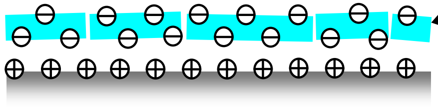

Nanosheet(1-layer)

heat

transition

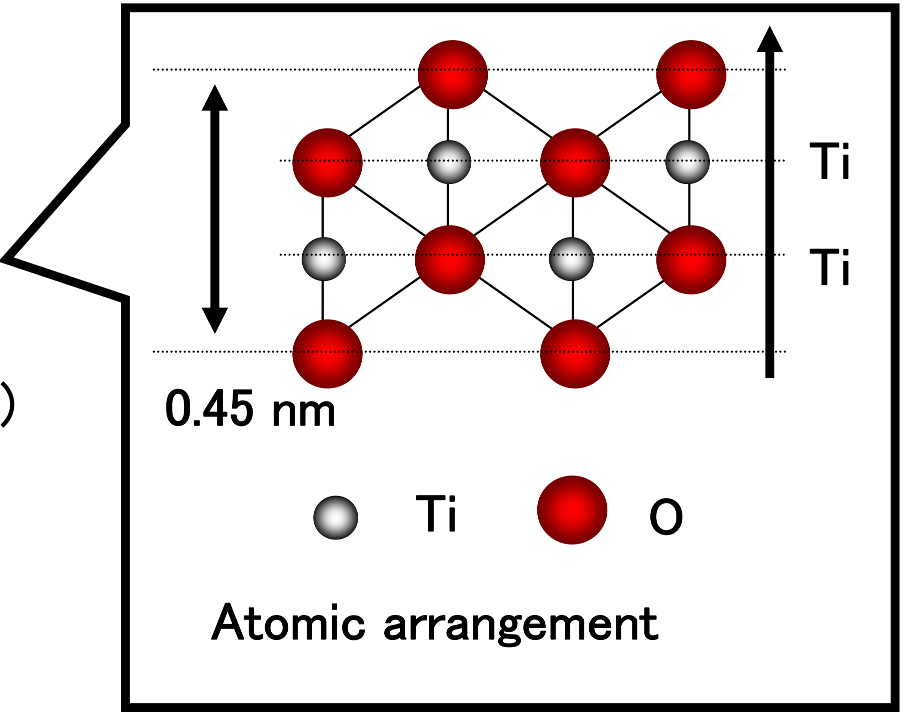

Atomic arrangement

How to construct the three dimensional structure

Ti K-edge XANES spectra as a function of temperature

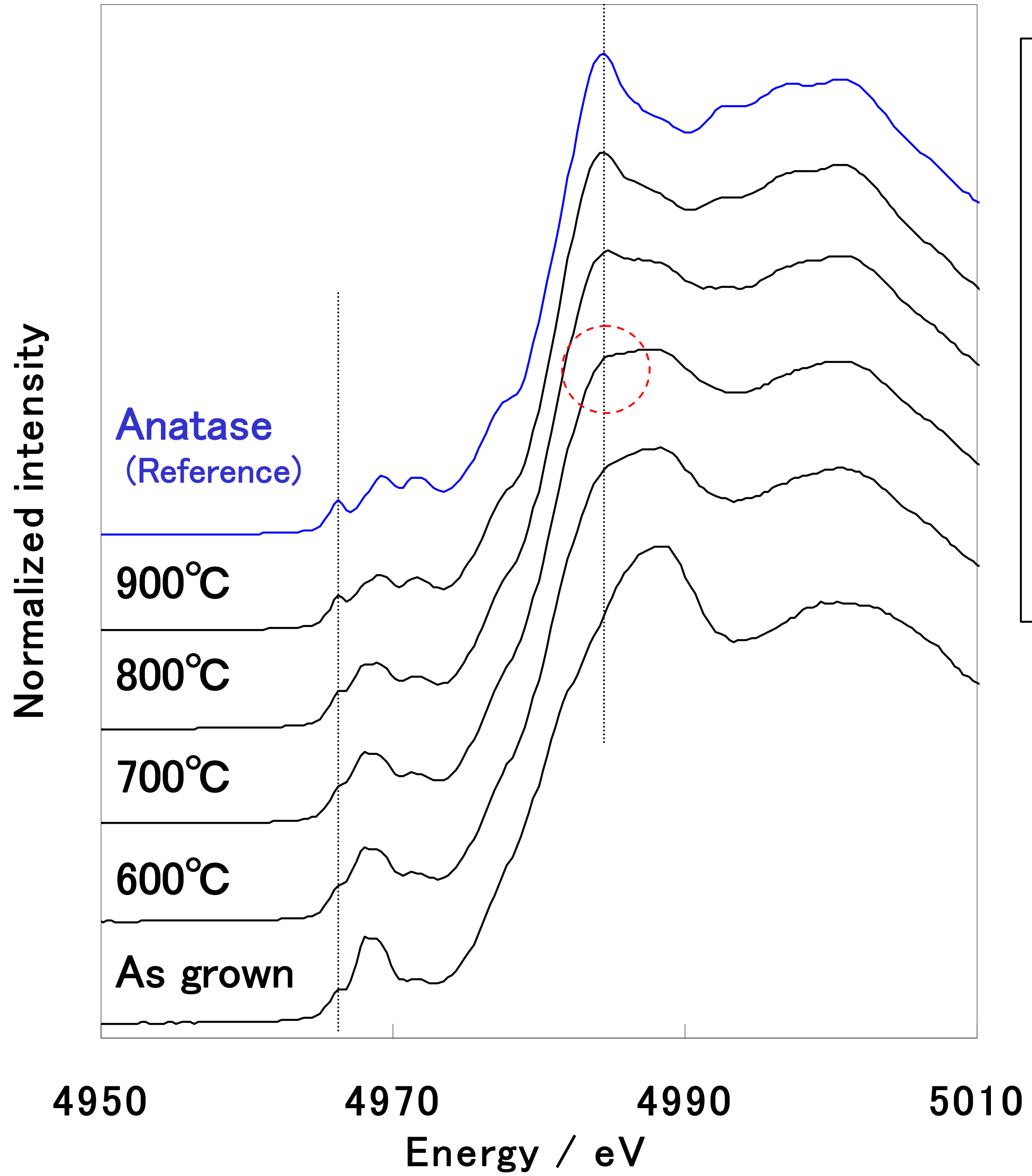

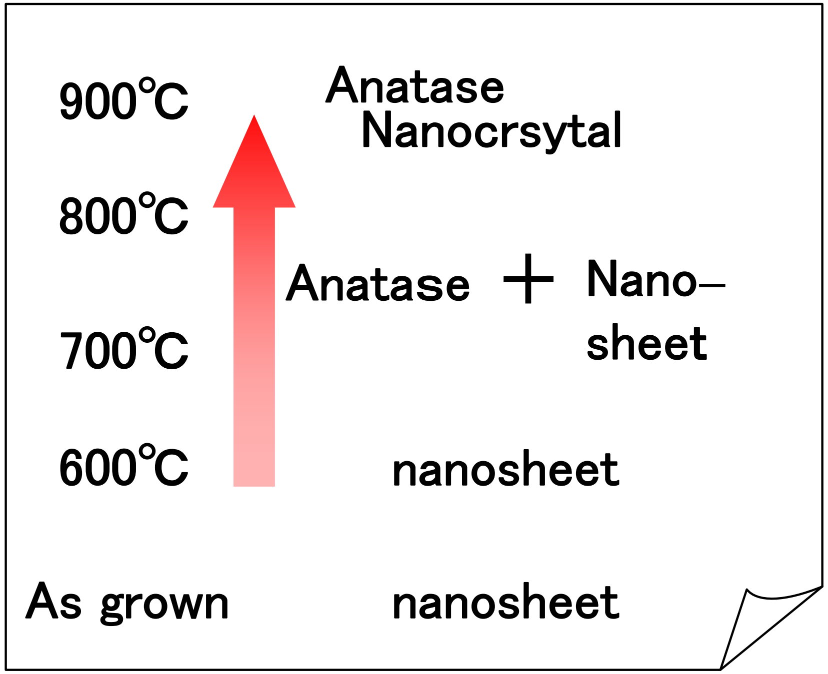

900℃ Anatase Nanocrsytal

800℃

Anatase ＋ Nano-sheet

700℃

600℃ nanosheet

As grown nanosheet

Bulk crystal: stable phase

800℃ → rutile

400℃ → anatase

©Fukuda&Nakai

（4)High energy X-ray

High energy SR-XRF

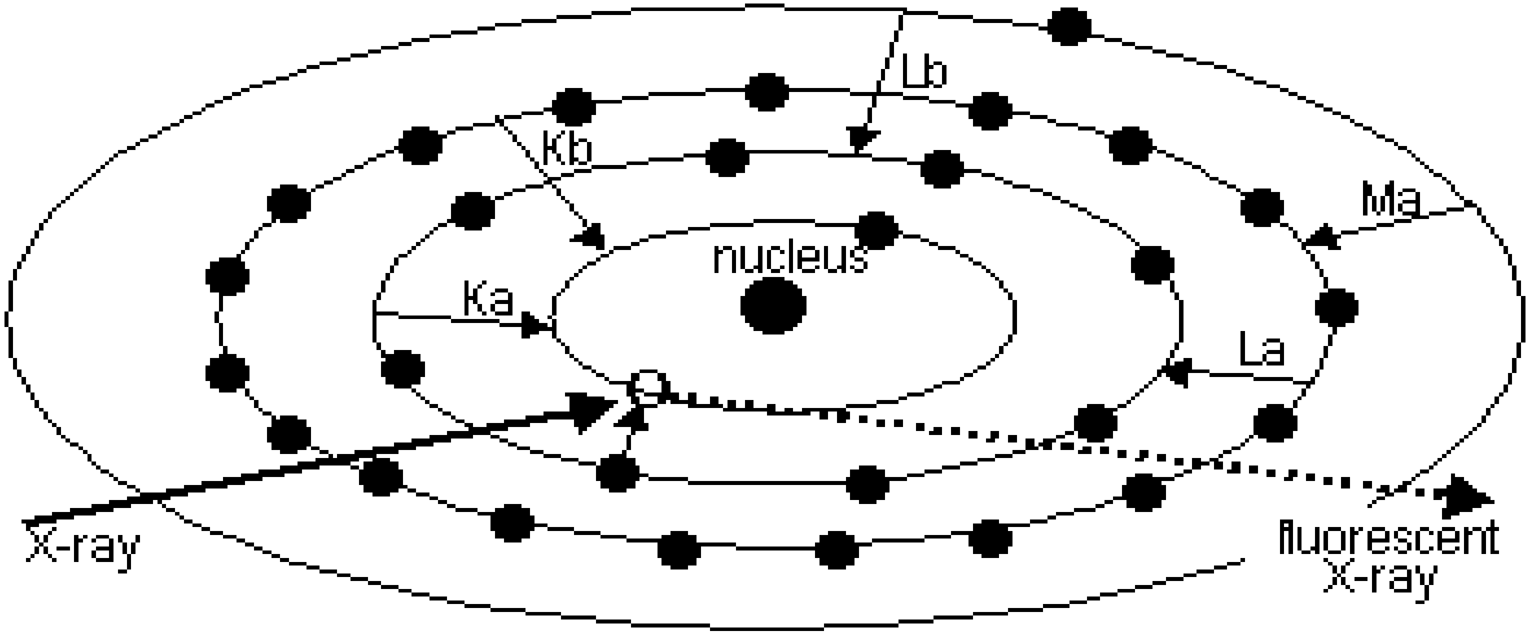

Bi Kα 76.35 E_b=90.57 U Kα 97.17 E_b=115.66keV

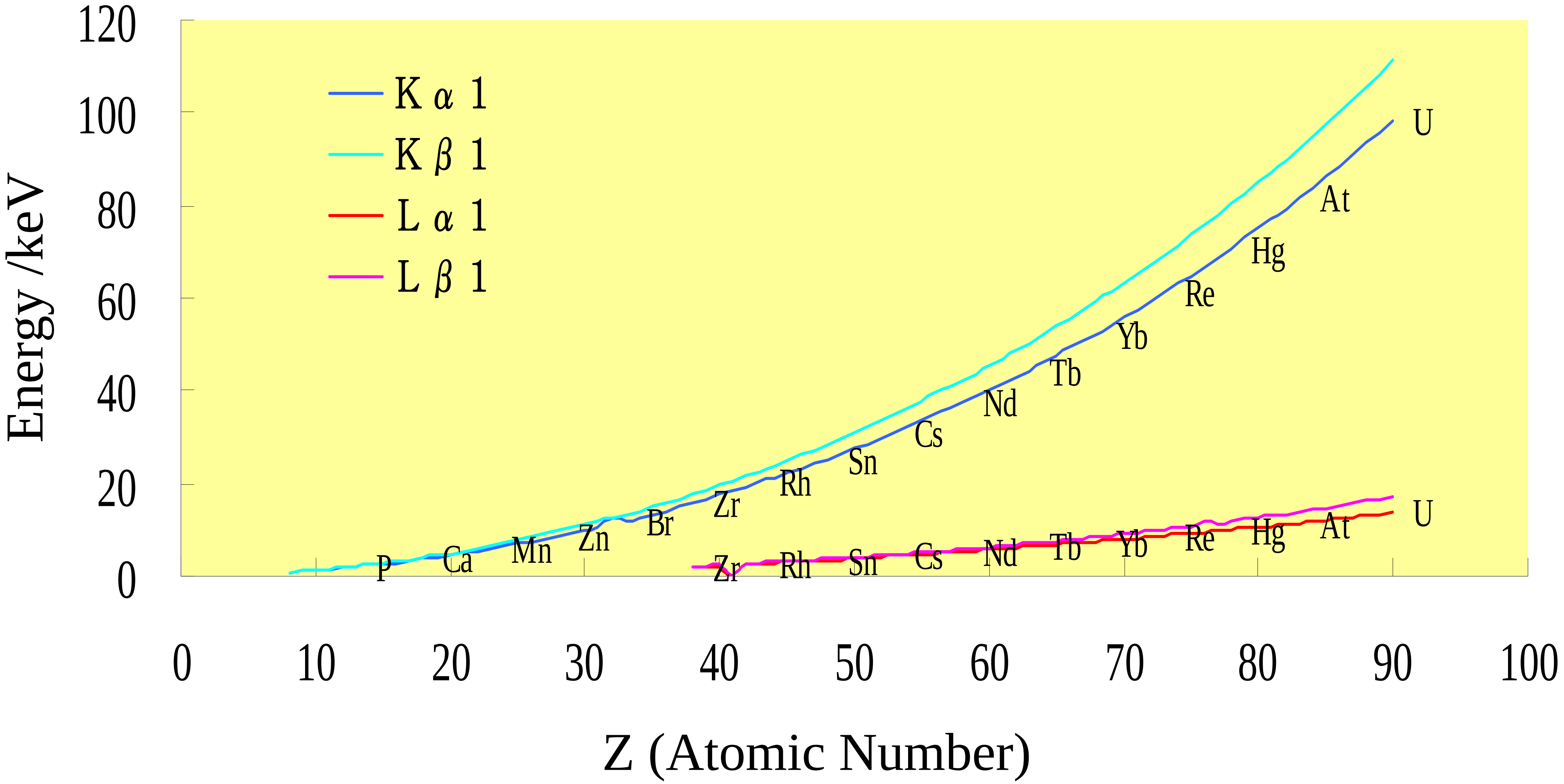

X-ray fluorescence energies of K & L lines v.s. atomic number

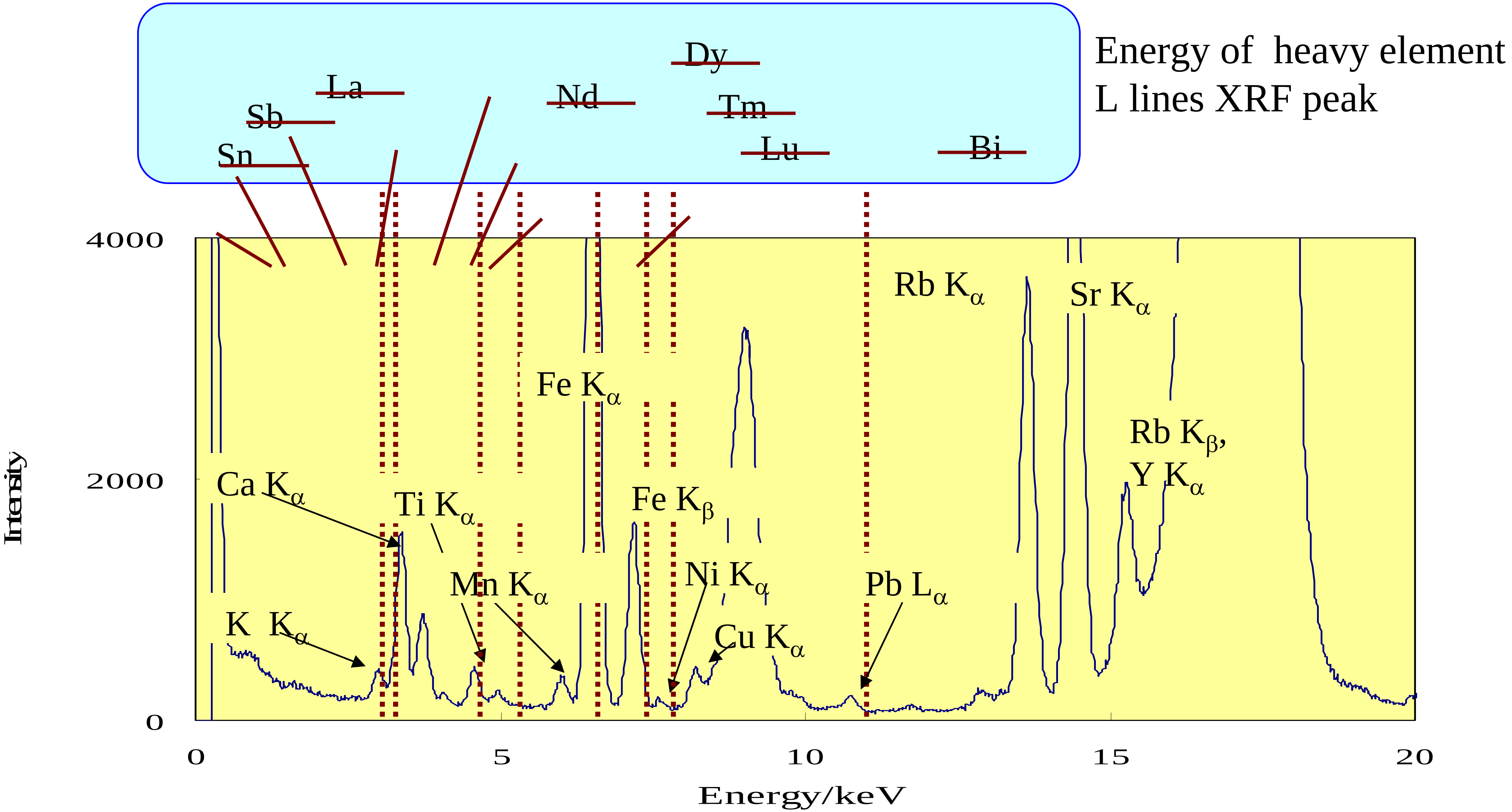

Problem of conventional XRF analysis
overlapping of heavy elements L lines as light elements K lines

Sample porcelain , Source：Mo Ka X-ray 40 kV-40 mA , time:1000sec

BL08W （for High-energy inelastic scattering experiments)

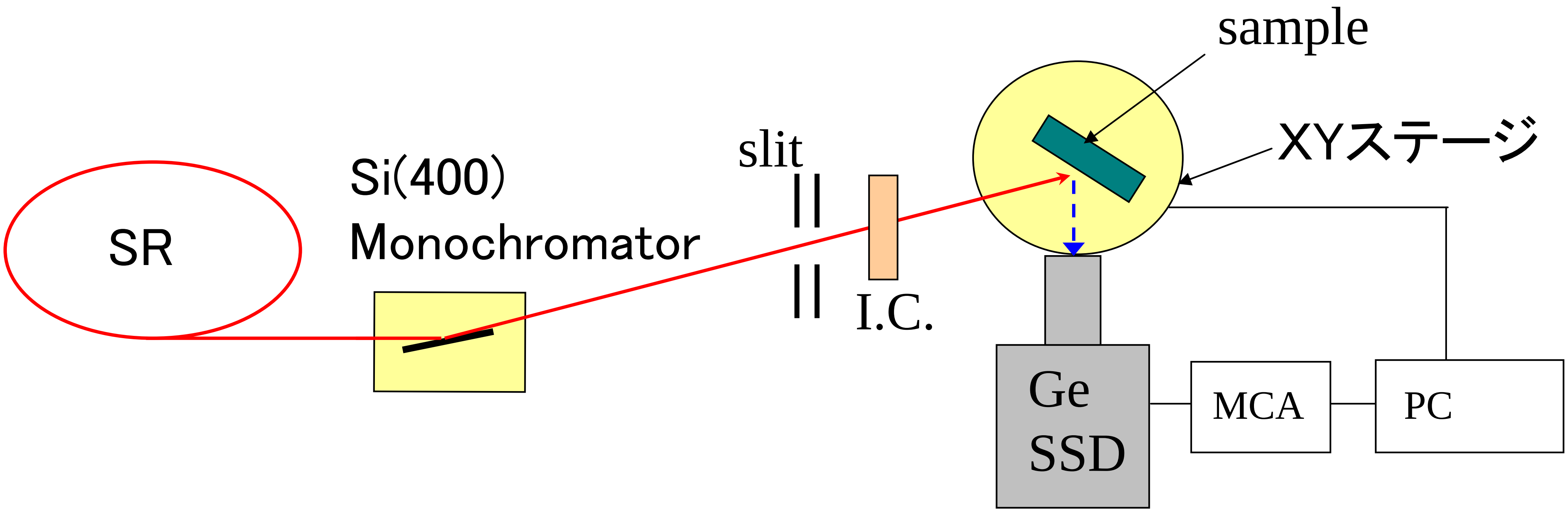

Eliptical multipole wiggler （Gap:160～25.5 mm）

Excitation energy:116 keV （100–150 keV）

Beam size : 1～0.1 mm^2

Experimental setup for high energy XRF

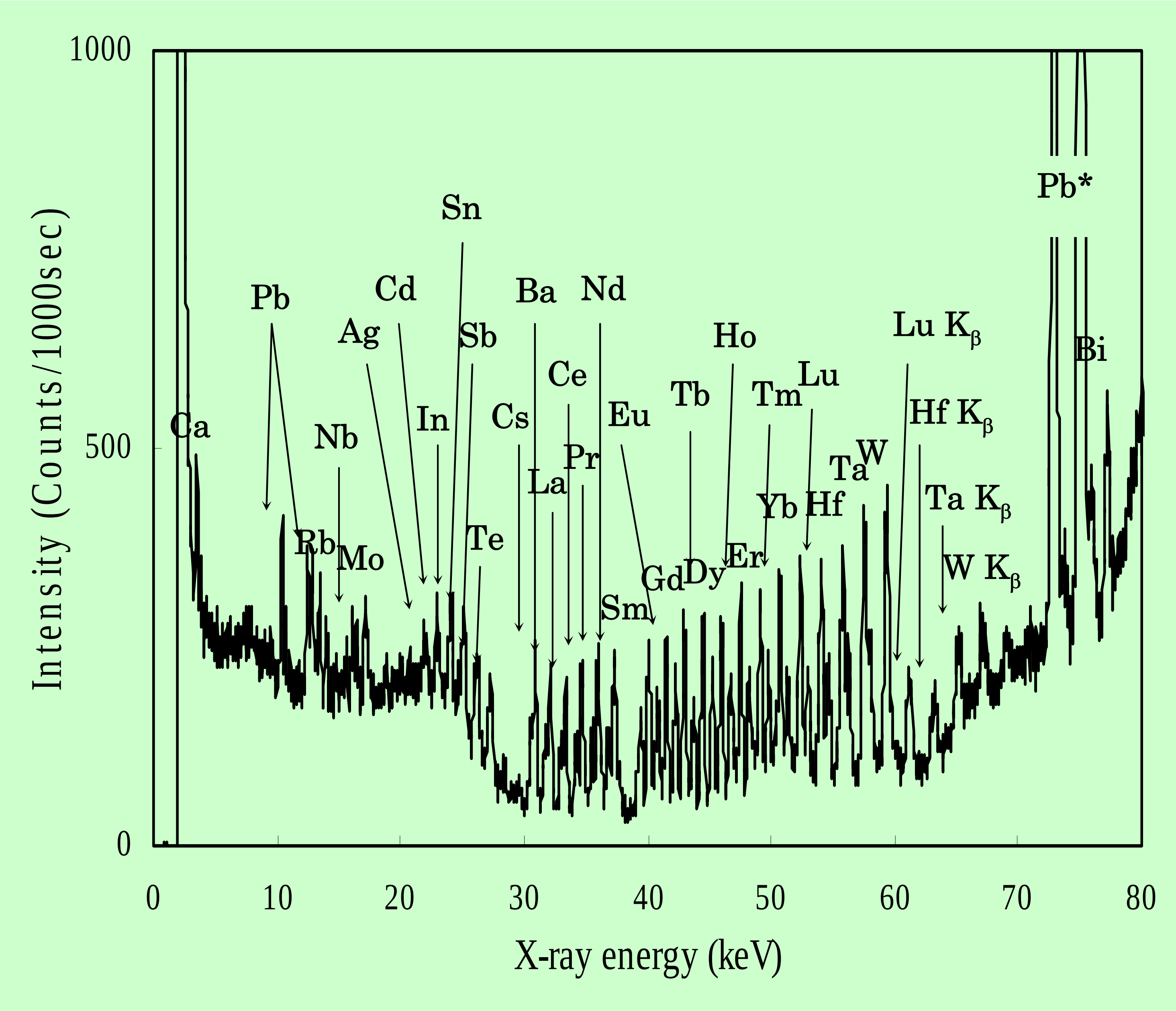

XRF spectrum of NIST SRM612 glass:
61 trace elements in 50ppm level(*scattering)

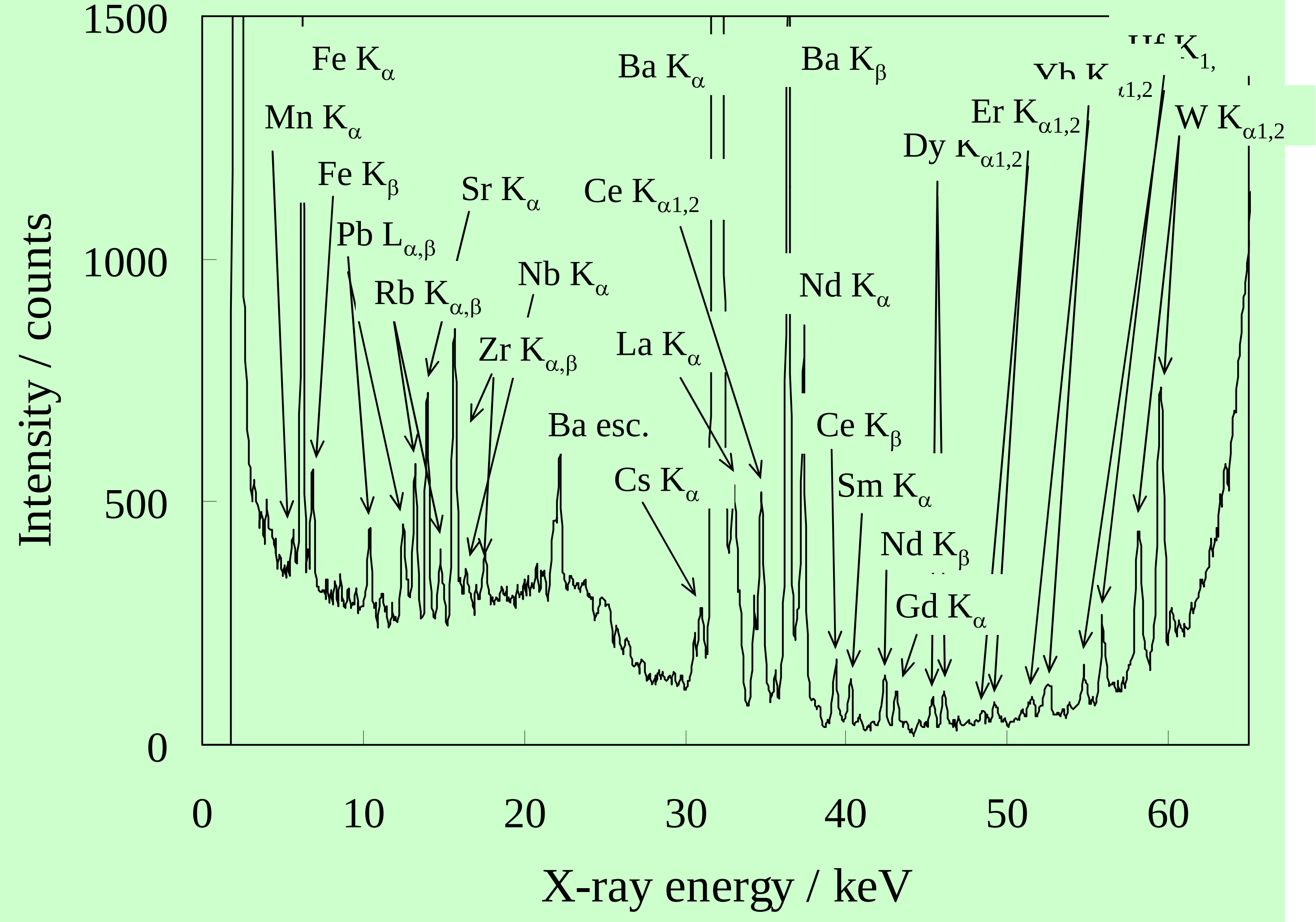

XRF spectrum of JG1 excited at 116keV for 1000sec.

MDL for JG1 sample

	Contents/ ppm	I_{peak}	I_{back}	MDL/ppm
Fe	2.02[a)]	1557	366	0.097[a)]
Rb	181	577	281	30.8
Sr	184	719	258	19.2
Zr[b)]	108	395	293.5	54.7
Cs	10.2	280	181	4.2
Ba	462	7205	354.5	3.8
La	23	535	355.5	7.2
Ce	46.6	520	86	3.0
Nd	20	862	154.5	1.1
Sm	5.1	136	45	1.1
Gd	3.7	108	42.5	1.1
Dy	4.6	110	41	1.3
Er	1.7	86	51.5	1.1
Yb	2.7	125	61	1.0
Hf	3.5	268	98.5	0.6
W	1.7	737	199.5	0.1

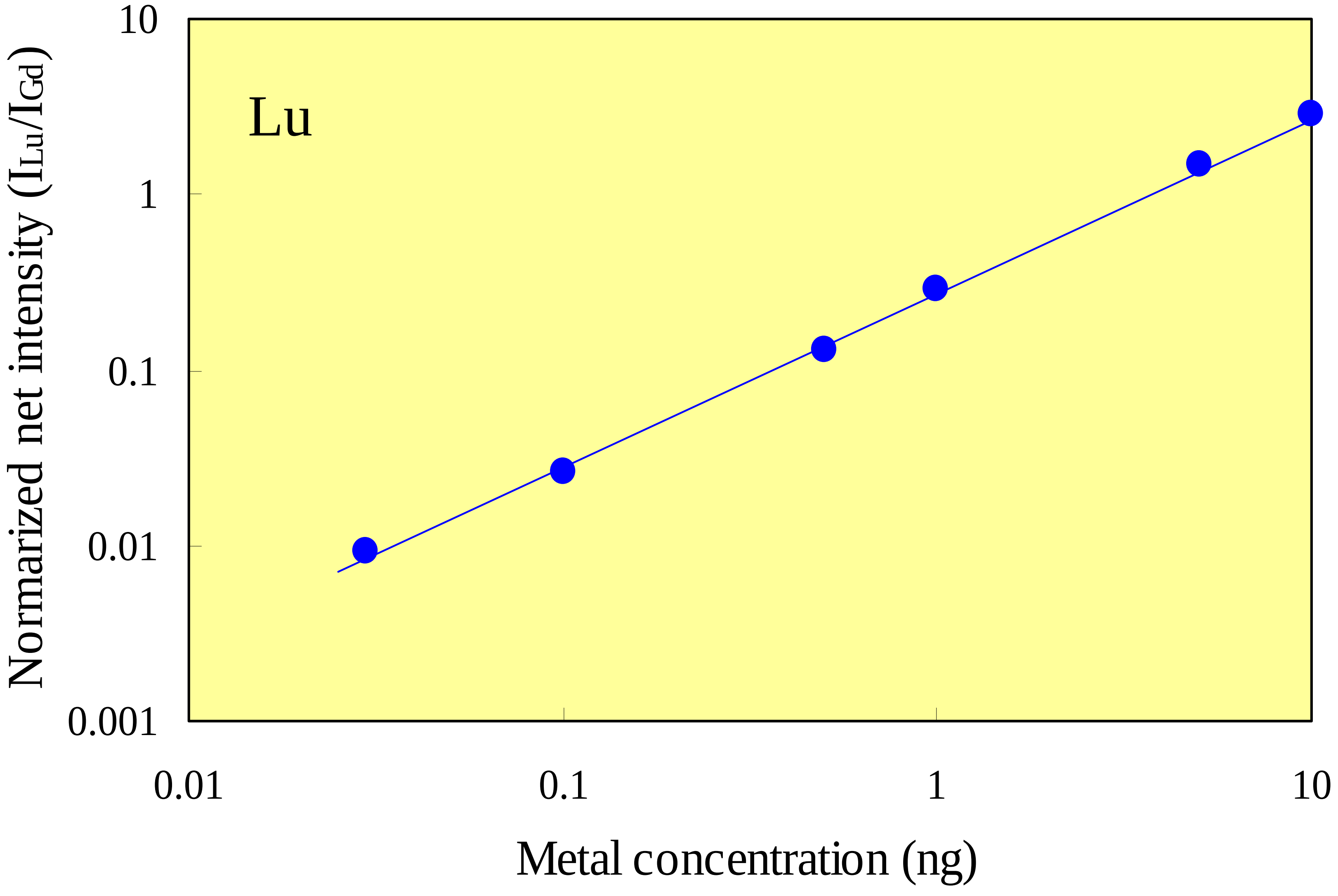

**Calibration curves for Lu
using K-lines XRF spectra**

Application field of high energy XRF

- Archaeology for nondestructive provenance analysis
- Forensic analysis
- Industrial chemical analysis of high-Tech materials
- Geochemistry

Principle of Provenance Analysis of Cultural Heritages

Raw material → Porcelain Stone

Trace element composition tells the locality

Role of Heavy Elements

Good fingerprint elements

- Cosmic abundances of the heavy elements with atomic number larger than 26 (Fe) are small compared with the lighter elements.
- They exhibit characteristic distribution in earth, for the heavy elements such as rare earth and U often posses large ionic radii and high oxidation states.
- The trace elements often substitute for major elements, whose manner is largely affected by the nature of the elements such as the ionic radii, oxidation state as well as the PTC condition.

→ High energy SR-XRF analysis

・肥前(Arita)

加賀（Kutani)

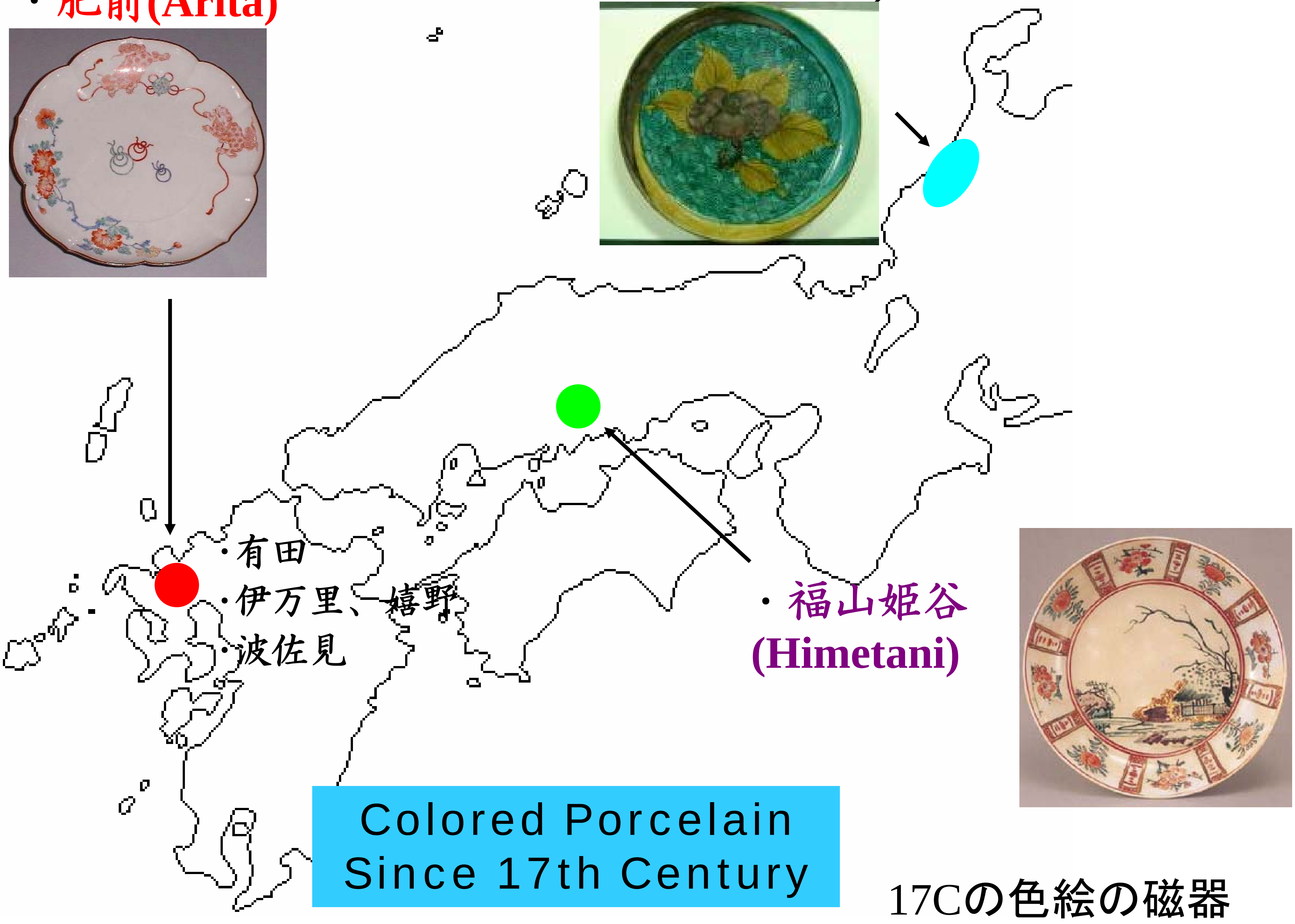

・福山姫谷
(Himetani)

Colored Porcelain
Since 17th Century

17Cの色絵の磁器

Provenance analysis of Old-Kutani China wares based on the information of their material history obtained by high energy XRF

Kutani china wares were first produced in the late 17th century in the Kaga Province in Japan. In 1710, however, after half a century of continuous production, the kiln was suddenly closed. Pottery from this early period is known as Old Kutani, which is extremely precious. However, there is a possibility that the Old Kutani might come from Arita, another famous production place of porcelain since 17th century in Japan. Therefore, identification of Old Kutani and Arita is an important and mysterious problem in Japanese art history. It was expected that high-energy XRF analysis utilizing synchrotron radiation from SPring-8 would reveal the origin of the source materials. This is the first nondestructive analysis of museum grade samples of Old Kutani.

Porcelain Stone tells the Locality

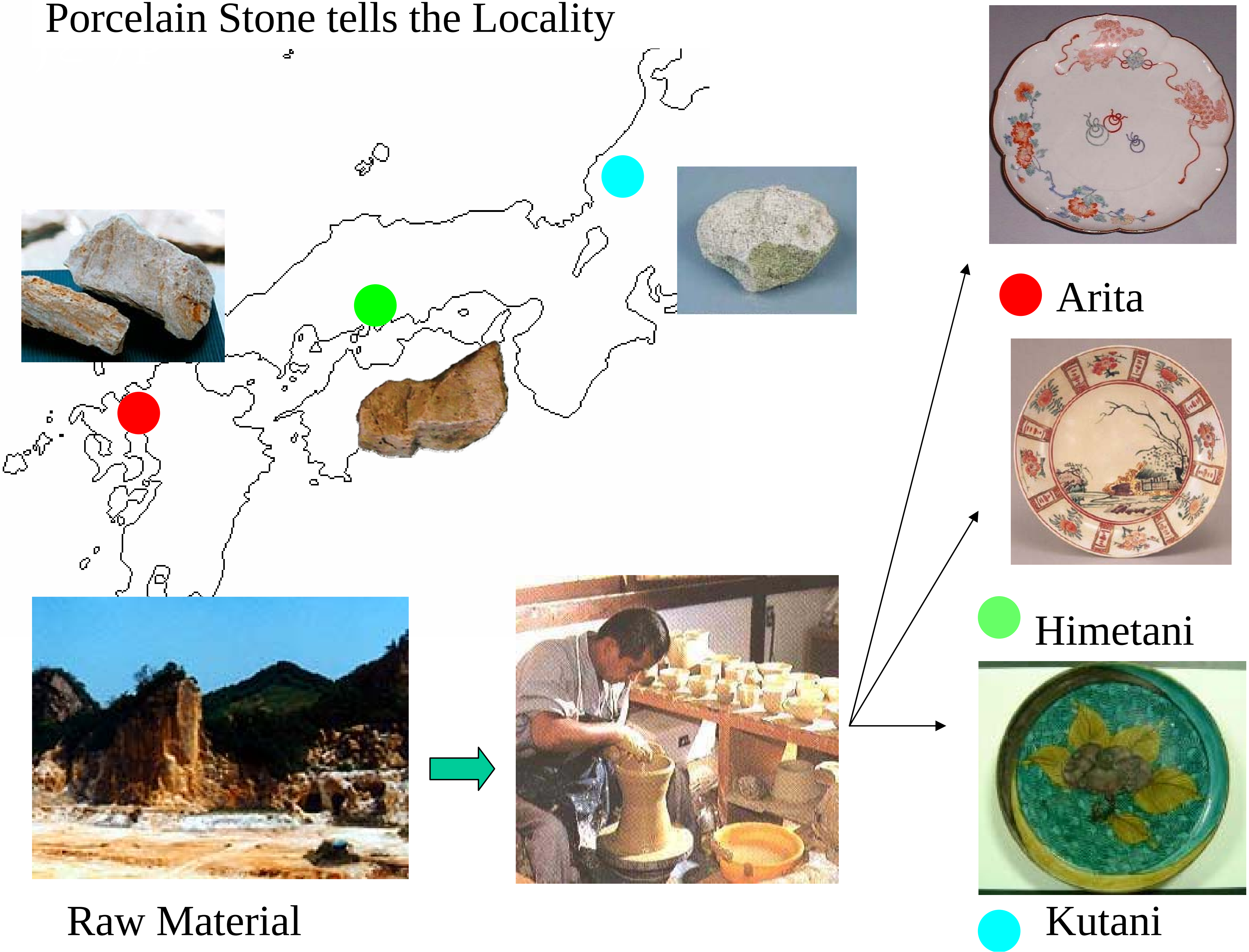

Raw Material

🔴 Arita

🟢 Himetani

🔵 Kutani

Samples

◆Fragments of porcelain excavated at each old kiln of Kaga, Arita, and Fukuyama.

Kutani: 121 Arita: 57 Fukuyama: 10

◆Museum grade samples which are thought to be original : 6

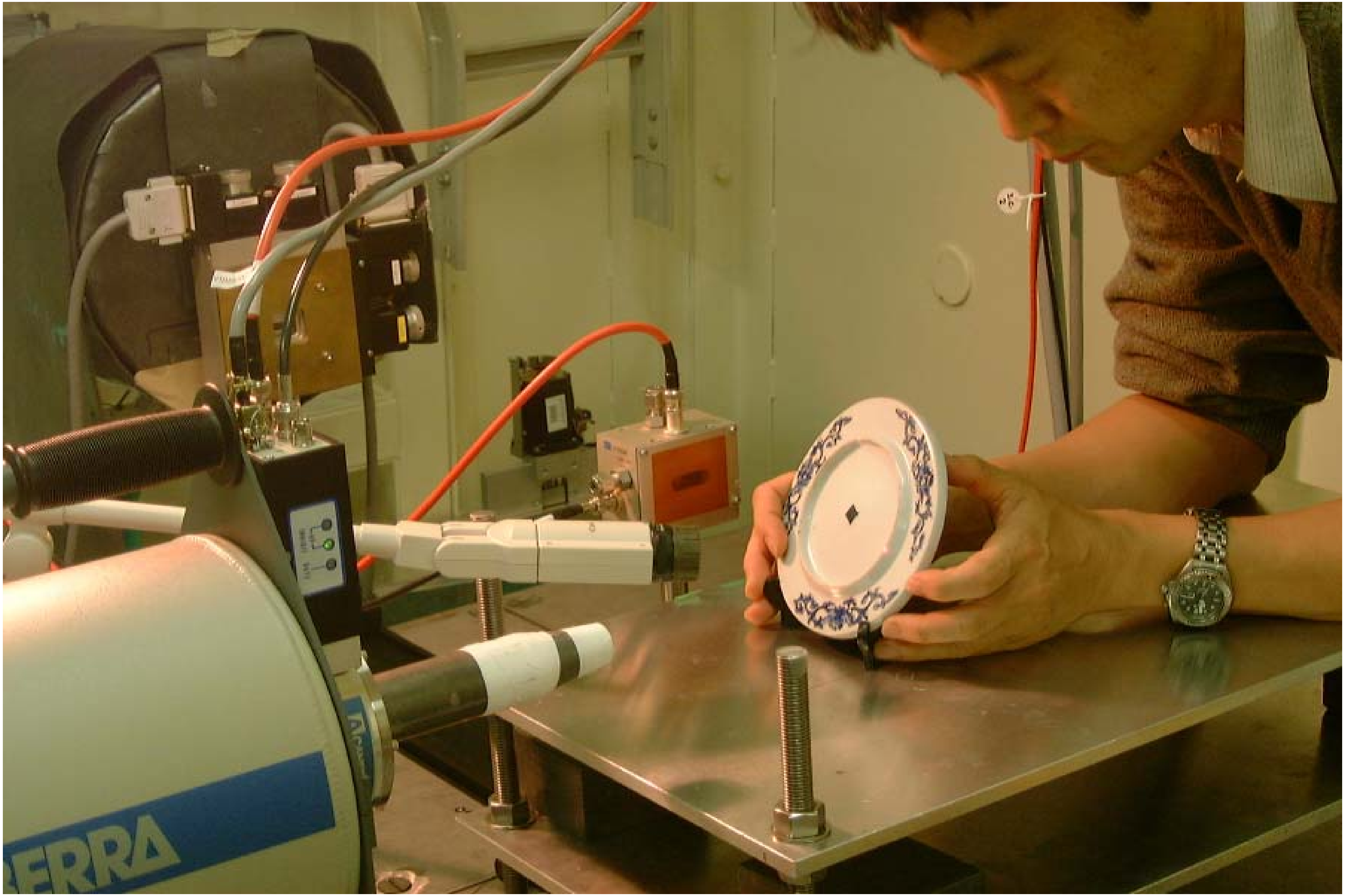
ERRA

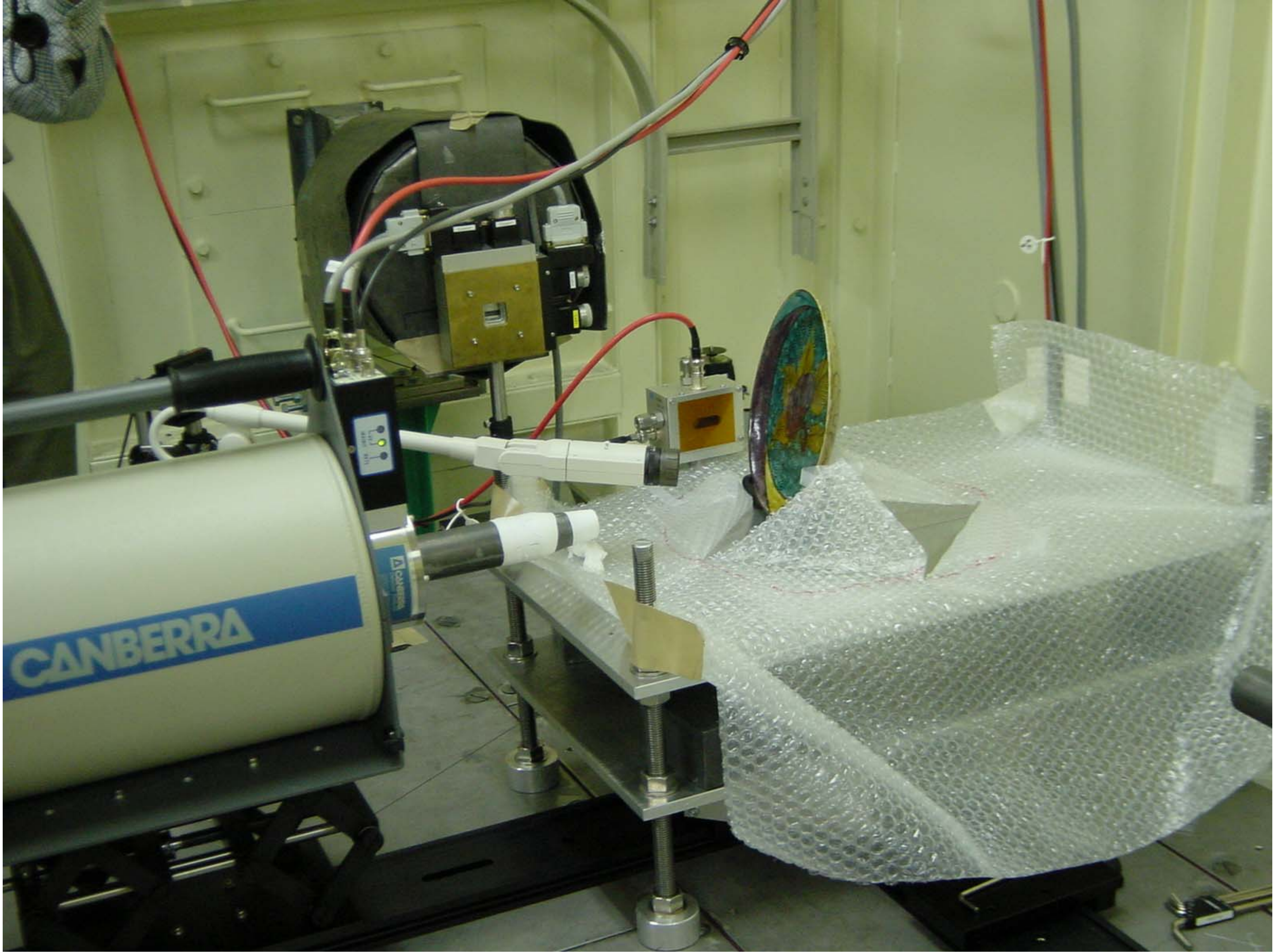
CANBERRA

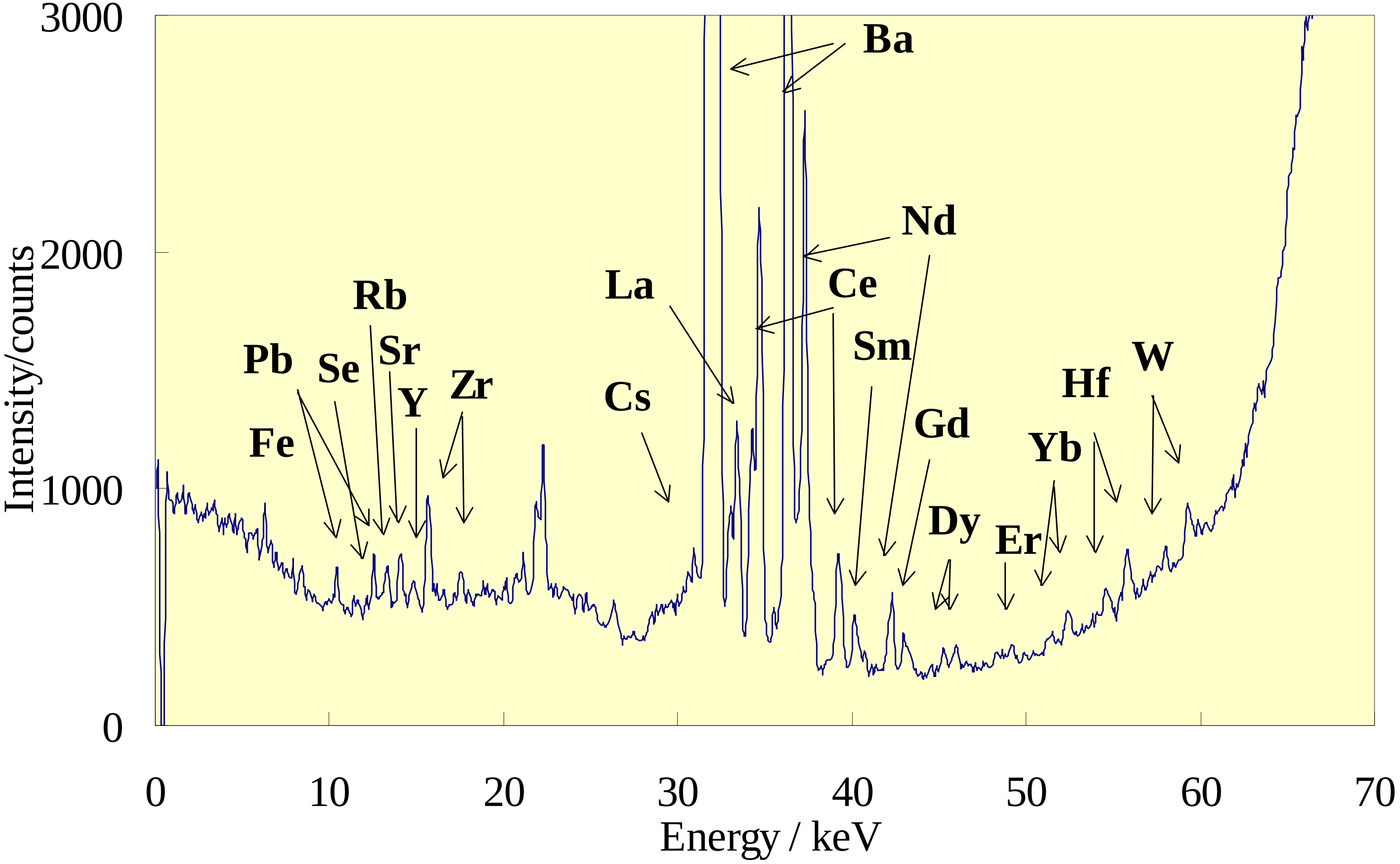

XRF spectrum of fragments of china ware excavated from Old Kutani kiln

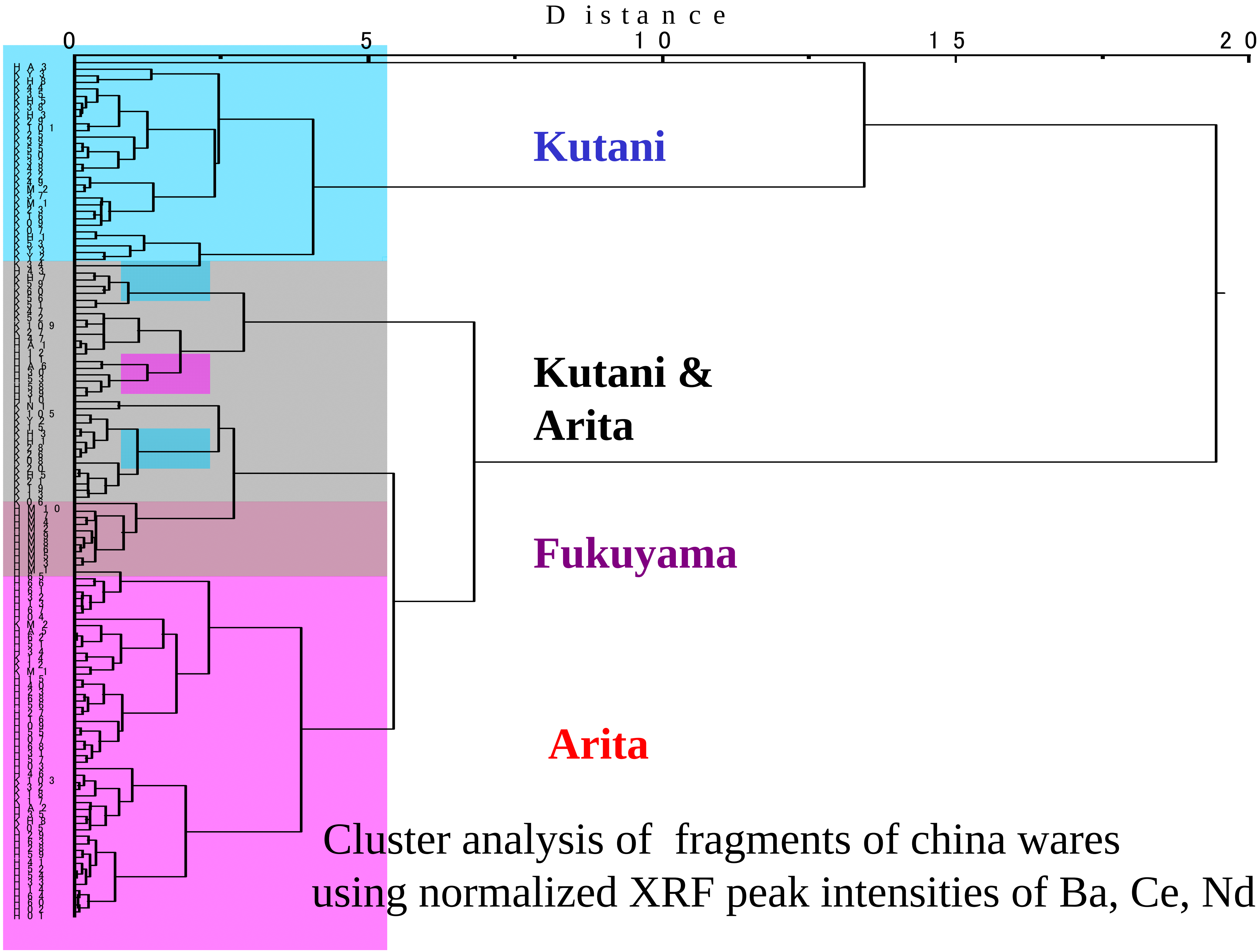

Cluster analysis of fragments of china wares using normalized XRF peak intensities of Ba, Ce, Nd

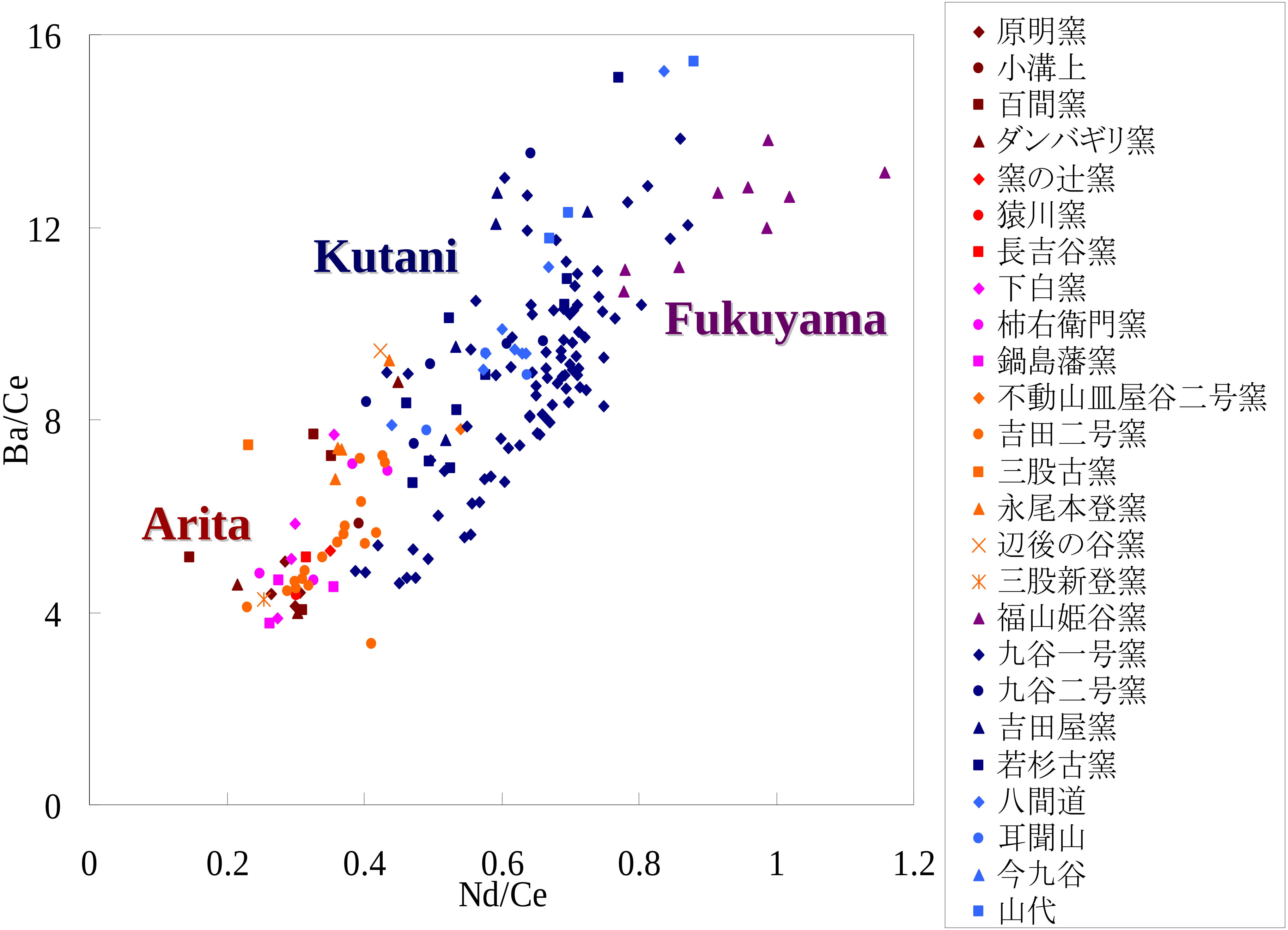

Ba/Ce-Nd/Ce plot

Material History

A latent record of information stored in a substance recording its origin and history

Every substance was produced in the past. The law of causality determines the chemical state of a substance.

During the formation and existence of a substance, the information of its material history is recorded in the substance in various forms such as the concentration, distribution, and chemical state of the trace elements as well as chemical composition, structure, isotope ratio of the major elements.

Material Evolution:material world is continuous

15 billions years ago

Stream of Time →

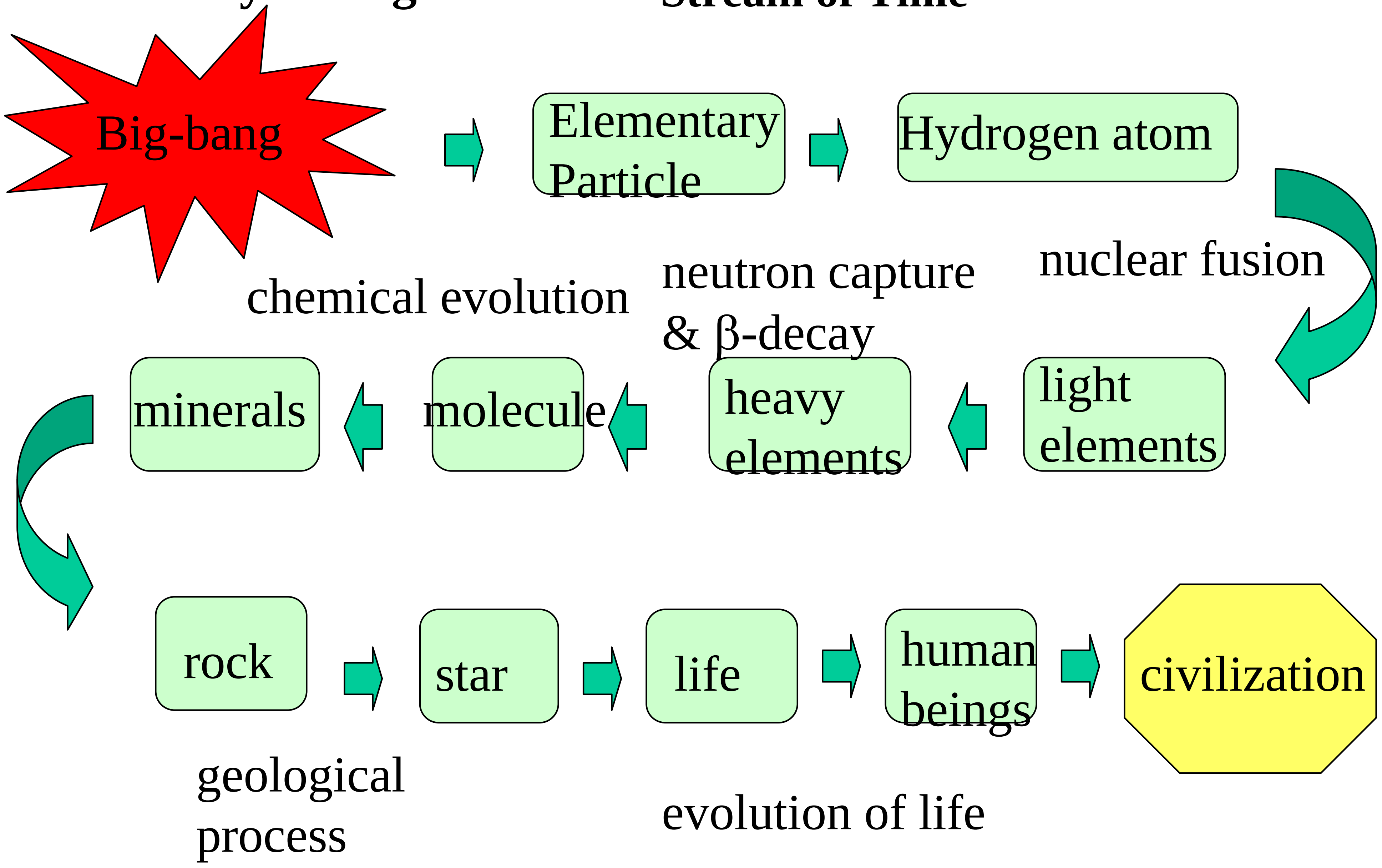

Big-bang

Elementary Particle

Hydrogen atom

nuclear fusion

light elements

neutron capture & β-decay

heavy elements

molecule

chemical evolution

minerals

rock

geological process

star

life

evolution of life

human beings

civilization

Application of the material history:
Information of the material history can be used in various scientific fields

- Archaeology, forensic analysis, geology,geochemisty
  →To reveal the past based on the material history.
- Biological sciences: life history, migration history, environmental problems
- Industrial application: prediction of source material, production method and patent related problems
- Environmental science: monitoring of environmental change→industrial, biological, and social activities etc.

Highly sensitive nondestructive X-ray analyses utilizing SR are most suitable techniques to reveal the material history of the sample.

Importance of trace element

Cobalt blue 0.0002% Co

Forensic application

S&W Gunshot Residue

SPring-8 BL08W

Characteristic element: Ba,Sb, Pb

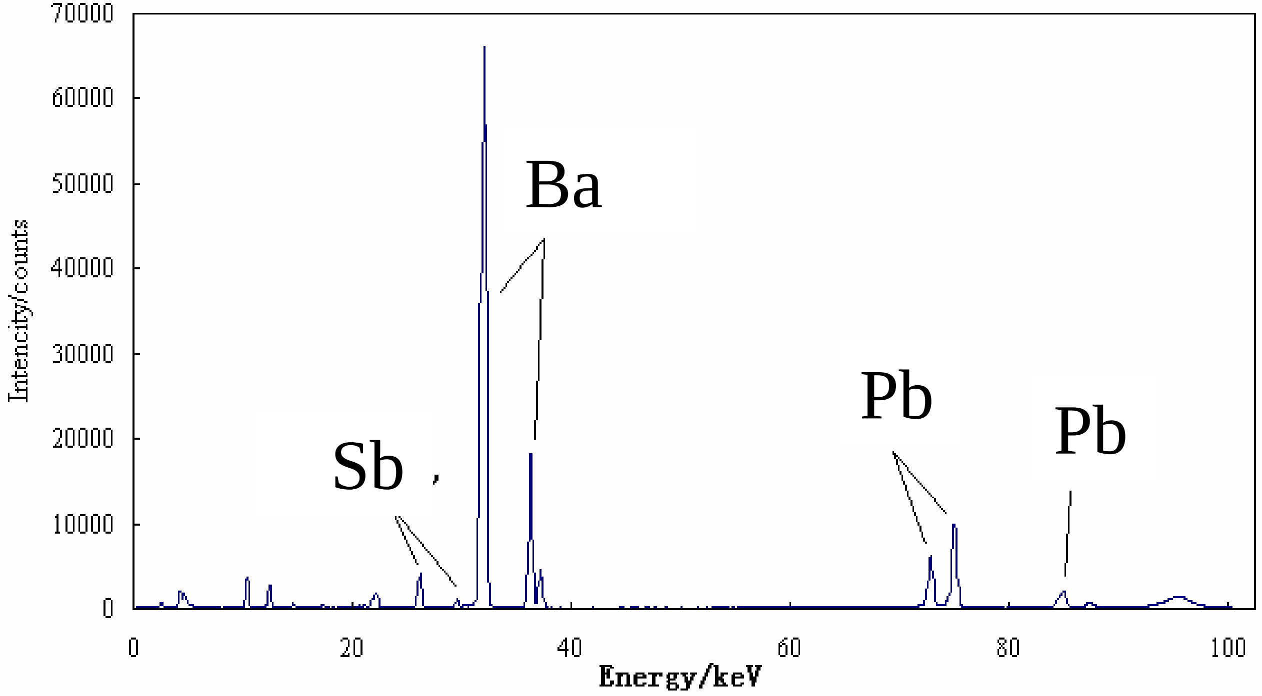

High energy SR-XRF characterization of trace gunshot residue

High energy XRF characterization of trace heavy elements in white car paints (paints A & B) compared with X-ray microprobe (bottom)

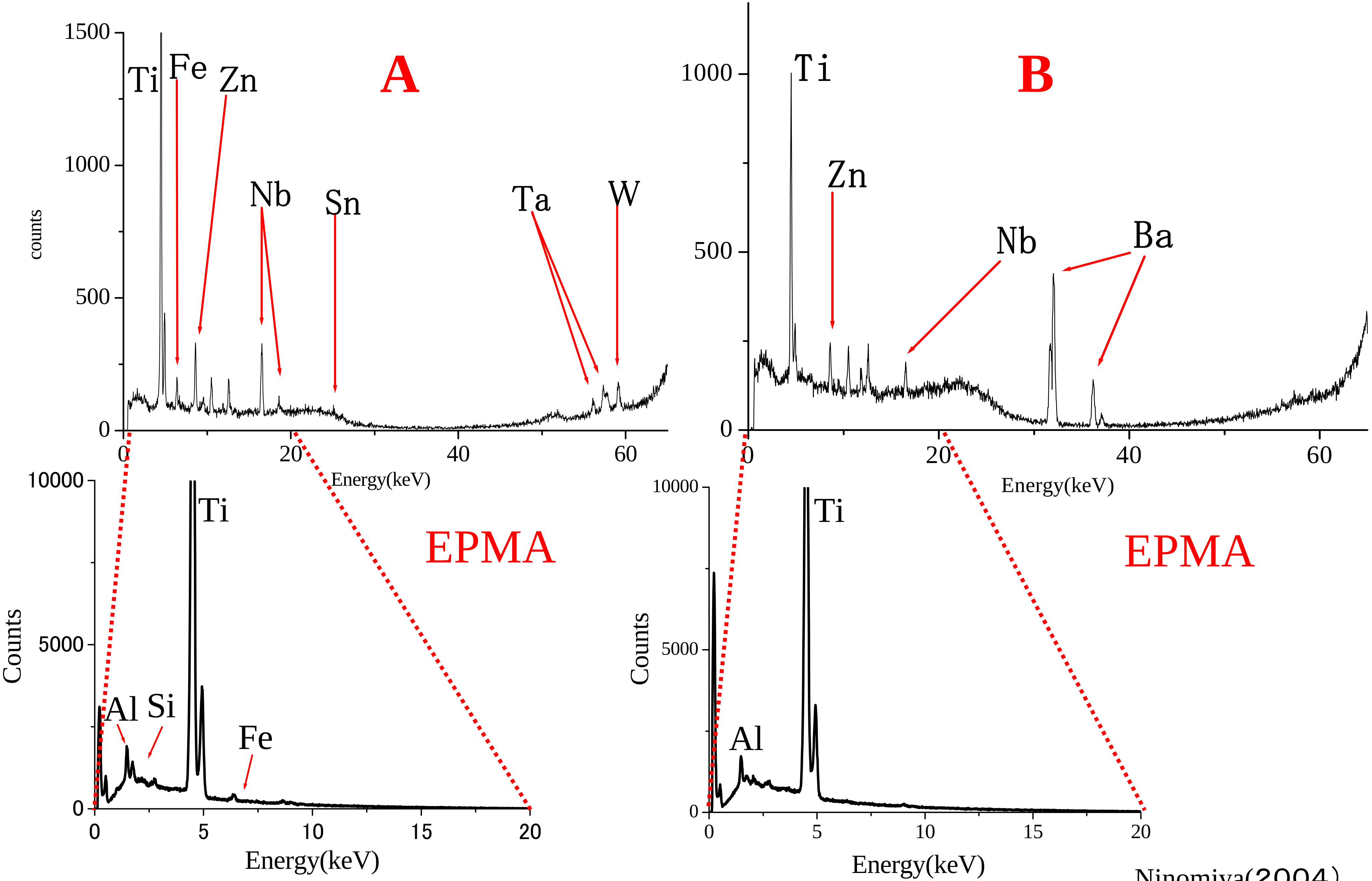

Ninomiya(2004)

(5) multiple X-ray analytical technique

μ-XRF imaging, m-XRD,XAFS and SEM

Chemical speciation of arsenic-accumulating mineral in a sedimentary iron deposit by synchrotron radiation multiple X-ray analytical techniques

S.ENDO,Y.TERADA,Y.KATO,I.NAKAI
Environ.Sci.Technol.2008,42,7152.

Comprehensive characterization of As(V)-bearing iron minerals from the Gunma iron deposit by

Sample the Gunma iron deposit of quaternary age

Background

Natural behavior of arsenic at volcanic region

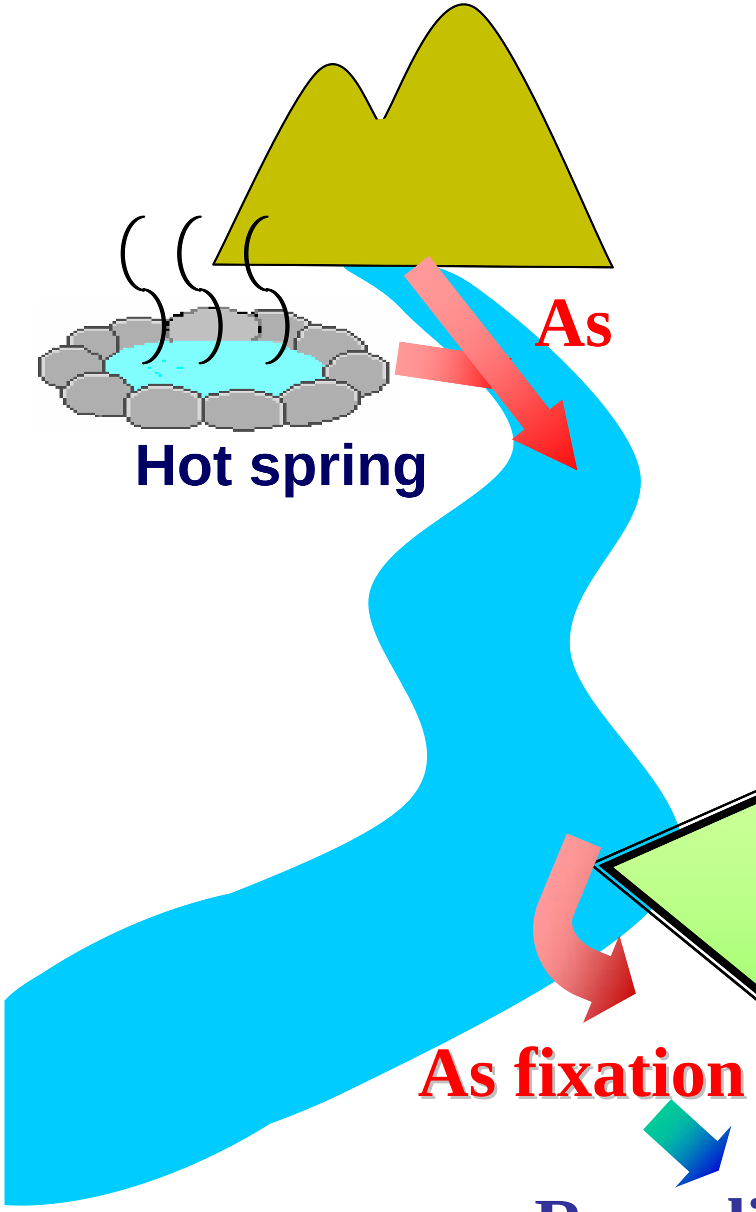

Decompositon of As containing minerals by acidic water

- **Precipiation**

ex.) $Fe^{3+} + AsO_4^{3-} \rightarrow FeAsO_4\downarrow$

- **Adsorption**

α-FeO(OH)

- **biological effect**

biomineral formation

Remediation of As poisoning

SR-μ-XRF XRF imaging

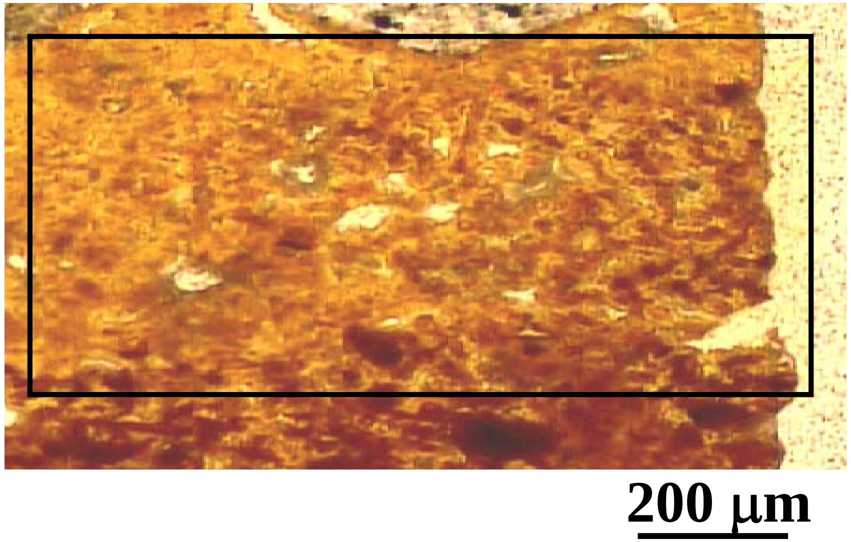

SPring-8 BL37XU

X-ray: **12.8 keV**

Beam size : 1.8 μm × 2.8 μm

Step size : 2.0 μm × 3.0 μm

Meas. time : 0.1 s/point

Detector : SDD

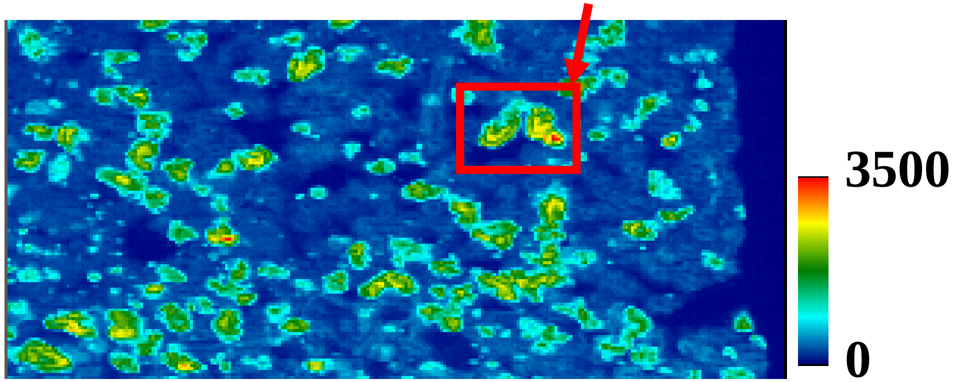

As

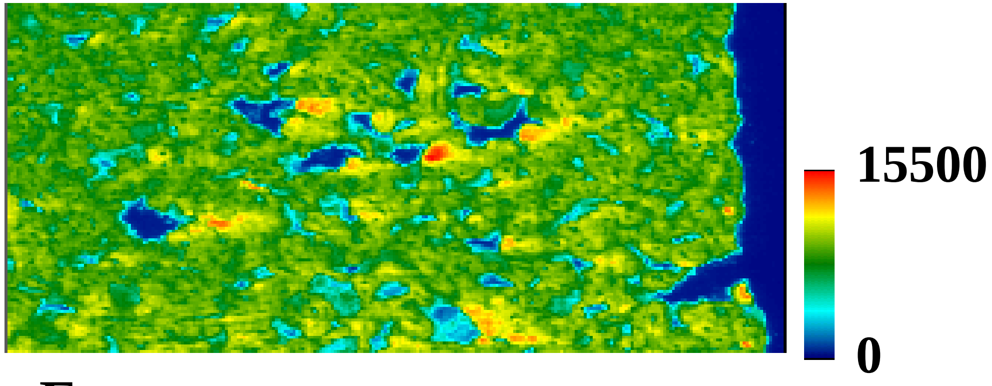

Fe

Purpose: which mineral accumulate arsenic?

strengite $FePO_4 \cdot 7H_2O$?
jarosite $KFe_3(SO_4)_2(OH)_6$?
goethite FeOOH?

SR-μ-XRF & SEM-EDS

strengite $FePO_4 \cdot 7H_2O$
jarosite $KFe_3(SO_4)_2(OH)_6$

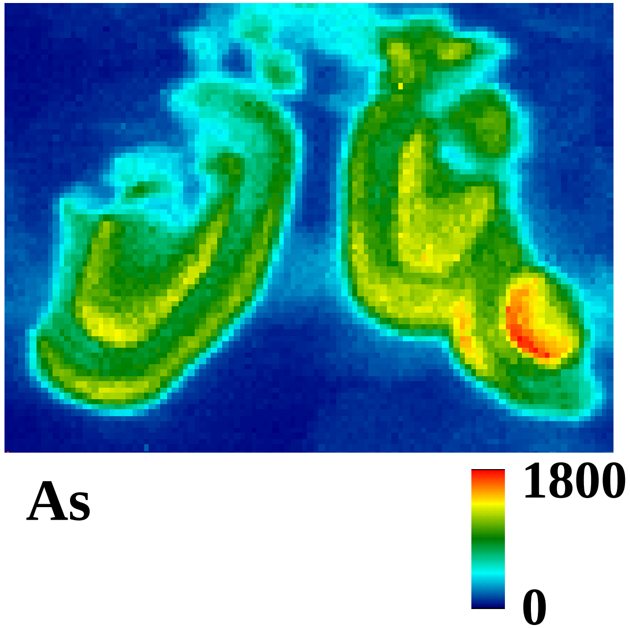

As

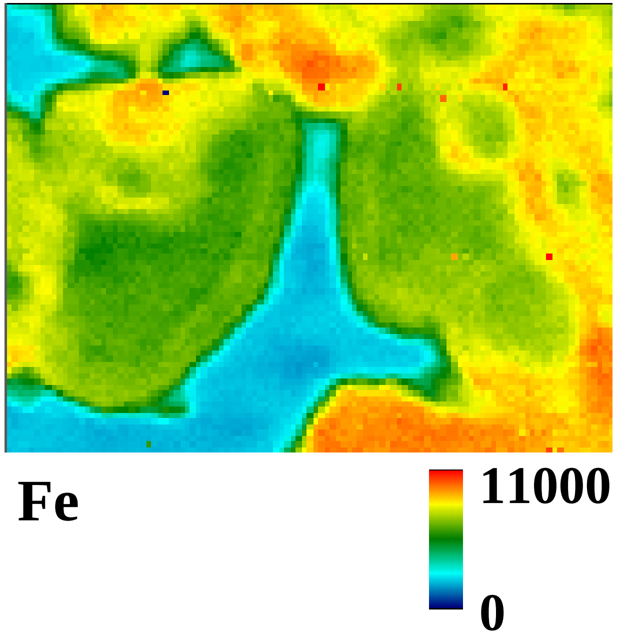

Fe

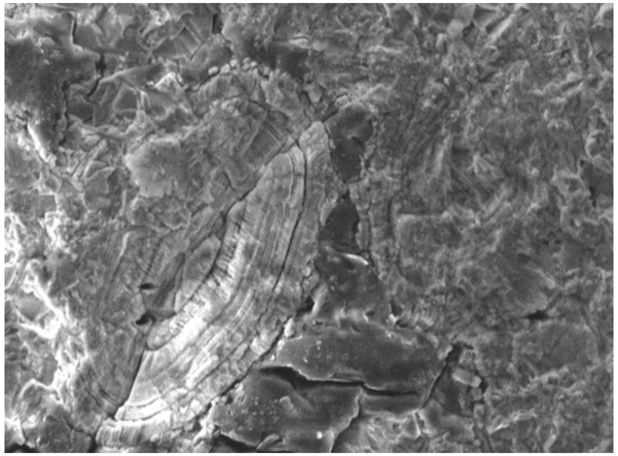

SEM image

Beam size: 1.8 μm×2.8 μm
Step size : 1.0 μm×1.0 μm

As at the region with peculiar concentric morphology

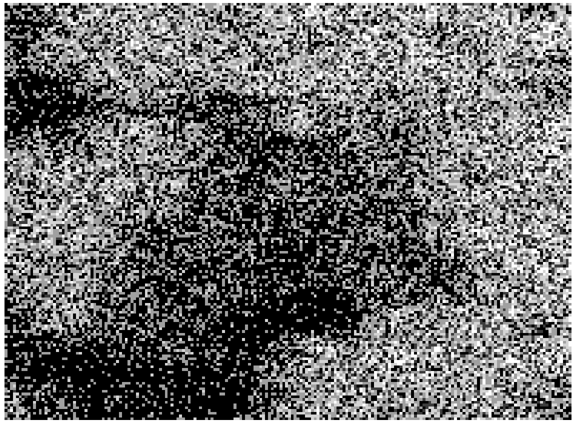

S (SEM-EDS)

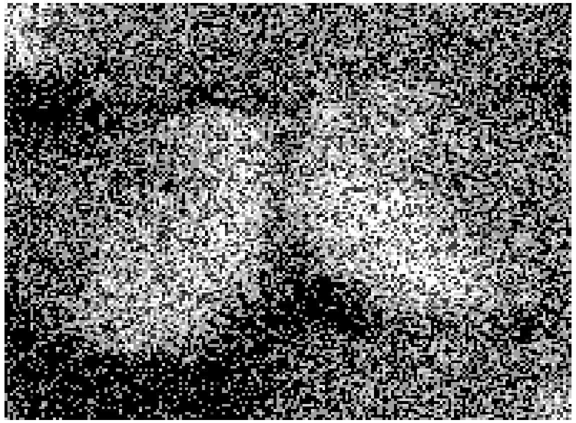

P (SEM-EDS)

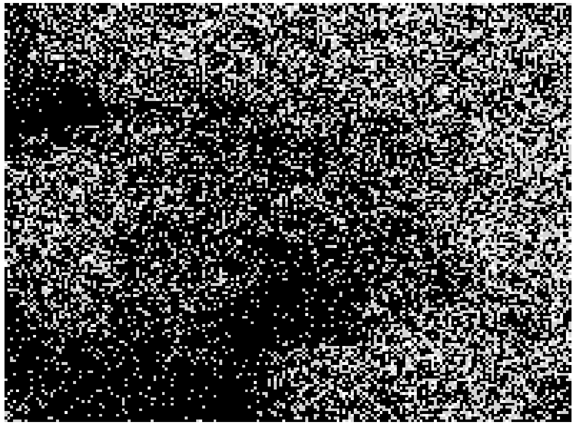

K (SEM-EDS)

Positive correlation between As and P, negative for S and K

SR-μ-XRF & SEM-EDS

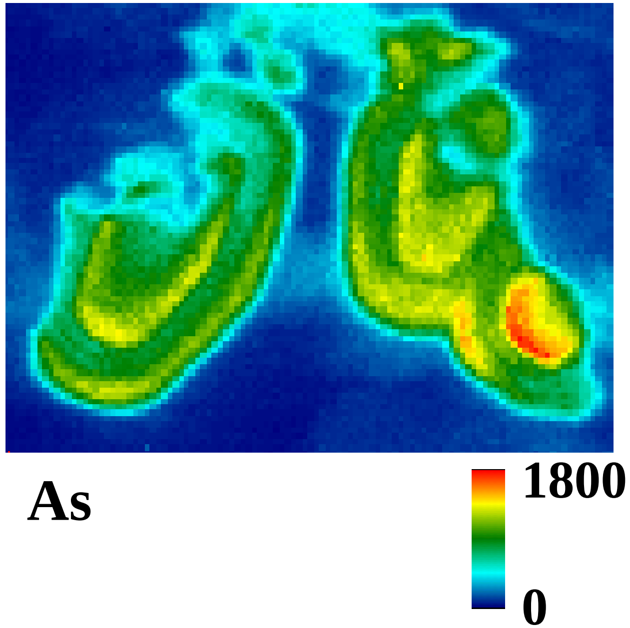

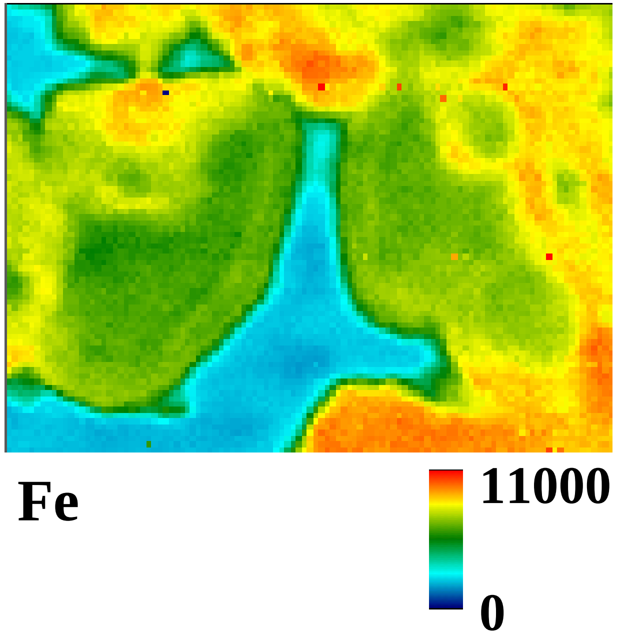

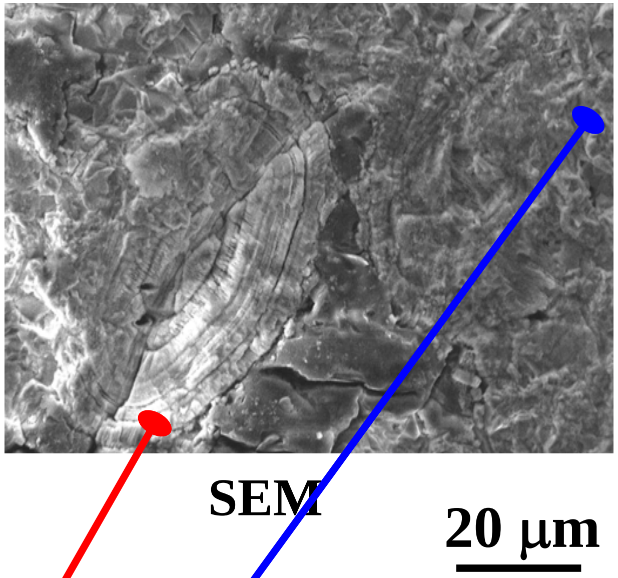

Beam size: 1.8 μm × 2.8 μm
Step size : 1.0 μm × 1.0 μm

Localization of As.

strengite $FePO_4 \cdot 7H_2O$
jarosite $KFe_3(SO_4)_2(OH)_6$

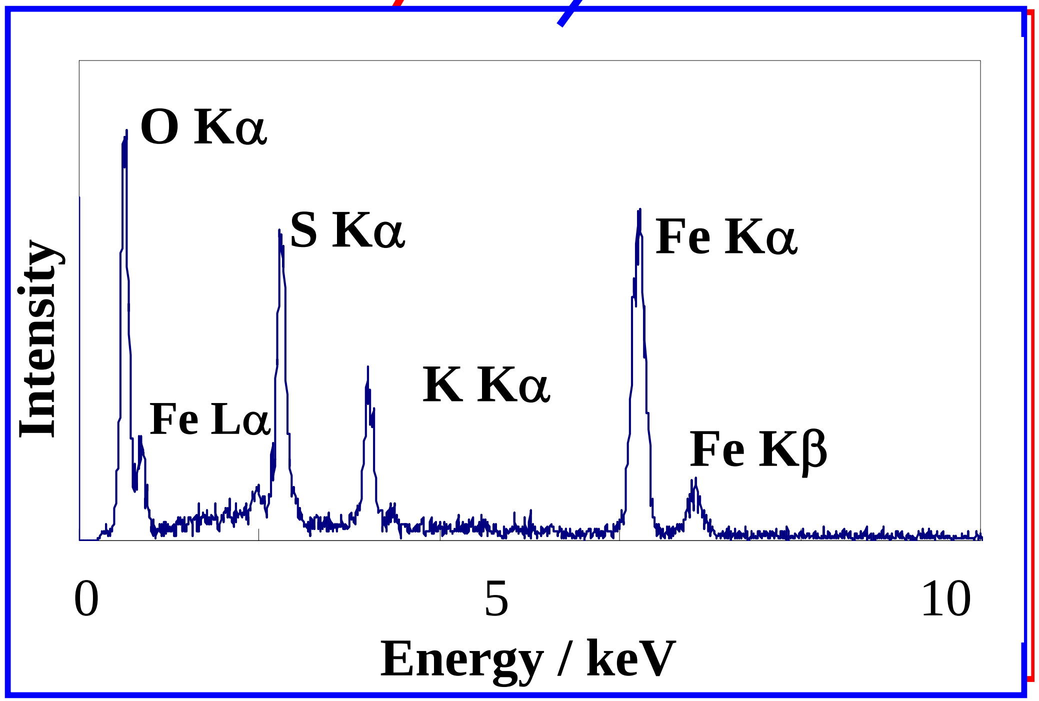

SEM-EDS spectrum

XRD

X-ray : 12.8 keV
Beam size : 50 μm × 50 μm
Meas.time **: 12 min. / sample**
IP (Imaging Plate)

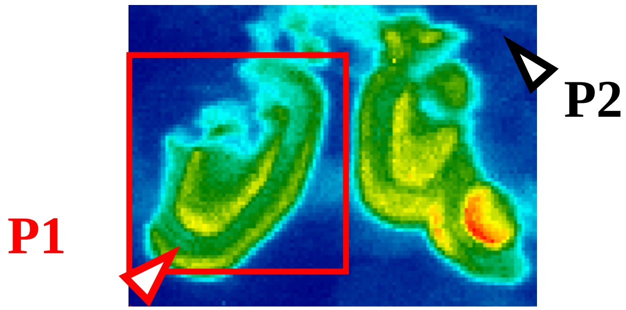

XRD point

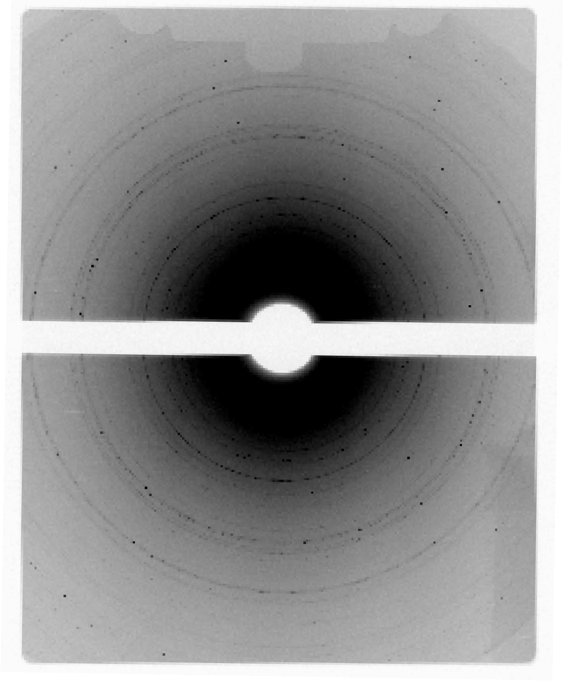

XRD pattern (P1)

P1		P2		strengite			jarosite		
***d* / Å**	**I / I$_0$**	***d* / Å**	**I / I$_0$**	***hkl***	***d* / A**	**I / I$_0$**	***hkl***	***d* / A**	**I / I$_0$**
		5.93	32				101	5.93	45
		5.75	14				003	5.72	25
5.49	55			111	5.509	60			
		5.10	56				102	5.09	70
4.95	43			020	4.954	30			
4.37	100			201	4.383	85			
4.00	22			211	3.996	45			
				121	3.959	13			
				112	3.719	25			
		3.63	32				110	3.65	40
3.27	21			221	3.281	17			
3.12	53	3.11	72	122	3.114	100	201	3.11	75
		3.07	100				113	3.08	100
2.99	16			311	3.002	45			
2.95	19	2.97	12	131	2.949	45	202	2.965	15
		2.88	8				006	2.861	30
				231	2.631	11			
2.56	45	2.55	20	132	2.546	50	204	2.542	30

*** strengite $FePO_4 \cdot 7H_2O$ PDF No. 33-667**
**** jarosite $KFe_3(SO_4)_2(OH)_6$ PDF No. 22-827**

μ-XANES

As K-edge XANES spectra
measured by 2μm X-ray beam

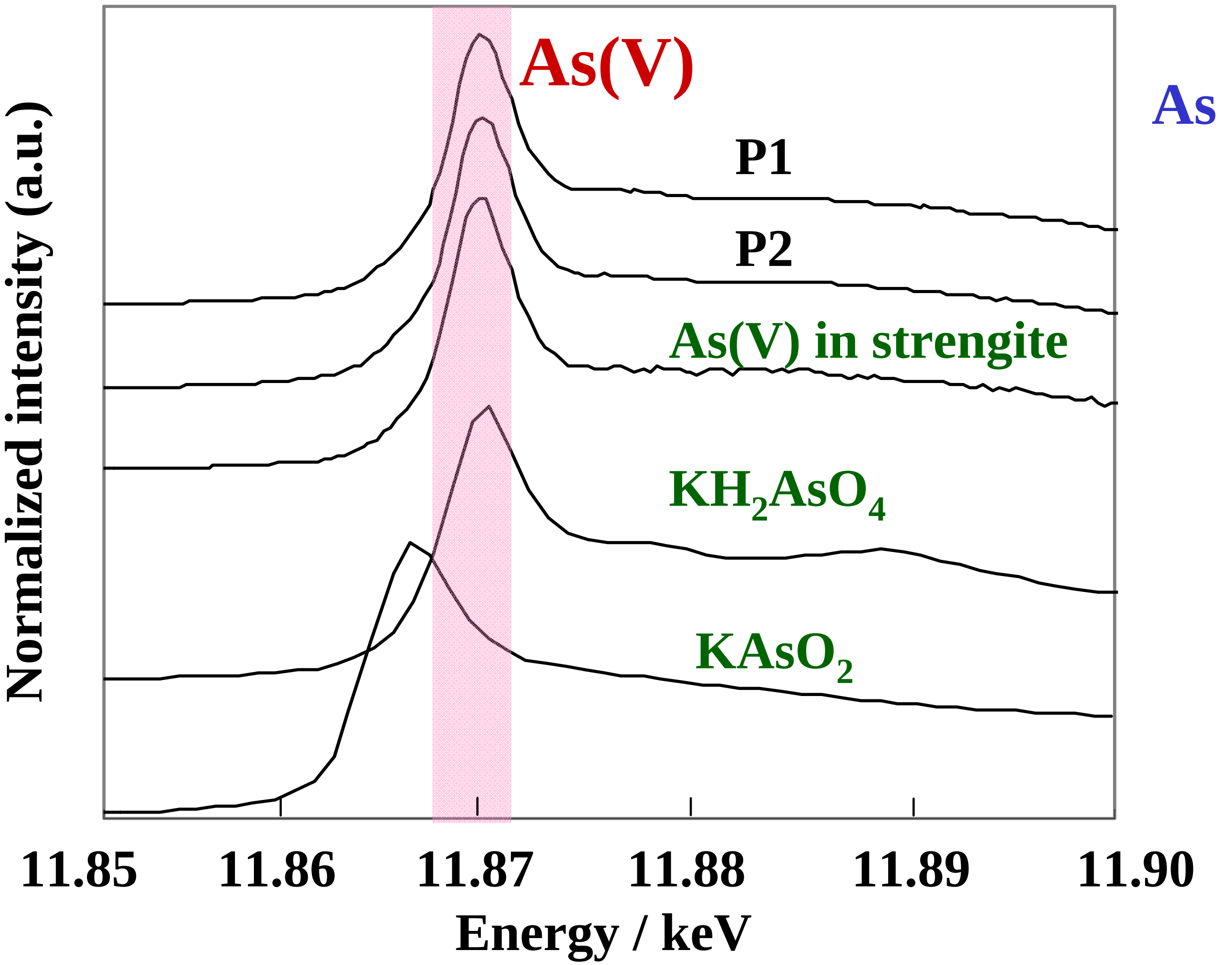

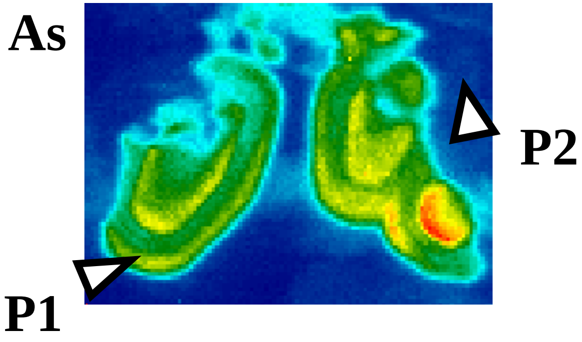

XANES points

As exists as As(V) in the sample
(AsO_4^{3-}, $HAsO_4^{2-}$)

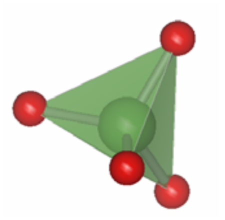

AsO_4^{3-}

strengite ($FePO_4 \cdot 2H_2O$)

μ-EXAFS

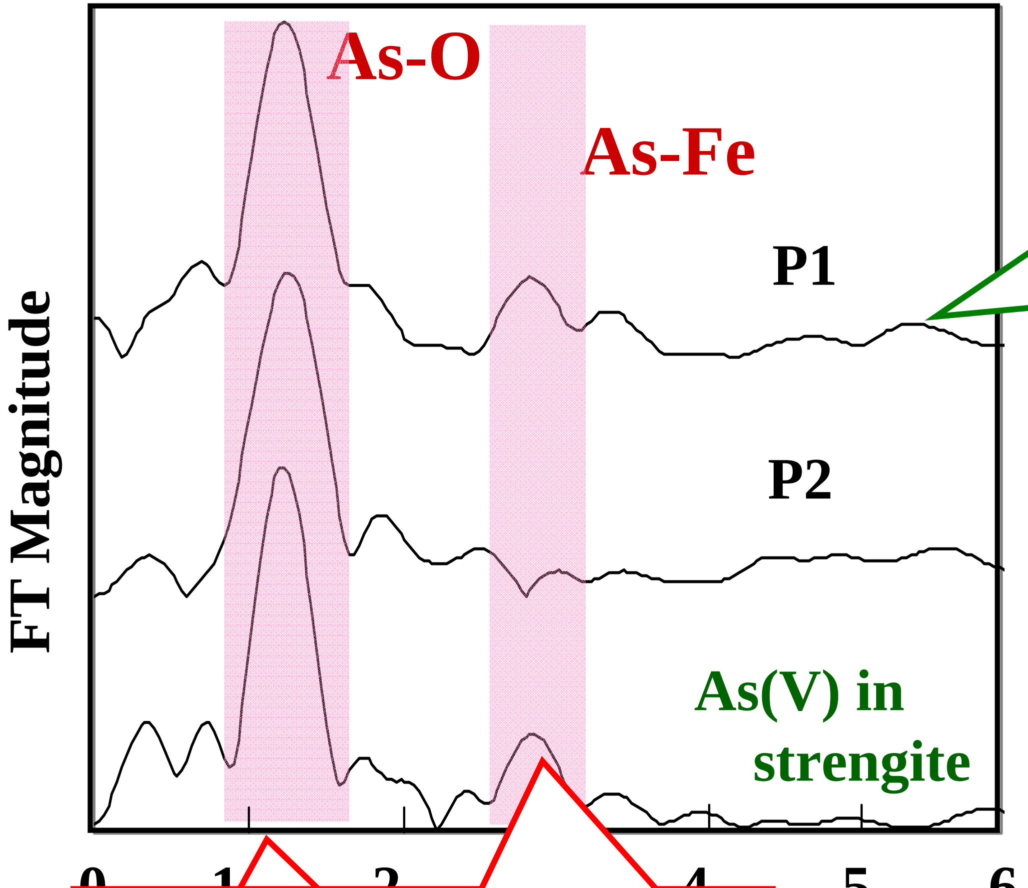

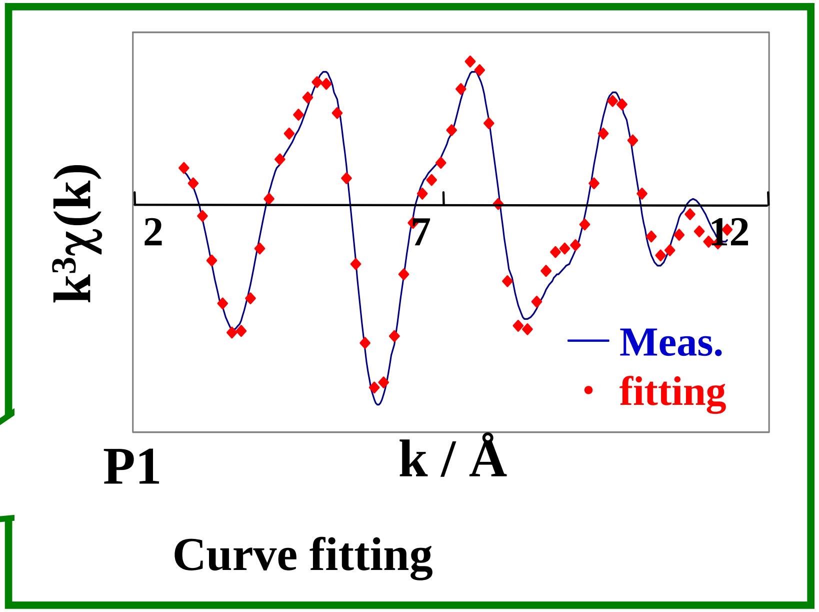

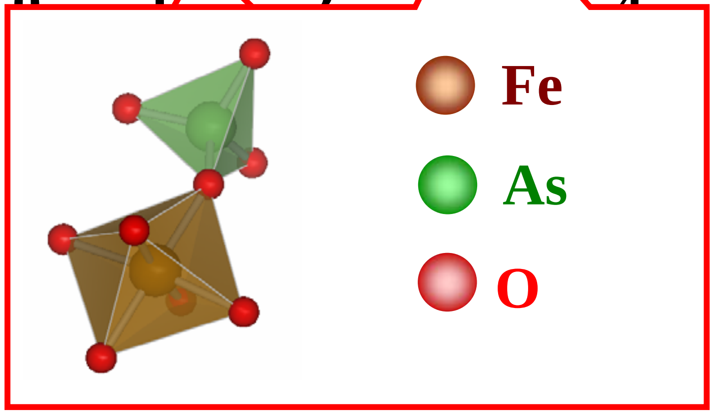

strengite FePO4·7H2O

EXAFS

	Atom	r / Å	CN
P1	O	1.68	4.0
	Fe	3.36	4.0
P2	O	1.69	4.0
As(V) in strengite	O	1.68	4.0
	Fe	3.35	4.0

As→AsO$_4$

AsO$_4$ tetrahedra-Fe(III)octahedra

As accumulation mechanism

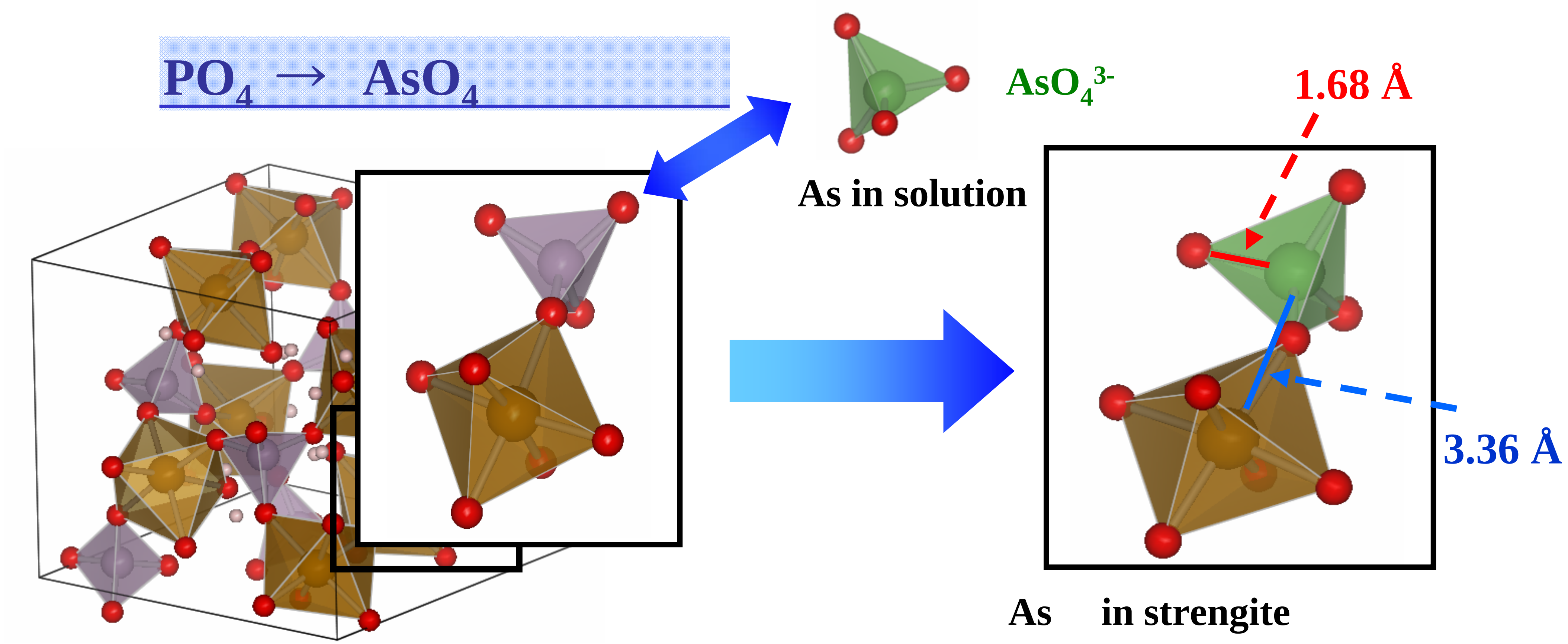

$PO_4 \rightarrow AsO_4$

AsO_4^{3-}

As in solution

1.68 Å

3.36 Å

As in strengite

Crystal structure of strengite ($FePO_4 \cdot 2H_2O$)

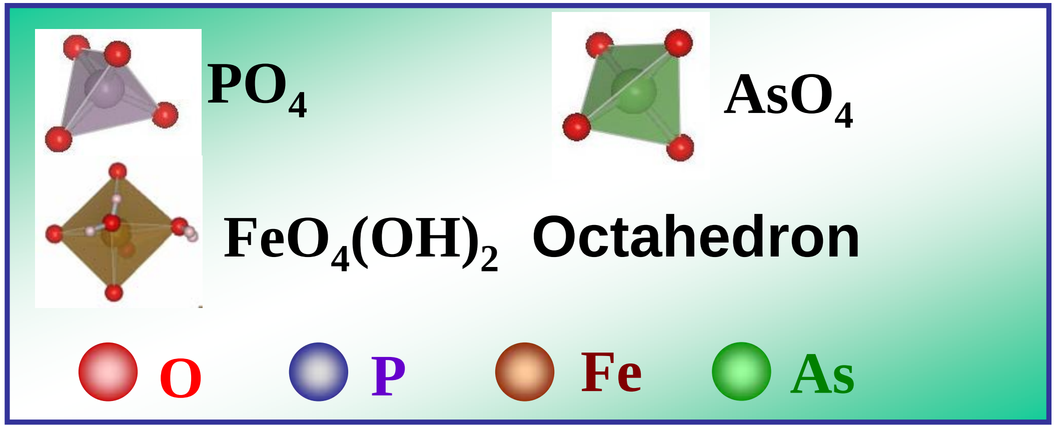

PO_4

AsO_4

$FeO_4(OH)_2$ **Octahedron**

O P Fe As

Substitution of PO4 tetrahedra in **strengite ($FePO_4 \cdot 2H_2O$)** by AsO_4 teterahedra

Conclusion

Limitation of the SR-XRF

1. **Microbeam analysis**

   i) the thickness of the sample should be in the order of beam size

   → preparation of thin sample is not easy

   ii) it takes long hours to carry out two dimensional mapping because of large numbers of measurement points

2. **Low excitation efficiency for light elements**

3. **Special efforts is necessary to carry out quantitative analysis**

4. **Sample damage should be considered if you use brilliant Undulator SR Source or white X-ray radiation. Especially, care must be taken about photo-reduction/oxidation of the component elements.**

However!

Attractiveness of SR-XRF

1．Nondestructive analysis, multielemental analysis

2. Two dimensional resolution

3. Easy to carry out the analysis and easy to understand the results

4. Basic optical system for EDS analysis is simple

SR → Monochromator → sample → detector

5．We can analyze almost any samples

size → from cell level to sculpture, paintings

in situ、in vivo、in air at any temperature

6. Information

concentration： major（%）, minor, trace（ppm) elements C ～Na ～ U

distribution: from nm level to cm level

chemical state (oxidation state, local structure) C ～ Si ～ U

7．Multiple SR-X-ray analysis: combination with X-ray diffraction and XAFS

Invitation to SR-XRF

SR-XRF is waiting for you.

Come and just try it !